Fault tolerant control of non-linear systems based on multiple model approach

Menglin He

Université Fédérale
Toulouse Midi-Pyrénées

THÈSE

En vue de l'obtention du
DOCTORAT DE L'UNIVERSITÉ DE TOULOUSE

Délivré par l'Université Toulouse 3 - Paul Sabatier

Cotutelle internationale : Guizhou University

Présentée et soutenue par

Menglin HE

Le 7 juillet 2021

Commande tolérante aux fautes des systèmes non linéaires basée sur l'approche multi-modèles

---

Ecole doctorale : **SYSTEMES**

Spécialité : **Automatique**

Unité de recherche :
LAAS - Laboratoire d'Analyse et d'Architecture des Systèmes

Thèse dirigée par
Boutaieb DAHHOU et Ze-Tao LI

Jury

M. Ahmed EL HAJJAJI, Rapporteur
M. Jing NA, Rapporteur
M. Mondher FARZA, Examinateur
M. Honglei WANG, Examinateur
M. Michel CABASSUD, Examinateur
Mme Wei WEI, Examinatrice
M. Boutaieb DAHHOU, Directeur de thèse
M. Zetao LI, Co-directeur de thèse

Acknowledgments

As time flies, my doctoral study has come to the end. Looking back on the past years, I gained various experiences, lots of friendships and rich knowledge. First of all, I would like to express my deepest gratitude to my supervisors, Prof. DAHHOU and Prof. LI. It is because of your wise advice, careful guidance and sincere care that enabled me to grow on the academic ground. Your broad scientific vision, profound knowledge, rigorous academic attitude and keen academic vision have benefited me greatly. I would like to thank my supervisors also for your efforts in creating the best research conditions and learning opportunities for me. I would like to express my special thanks to Prof. CABASSUD. You've gave me a lot of helps in the study of the chemical reactor and also the paper writing.

Many thanks to my colleagues in DISCO team in LAAS-CNRS! They are a group of active and lovely scholars. Activities with them leave me a great amount of good memories. I also would like to thank all my friends in Toulouse, and Paul Sabatier University, LAAS-CNRS, EDSYS and their kind staffs. The pink city, the beautiful campus, the advanced laboratory and the kind people I met here constitute my second hometown outside China, which I'll remember for a life-time.

I would like to thank all the teachers and students I met in the College of Electrical Engineering and all my colleagues in the Engineering Training Center of Guizhou University for their tremendous helps during my Ph.D. study. Thank you for your enlightenment and sincere friendships, which made every minute of my time at Guizhou University a happy one. I would like to thank the China Scholarship Council for providing me with such a rare opportunity and funding to study abroad. In particular, I would like to specially thank my family, my beloved, for the unconditional supports you gave me during this periods, such that I can continuously move on without any worries. Every point of my progress and achievement contains your efforts and dedications.

Finally, I would like to express my sincere gratitude to the experts who took time out of their busy schedules to review my thesis. Thank you in advance for your kind guidance and valuable comments.

Résumé

Avec le développement de la science et de la technologie, le processus d'industrialisation continue de s'accélérer. La demande de sécurité des systèmes géants modernes augmente également très rapidement. En tant qu'axes de recherche clés pour améliorer la fiabilité et la sécurité des systèmes dynamiques, le diagnostic des fautes (FD) et les méthodes de la commande tolérante aux fautes (FTC) ont reçu de plus en plus d'attention. Bien que des résultats très probants ont été obtenus dans ces directions au cours des dernières décennies, la théorie du diagnostic des fautes et de la commande tolérante aux fautes semblent encore insuffisants face aux problèmes rencontrés lors de la commande des systèmes industriels complexes non linéaires de grande taille. Par conséquent, les études concernant le diagnostic des défauts et les théories de FTC doivent continuer à se developer pour garantir la sécurité et la stabilité des systems industriels.

Dans cette thèse, nous avons fait quelques extensions à la méthode de FTC basée sur l'approche des modèles multiples et nous avons proposé plusieurs algorithmes de diagnostic de fautes et de FTC basés sur des stratégies de correspondance de modèles. Ceci dans le but de concevoir des stratégies FTC pour des systèmes non linéaires complexes en utilisant des idées et des logiques simples. Plus précisément, l'approche multi-modèles est d'abord utilisée pour représenter le système complexe par un ensemble de modèles simples. L'approche classique des modèles multiples est ensuite étendue en augmentant ses dimensions pour créer un système qui peut s'adapter à différentes situations de défaillance. On obtient ainsi un ensemble de modèles multidimensionnels qui peuvent être adaptés au système réel dans des états normaux ou en cas de défaillance. La banque de contrôleurs multidimensionnelle correspondante est conçue en fonction des paramètres des modèles locaux. Comme les modèles locaux sont généralement linéaires, leurs contrôleurs peuvent être conçus facilement.

Lorsque l'ensemble de modèles multiples multidimensionnels est construit, deux stratégies de commande tolérance aux fautes sont proposées. La sortie du système est comparée à l'ensemble de modèles pour déterminer l'intervalle dans lequel se trouve le système, puis les contrôleurs, correspondants aux sous-modèles du système actuel, peuvent être sélectionnés pour effectuer le calcul de la commande. Pour la partie planification de la banque de contrôleurs, la stratégie classique de commutation ou de mélange peut être utilisée. En cas d'utilisation de la stratégie de mélange, la somme pondérée des sorties des multicontrôleurs représente la sortie de la banque de contrôleurs. Les

valeurs de pondération ont également un espace de recherche relativement large. Elles peuvent être pondérées linéairement, non linéairement ou sélectivement. Une telle sortie intégrée peut également être réalisée en deux dimensions, par exemple, au sein d'un ensemble de contrôleurs et entre des ensembles de contrôleurs tolérants aux fautes.

Inspiré par le concept de modèle adaptatif, une approche multi-modèles à deux couches est utilisée comme base pour développer la stratégie FTC. Les paramètres des modèles sélectionnés dans l'ensemble de modèles multiples multidimensionnels qui représentent les paramètres des modèles intégrés dans l'ensemble de modèles multidimensionnels multiples qui représentent le système réel sont utilisés pour initier les modèles adaptatifs afin de se rapprocher du système réel avec des paramètres inconnus. le système réel est utilisé pour lancer les modèles adaptatifs pour se rapprocher du système réel avec des paramètres inconnus. De cette manière, on peut atteindre lobectif du contrôle du système en identifiant ses paramètres. Un module de diagnostic de défauts permet la surveillance du système en temps réel et détermine son domaine de fonctionnement dans l'ensemble de modèles multiples à deux couches est conçu.

Lorsqu'un changement important est détecté, le bloc du diagnostic ndique un défaut. L'information sur le défaut est transmise au module de la commande tolérante aux fautes, qui lance un processus d'adaptation pour faire correspondre le système réel aux paramètres des nouveaux modèles. Dans cette situation, un contrôleur supplémentaire est défini pour corriger et atteindre lobjectif du contrôle.

Plusieurs simulations démontrent l'efficacité de la stratégie FTC d'adaptation de modèle proposée pour différents systèmes.

Mots clés: diagnostic de défauts, commande tolérante aux fautes, correspondance de modèles multiples, contrôle adaptatif

Abstract

With the development of science and technology, the industrialization process continues to speed up. The demand for the safety of modern giant systems grows very fast, too. As key research directions to improve the reliability and safety of dynamic systems, fault diagnosis and fault tolerant control (FTC) methods have received more and more attention. Though very rich results have been achieved in these directions during the past decades, fault diagnosis and fault-tolerant control theory still seem to be weak when facing high nonlinear complex industrial systems that iterate even faster. Otherwise, the most advanced creations of science and technology like space shuttles, and civil air-crafts, would not encounter disasters like explosions or crashes. Therefore, fault diagnosis and FTC theories must keep pace with the fast-changing world to ensure safety and stability.

In this thesis, we did some extensions to the multiple model approach based fault tolerant control method and proposed several fault diagnosis and FTC algorithms based on model matching strategies. This is under the consideration of designing FTC strategies for complex nonlinear systems using simple ideas and logic. Specifically, the multiple model approach is first used to represent the complex system by a set of simple models. The classical multiple model approach is then extended by increasing its dimensions to create a system that can adapt to different faulty conditions. This results in a multi-dimensional multiple model set that can be adapted to the real system in normal states or under faults. The corresponding multi-dimensional controller bank is designed according to the parameters of the local models. Since the local models are generally set as linear ones, their controllers can be designed easily.

When the multi-dimensional multiple model set is constructed, two model matching fault tolerant strategies are proposed. For the traditional system, its output is compared with the model set to determine the interval in which the system is located, and then the controllers, corresponding to the sub-models which are matched to the current system, can be selected to conduct the control calculation. For the controller bank scheduling part, the classical switching or mixing strategy can be used. When using the mixing strategy, the weighted sum of the multi-controller outputs represents the output of the controller bank. The weighting values also have a relatively large research space. They can be linearly weighted, non-linearly weighted, or selectively weighted. Such an integrated output can also be performed in two dimensions, e.g., within one controller set and between fault tolerant controller sets.

Inspired by the concept of adaptive model, a two-layer multiple model structure is used as the basic framework to conduct the FTC strategy. In the actual operation, the pre-defined local models set is like a source pool. Parameters of the interval vertex models selected from the multi-dimensional multiple model set that encloses the actual system are used to initiate the adaptive models to approximate the actual system with unknown parameters. In this way, it achieves the purpose of controlling the unknown system while identifying it. A fault diagnosis module monitors the actual system in real time and determines its operating interval within the two-layer multiple model set. When a big change is detected, it indicates a fault. The fault information is transmitted to the fault tolerant module, which initiates an adaptation process to match the actual system according to the new vertex models parameter. Here, an extra controller is set to the reference model in this process to achieve the control goal by following the original reference while the adaptation process approximating the actual system.

Several simulations demonstrate the effectiveness of the proposed model matching FTC strategy for different systems and are worthy of promotions and further study.

Key words: fault diagnosis, fault tolerant control, multiple model matching, adaptive control

List of Figures

2.1 Fault classification with respect to location 14
2.2 Fault classification with respect to time [121] 15
2.3 Basic models of faults: (a) additive fault; (b) multiplicative fault [4] . . 15
2.4 Fault diagnosis technology based on analytical model 16
2.5 Structure of signal based fault diagnosis method 20
2.6 Structure of data-driven based fault diagnosis 21
2.7 Structure of passive fault tolerant control[59] 23
2.8 Structure of active fault tolerant control[59] 24

3.1 Global controller structure of multiple model method [115] 30
3.2 Local controller structure of multiple model method 31
3.3 FTC strategy using two-layer multiple model structure [48] 42
3.4 Two-layer multiple model structure based multiple adaptive model matching FTC [48] 44

4.1 Details of the heat exchanger/reactor: (a) Process channel; (b) utility channel; (c) the heat exchanger/reactor after assembly [9] 47
4.2 Block modeling description, showing (a) utility plate, (b) process plate, and (c) plate wall 49
4.3 Description of units dividing 50
4.4 Internal description of one computing unit and convective heat exchange 50
4.5 Representation of a cell k of process plate 51
4.6 Representation of a cell k of utility plate 53
4.7 (a) Representation of a cell k of plate wall with process plate in the left and utility plate in the right; (b) Representation of a cell k of plate wall with process plate in the right and utility plate in the left 54
4.8 The matched UA as a function of $\dot{M}_p$ and $\dot{M}_u$ (hexagonal stars are computed from experimental data) 56

4.9 Parity plot of UA calculated from experimental data against those given by Equation (21) using the searched values of α, β, and R_f 57
4.10 Localization of five thermocouples in the first process plate [105] 62
4.11 Simulation results of the process fluid temperature along the process channel for different utility flow rates, with $\dot{M}_p = 10kg \cdot h^{-1}$ and $T_{p-in} = 77^{\circ}C$ 62
4.12 Simulation results of the process fluid temperature along the channel for different process flow rates, with $\dot{M}_u = 152kg \cdot h^{-1}$ and $T_{u-in} = 15.6^{\circ}C$. 63
4.13 Comparison of inner temperature distribution of Experiment 5 with $\dot{M}_p = 10kg \cdot h^{-1}$ and $T_{p-in} = 77^{\circ}C$ 64
4.14 Comparison of inner temperature distribution of Experiment 8 with $\dot{M}_u = 152kg \cdot h^{-1}$ and $T_{u-in} = 15.6^{\circ}C$ 65
4.15 Simulated temperature profiles for experiment 1 (reaction was introduced at $150s$) 67

5.1 The interval inputs and outputs from virtual experiments (The color indicates the IO pair). 72
5.2 Verification of the first layer model bank using inputs of integral range. 73
5.3 The accuracies of multiple model bank with different total number of local models. 74
5.4 Two-layer multiple models. 74
5.5 Performances of controller banks under the same reference Tp-ref after tuning. 78
5.6 FDI process using interval unscented Kalman filters 81
5.7 The simulation considering faulty parameter drops to 65% of its nominal value 82
5.8 The simulation considering faulty parameter drops to 45% of its nominal value 83
5.9 The simulation considering faulty parameter drops to 18% of its nominal value 83
5.10 The simulation of $45\%h$ fault case considering measurement noise 85
5.11 The simulation of interval residuals of T_{uin} fault 86
5.12 FTC simulation of T_{uin} fault 86

6.1 Model reference adaptive control 93
6.2 Introduction of MPC for reference model 94
6.3 Strategy of fault tolerant control using multiple adaptive models 96

6.4 Strategy of fault tolerant control using multiple adaptive models 98
6.5 Simulation result of single adaptive models under normal condition . . . 99
6.6 Simulation result of multiple adaptive models under normal condition . 100
6.7 Comparison of output error between single and multiple adaptive models 100
6.8 Fault tolerant control simulation of multiple adaptive models (plant fault is introduced at $t = 124s$) 102
6.9 Error curves of the FTC Simulation 103
6.10 Multiple adaptive models approaching to the parameter unknown system in initialization and faulty condition 103

List of Tables

4.1 Geometrical properties of the heat-exchanger/reactor [105] 48
4.2 Experimental conditions for simulating the heat exchange experiments [105] 61
4.3 Comparisons of experiment and simulation data with reaction 65

5.1 Key information about the simulation 82

List of abbreviations

FTC	Fault tolerant control
FDI	Fault detection and isolation
FDD	Fault detection and diagnosis
IFAC	International Federation of Automatic Control
MRAC	Model reference adaptive control
LGC	Laboratoire de GénieChimique à Toulouse
HEX/Reactor	Heat exchanger/reactor
UKF	Unscented Kalman Filter
QTA	Qualitative trend analysis
SGD	Signed directed graphs
PCA	Principal component analysis
PLS	Partially least squares
ICA	Independent component analysis
SVM	Support vector machine
FL	Fuzzy logic
PFTC	Passive fault tolerant control
AFTC	Active fault tolerant control
PIM	Pseudo-Inverse Method
LMI	Linear matrix inequality
PDC	Parallel distributed compensation controller
HIP	Hot isostatic pressing
DAE	ifferential and algebraic equations
ODE	Ordinary differential equations
AE	Algebraic equations
MPC	Model predictive control
EKF	Extended Kalman filter
LTI	Linear time invariant

Contents

1 Introduction **1**

1.1 Motivations of this thesis 2

1.2 Basic descriptions of the current research 3

1.3 Main contributions 6

1.4 Thesis organization 7

2 Fault Diagnosis and Fault Tolerant Control Techniques **11**

2.1 Basic concepts 12

2.1.1 Basic terminologies and definitions 12

2.1.2 Fault classification 13

2.2 Analytical model based fault diagnosis 16

2.2.1 State estimation method 17

2.2.2 Parameter estimation method 18

2.2.3 Parity space method 19

2.3 Signal based fault diagnosis 20

2.4 data-driven fault diagnosis 21

2.5 Fault tolerant control methods 22

2.5.1 Passive fault tolerant control 23

2.5.2 Active fault tolerant control 23

2.6 Summary 25

3 Multi-dimension Multiple Model Structure Based Fault Tolerant Strategy **27**

3.1 Multiple Model Approach 28

3.1.1 The decomposition and synthesis problem of multiple model approach 28

3.1.2 The construction problem of multiple model approach 31

3.1.3 The stability problem of multiple model approach 33

3.2 The multiple model approach based fault tolerant control 35
3.2.1 The multi-dimensional multiple model structure concerning faults 35
3.2.2 Control problem under multi-dimensional multiple model structure 36
3.2.3 Basic concepts and FTC ideas 39
3.3 The FTC method based on multi-dimensional multiple model structure and model matching strategy 41
3.3.1 FTC strategy through direct multiple model matching 41
3.3.2 FTC strategy through multiple adaptive model matching 43
3.4 Summary 44

4 Development of the Nominal Model of the Heat-exchanger/Reactor 45
4.1 Background 46
4.2 Physical structure of the reactor 47
4.3 Modeling 48
4.3.1 General Modeling of the Reactor 48
4.3.2 Modeling of the Process Plate 50
4.3.3 Modeling of the Utility Plate and Plate Wall 52
4.3.4 Calculation of Heat Transfer Coefficient 55
4.3.5 Reaction Modeling 57
4.3.6 Calculating the Model in Matlab/Simulink 59
4.4 Simulation of the Model 60
4.4.1 Initial States of the Simulations 60
4.4.2 Simulation Results of Heat Exchange Procedure 60
4.5 Validation 63
4.5.1 Validation of Heat Exchange Procedure 64
4.5.2 Simulation Results of Heat Exchange with Reaction 65
4.6 Summary 67

5 FTC Strategy through Direct Multiple Model Matching and Its Application to the HEX/Reactor 69
5.1 Two-layer multiple model bank construction 70
5.1.1 Mathematical model of the HEX/Reactor 70
5.1.2 Construction of the first layer multiple model 71
5.1.3 Construction of the second layer model bank 73
5.2 Two-layer controller bank design 75
5.2.1 Controller bank design 75

5.2.2 Tuning of the second layer controller banks 78
5.3 Fault detection and isolation section 79
5.3.1 The Unscented Kalman Filter 79
5.3.2 UKF based fault detection and isolation 80
5.4 FTC simulation and analysis of the HEX/Reactor 81
5.4.1 FTC simulation for heat exchange fault 82
5.4.2 FTC simulation for the utility input temperature fault 84
5.5 Summary 87

6 FTC Strategy through Multiple Adaptive Model Matching 89
6.1 The concept of multiple adaptive models 90
6.1.1 Adaptive control problem and identification model 90
6.1.2 Multiple adaptive model 92
6.1.3 Controller Design for Reference Model 93
6.2 Multiple adaptive model based FTC stategy 94
6.3 Simulation results 97
6.3.1 System parameters and initial setting 97
6.3.2 Simulations of multiple adaptive model 98
6.3.3 FTC simulation under multiple adaptive model matching strategy 99
6.4 Summary 104

7 Conclusions and Future Works 105
7.1 Conclusions 106
7.2 Future works 107

Chapter 1

Introduction

Modern technologies have achieved a very high level in the domain of automatic control, which brings us with the comfortable life and high efficiency industries. However, safety is one of the fundamental aspect in our daily life. Great amount of efforts should be put on to the researches and measurements for ensuring safety.

1.1 Motivations of this thesis

As is known to all, human beings have experienced 3 main industrial revolutions. The first one is mechanization which occurred in the 19^{th} century. For the second one that took place in the early 20^{th} century, we knew how to generate and use electricity. After the third industrial revolution in the late 20^{th} century, we entered the digital era. Now, our world is in the period of the ongoing fourth industrial revolution (or Industry 4.0). Through out all the history of the development of science and technology, one thing in common is that the newly invented systems are getting more and more complex. For example, transportation vehicles changed from steamers to high speed trains, from double wings to space shuttles, etc. Two hundred years ago, goods were produced through small workshops. Now we have super giant factories which are highly automated like in Tesla.

As human beings enjoying the comforts and conveniences that the development of science and technology brings to us, numerous losses of lives and properties in serious accidents, for instance, the failures of the space shuttle missions of the Challenger and Columbia, the nuclear plant explosion in Chernobyl, the recent two crashes of Boeing 737 Max, and the newly accident of auto-drive cars, etc., keep reminding us just how important the securities of modern systems are! It is claimed that petrochemical industry of the United States suffers from losses of 20 billion dollar every year due to poor management in abnormal situations [57]. One extra example, which can lead to a reduction of reactor power output by as much as 3% in the U.S., is the sensors drift of feed water flow in steam generator [43]. It's reasonable that we chase for a better life by developing science and technologies. However, safety is one of the basic issues that should be assigned a lot of works to account for. Cause no one wants to work in an in-secured environment nor entertain while facing the safety risk. Security demand is getting stronger and stronger.

The discipline of automation plays a key role in this new revolution as it is the base of many popular technologies and new trends like artificial intelligence, internet of things and smart manufacture, etc. Accompany with the quick development of the highly automatic systems, their safety issues are becoming more and more significant. Researches in fault detection and isolation (FDI), fault detection and diagnosis (FDD), fault tolerant control (FTC) are focusing on the safety direction. These studies maintain the safety issues in two levels. For the first, FDI and FDD concern about the supervision of the system in real-time. They will use model-based or data driven approaches to constantly watching the system and give out the diagnosis result when a fault occurs.

For the second, FTC aims at maintaining the system performance in an acceptable level under the faulty situation using the information given by the previous step when it is needed. In this way, we got the basic strategy to handle the security problems of the modern systems.

However, due to the complexity of modern nonlinear systems, there is not yet an universal method for the FTC design which can meet the requirements of all the situations. Researches on the FTC strategy for nonlinear systems are still demanding tasks.

1.2 Basic descriptions of the current research

Fault diagnosis focuses on how to detect a fault's occurrence in a system, determine its location, type, and calculate the size. The direction of fault diagnosis has received a lot of attentions in the past decades and has achieved fruitful results in the field of linear systems. According to the definition of International Federation of Automatic Control (IFAC) Technical Committee on Process Safety, a fault is "an impermissible deviation of at least one characteristic or parameter of a system from acceptable/normal/standard conditions". According to an international authority on fault diagnosis, Professor P.M. Frank [35], system fault diagnosis methods can be classified as: signal processing-based methods, model redundancy-based methods, and data-driven methods, as well as a synthesis applications [132].

Analytical redundancy based fault diagnosis includes state observer methods, parameter estimation methods, etc. Using the mathematical model of the target system and measurable information [132], such as the current and voltage in the circuit, the corresponding observers can be designed, and the residuals are constructed from the difference between the actual output of the system and the output of the observers. After that, fault detection and diagnosis are achieved by processing, analyzing, and evaluating the residuals. That is the general design steps of the state observer-based fault diagnosis [34]. If an accurate mathematical model of the system is available, the observer-based fault detection and diagnosis method is very effective for fault diagnosis. The observer-based fault detection and diagnosis methods for linear systems has a good theoretical foundation, and its researches have been very mature [111] [109] [110]. These researches focuses on the establishment of mathematical models, the improvements of sensitivity to early faults and the robustness to modeling errors, disturbances and other unknown inputs. For nonlinear systems, most of the observers have been

designed using methods that linearize in a small range near the operating point. Longberg observer, sliding mode observer, high gain observer and adaptive observer are the most commonly used observers. The fault diagnosis method based on parameter estimation [68] detects and diagnoses faults based on the system parameters and the variation of the process coefficients of the response. The method requires the controlled process to be fully excited and find out the relations between the system parameters and the process parameters. It therefore has good fault isolation performance.

Because of the supports from rich theoretical knowledge, the analytical model-based fault diagnosis method has excellent monitoring capability. However, it is sometimes very difficult to obtain models of complex systems with strong nonlinearity, strong coupling, time-varying and frequent changes in production conditions. Thus it has some limitations in fault diagnosis of complex nonlinear systems. Signal processing-based diagnosis methods [21][118] use signal models to extract feature values such as variance, amplitude, and spectral components by directly analyzing the measurable signal for the purpose of diagnosing the type and location of faults. Signal-based diagnosis methods usually include PARK transform, Fourier transform, wavelet transform, spectrum analysis, and information calibration [23]. Signal-based diagnosis meets the needs of complex systems and has good robustness. At the same time, its diagnosis is fast and sensitive, and it can be diagnosed online in real time, thus it is widely used. However, this method has problems such as insufficient diagnosis of early faults, weak fault separation identification ability, and difficulty in selecting the correct fault feature discrimination parameters due to its non-analytic nature. Therefore, it cannot be directly used for fault location in most cases. Data-driven fault diagnosis of complex systems has good adaptability to nonlinear systems [39]. But the industrial data has the feature that is has more normal operation data and less fault operation data. This makes the diagnosis system has insufficient data.

"Fault tolerance" is originally a concept in computer system. fault tolerant control refers to the control that can maintain the system performance or moderate degradation of performance at an "acceptable" level after a fault's occurrence. Because of this, fault tolerant control has received increasing attentions [73][119]. The idea of fault tolerance first appeared in 1971, marked by the concept of integral control proposed by Niederlinski et al [80] [131]. According to the usage of real-time fault diagnosis information of the system, fault tolerant control is divided into two categories, passive fault tolerant control and active fault tolerant control [69].

Passive fault tolerant control method has some similarities with robust control [122]. It is often divided into reliable stabilization, joint stabilization and integral control.

Reliable stabilization targets at controller faults. It uses multiple fault compensators to stabilize the same controlled object in parallel. In recent years, its related results are also more abundant [90]. Associative stabilization is essentially the design of a controller to stabilize multiple models of a dynamic system. Integral control is a fault tolerant control mainly for sensors and actuators. When the actuator and sensor of the controlled system fail at the same time, designing a fault tolerant controller to make the system stable. This means the closed-loop system has integrity. The integral control design problem is also referred to the controller design problem for simultaneous stabilization. There are two mainly ways for the design of integral controller: state feedback based method and parameter space based method.

Passive fault tolerant control is similar to robust control, which is effective only for a specific range of faults and is relatively conservative. Because it doesn't requires FDD section nor control law reconfiguration [59], the passive fault tolerant control is relatively easier to design and implement. In contrast, there are active fault tolerant control techniques. Active fault tolerant control was first proposed in the 1980s. The general idea is to combine with fault diagnosis technology and redesign the controller on-line according to the real-time fault information of the system in order to reduce the impact of the fault. The fault information is provided by the fault diagnosis unit and the controller redesign generally includes the following techniques: control parameters resetting, control law adjustment, and control reconfiguration. Active fault tolerant control is the most important and the most popular area of fault tolerant control technology. The premise of active fault tolerant control is fault diagnosis technology, and the demand for active fault tolerant control greatly stimulates the development of fault diagnosis technology also, which in turn provides theoretical reserve for the development of active fault tolerant control with the fruitful results of fault diagnosis technology.

Among these active FTC approaches, studies on multiple-model based reconfigurable control have drawn increasing attentions [128]. The idea of multiple model approach was originally proposed in [71] and systematically described in [76]. As the development of computing devices, parallel calculation of multiple models is no longer a problem to hardware, which intensively boosts the growth of multiple model approach. It is not only used for controller design, see [27][75], but is also applied in the domain of system reliability like fault diagnosis and fault tolerant control, as in [15][72]. Multiple model approaches deal with fault diagnosis problems in a way to avoid the complicated process of observer and controller design of the real system. However, complexities still exist in integrated controller design for sub-models, especially when the considering

system is complex and highly nonlinear.

1.3 Main contributions

The main work of the thesis lies in the researches on fault diagnosis and fault-tolerant control methods. The proposed strategies are then applied to the fault problems of heat exchanger/reactor (HEX/Reactor), and also the structural fault of power electronics systems. One effort the thesis made is the nominal model development of the target heat exchanger/reactor. The heat exchanger/reactor is then studied on both its heat exchange performances and the features when a typical exothermic chemical reaction is considered. Based on the idea of classical multiple model approach, the thesis proposes a multi-dimensional multiple model bank structure considering both nonlinear system representation and fault scenarios. Start from this structure, the thesis researches on fault diagnosis and fault-tolerant control by applying model matching strategy. It aims at carrying out the proposed strategies for nonlinear and complex systems. The main innovations of the thesis are the following items.

(1) FTC strategy through direct multiple model matching

The two-layer multiple model structure for the target system is constructed based on its priori knowledge. The construction process considers the nominal states, operating points, and faulty modes of the system. The fault range is determined after the standard that it covers the maximum faulty space or it is the maximum diagnosable/fault-tolerant range. As a result, the system states will fall into the intervals of the model banks at any time point. Therefore, the sub-model or sub-set of models within the multidimensional model bank structure that is closest to the current system can be activated and matches to the actual system with an appropriate weighting strategy. This matching behavior covers either normal or faulty scenarios. In order to achieve fault tolerance, the corresponding controller banks are synthesized in the same way to control the actual system.

The difference between this strategy and previous studies is that it considers both the multiple model representations of nonlinear systems and multiple model representations of the system with different fault parameters. The strategy proposed in this thesis increases the dimension of multiple model banks and builds a library based on a priori knowledge from both operating points and fault parameters. This makes the matching process of the models to the real system to be more accurate and fast.

(2) FTC strategy through multiple adaptive model matching

Starting from the concept of adaptive model in the literature [46], this thesis proposed a multiple adaptive model matching FTC strategy by incorporating the related concepts of model reference adaptive control (MRAC). The basic implementation idea is to firstly construct a multi-dimensional multiple model bank based on a priori knowledge. Then it designs a fault detection module. The strategy determines the vertex models that encloses the current system in the parameter space by analyzing the actual system output and the model set output. An accurate matching of the actual system is achieved by initialize the adaptive models from the vertex models. At the same time, the strategy designs a controller for the reference model and uses the output of this controller as the reference input of the adaptive process. In this way, it indirectly makes the unknown parameter system to be approached while follows the most original reference input. When a fault occurs, it can be equivalent to a relatively large parameter change in the actual system. The fault diagnosis module gives a fault interval in which the fault-tolerant strategy restarts the above adaptive processes to complete the fault-tolerant control of the faulty system.

Compared with the previous studies on a single direction, the proposed strategy can quickly jump to a smaller space when the system has a fault. This is due to the joining of multi-dimensional multiple model structure. On the other hand, the adaptive process also ensures the precise approximation of the unknown faulty system. It thus obtains a more accurate control effect.

1.4 Thesis organization

This thesis is organized of 8 chapters. The first two chapters serve as introduction of the background techniques. The third chapter reviews the multiple model approach and then presents the main ideas of this thesis. The following 4 chapters give out the details and contributions of this study while the last one makes a conclusion of all the thesis.

Among them, Chapter 1 gives the problem statement, the motivations, outlines of the contributions and organizations of the thesis.

Chapter 2 focuses on the introduction of fault diagnosis and fault tolerant control techniques. This chapter talks about the architectures of the strategies and their classifications. Some well-known methods for FDD, FDI and FTC are also presented and discussed.

Chapter 3 gives a brief introduction about the multiple model method. It gives

the steps and philosophy of using this famous engineering approach and discusses also about how a multiple model structure is obtained. Applications in different occasions are described in short. This chapter also gives out the main ideas of the thesis on how to carrying out FTC with the proposed strategies.

Chapter 4 introduces the modelling process of an intensified heat-exchanger/reactor. This reactor is designed by our collaborate laboratory LGC (Laboratoire de Génie Chimique à Toulouse) and their partner enterprise. This HEX/Reactor combines a heat-exchanger and a plug-flow reactor in only one unit, which makes it not only meets the demand of miniaturization and low cost of the chemical plant, but also has better heat and mass transfer ability. Along with considered highly exothermic reactions, it becomes a very complex nonlinear dynamic system. Since a part of the motivation of this thesis is to design an FTC strategy for this HEX reactor, this chapter described the detailed process for obtaining a nominal numerical model of it. Simulation results of the final model has been compared with the records of the experiments to check its modelling accuracy.

Chapter 5 discusses the process of multiple model creation by deconstructing the nominal model of the HEX/Reactor. Model bank containing simple linear local models is then achieved by system identification approaches and used to help the corresponding controller bank design. A two-layer multiple model structure is then constructed by repeating the system identification process under the consideration of different faulty situations. Corresponding two-layer multiple controller banks are created using the information of the models. This chapter also presents the precision of the model banks toward the corresponding real system and its relationship with the number of local model in a model bank. The controller tuning process is described in detail, too. This chapter then presents the direct model matching FTC scheme for the HEX/Reactor using two-layer multiple model structure. An FDI module is created first. In this step, unscented Kalman Filter (UKF), for its convenience and accuracy, is chosen to form the state estimation part of the module. After that, the fault interval can be determined. Thus corresponding controller banks of the model banks covering the current faulty system will be activated. Controller scheduler uses mixing strategy to form a new control signal to the process. In this way the system in faulty situation is compensated. Several simulation results are given in different situations, like noisy and noise-free cases, and also different fault scales.

Chapter 6 shows our efforts on introducing and combining the concept of multiple adaptive model with the currently proposed two-layer multiple model structure. The objective is to form a novel approach for FTC design. This combination makes the

new strategy having a feature of soft scheduling. The FDI module will supervise the real system and give out the index of interval when the fault occurs. By checking the interval in the two-layer multiple model banks, surrounding local models of the current system could be determined. These models are set to initiate the adaptation process. Several adaptive models will have the abilities to converge to the real system quickly. Under the reference given by the controller of the reference model of the adaptive models, the adaptation process will assure to meet the original control goal. Performances of the adaptation process using just one adaptive model and multiple adaptive models are also compared and discussed. A conclusion that multiple adaptive models act way better than the single case is then made. In general, this chapter presents new attempts for the FTC design using multiple model and adaptive control approach. It can be concluded that the proposed strategy is a promising attempt and has the potential ability to implement in industries.

Chapter 7 makes a summary of this thesis and points out some potential directions in this area. Future works are also mentioned and discussed in this chapter.

Chapter 2

Fault Diagnosis and Fault Tolerant Control Techniques

This chapter focuses on the introduction of fault diagnosis and fault tolerant control techniques. It talks about the architectures of the strategies and their classifications. Some well-known methods for FDD, FDI and FTC are also presented and discussed.

2.1 Basic concepts

With the development of science and technology, there is an increasing demand for reliability and safety of industrial systems. Therefore, early detection and identification of all types of potential failures is crucial. In order to achieve fault-tolerant control of systems and minimize their performance degradation or avoid more dangerous situations when encountering faults, researchers have proposed many approaches[38][97][129]. For example, in 2003, a very complete series of fault diagnosis literature consisting of three parts reviewed the methods in details [111][109] [110]. They classified fault diagnosis methods into three aspects: quantitative model analysis, qualitative analysis, and historical processes. Similarly, [132] also classified the existing fault diagnosis methods under the framework of quantitative model analysis and qualitative analysis, and introduced the basic ideas and typical applications of each method. In [38][39], fault diagnosis methods were classified into four major categories: analytical model-based methods, signal processing-based methods, data-driven methods, and hybrid methods. In [129][59][5], the authors present the classification and methods of fault-tolerant control. Unlike fault diagnosis techniques that have multiple classifications, fault-tolerant control is generally classified into two major categories: active fault tolerance and passive fault tolerance.

Regardless of the classification method, the main purpose of this research direction is to complete fault diagnosis and fault-tolerance control quickly when a fault occurs in order to prevent worse effects. In the following paragraphs, we first introduce some basic concepts, research methods and tools mentioned in the literature, and then present the current research states of fault diagnosis and fault-tolerant control for dynamic systems.

2.1.1 Basic terminologies and definitions

For the basic concepts and terminologies, most of them have been defined by the SAFE-PROCESS committee in IFAC[53].

Normal operation state: When the states, inputs and outputs of the system are all close to its nominal values, we say the system is in normal operation state. Generally, no faults occur in this situation.

Fault: At least one variable or parameter of the system has unacceptable deviation from the value in its usual or standard condition.

Failure: The system loses the ability to achieve its designed function permanently.

Error: The difference between the calculated or measured value of the output

variable and that of the true, specified or theoretically correct value.

Disturbance: The uncontrolled and unknown input that acts on the system.

Residual: It is a fault indicator which based on a deviation between measurements and model-equation-based calculations.

Qualitative model: Use of statistic and dynamic relations among system variables and parameters in order to describe a system's behaviour in qualitative terms.

Quantitative model: Use of statistic and dynamic relations among system variables and parameters in order to describe a system's behaviour in quantitative mathematical terms.

Fault detection: Determination of the faults present in a system and the time of detection.

Fault isolation: Determination of the kind, location and the detection time. It follows fault detection.

Fault identification: Determination of the size and time-variant behaviour of a fault. It follows fault isolation.

Fault diagnosis: Determination of the kind, size, location and detection time of a fault. It includes all the fault detection, isolation and identification sections.

The presented terminologies and definitions may be mentioned repeatedly in the following sections. Besides these terms, we do a classification of the fault in the next sub-section to carry out the work of fault diagnosis.

2.1.2 Fault classification

As is mentioned before, when one variable or parameter of the system deviates from its nominal value evidently, we think there's a fault. A fault could be in any part of the system due to the complexity of the system. Thus, there's different classifications of the faults according to their locations and behaviours.

Faults are classified into actuator fault, plant fault and sensor fault by their location of occurrence, as is shown in Figure 2.1.

Actuator fault: Actuator is defined as module that acts on the system by converting the control signal to acting signal. When the actuator has a fault, the input control signal will have difference to the actuator output. This deviation may harm the control strategy to the overall system and lead to a failure to the expected objective. Generally, actuator fault has 4 modes: floating, stuck, damage and saturation. It is

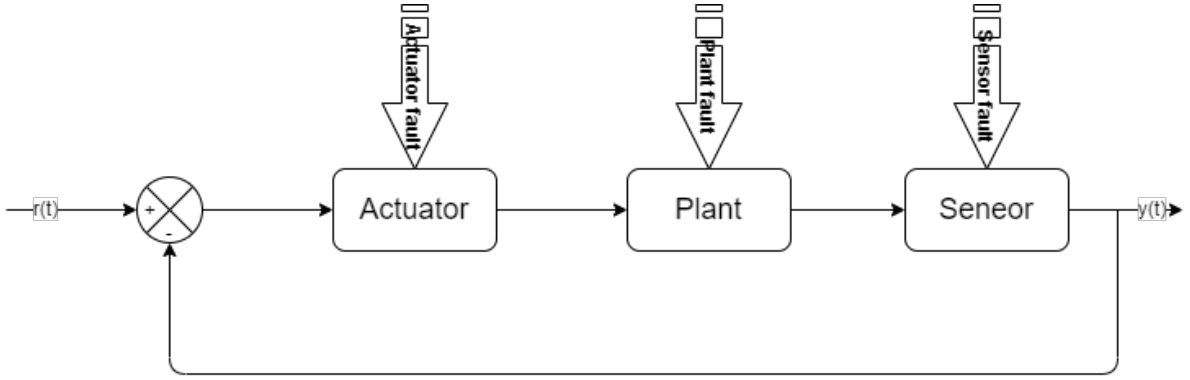

Figure 2.1: Fault classification with respect to location

expressed as follows:

$$u_{out} = \begin{cases} u & \textbf{normal state} \\ ku & \textbf{damage, } 0 < k < 1\text{, k is the damage percentage} \\ 0 & \textbf{floating} \\ u_a & \textbf{stuck, } u_a\text{is the stuck angle} \\ u_{omin} \text{ or } u_{omax} & \textbf{saturation} \end{cases} \tag{2.1}$$

where u_{out} is the actuator output. u is the actuator input. u_{omin} and u_{omax} are the minimum and maximum output of the actuator respectively.

Plant fault: This is the fault that affect the system itself. It concerns the performance deterioration of components due to the inner parameter change.

Sensor fault: Sensors are used to convert physical states into measurable signals that can be processed by a computer. They are the interface of the system and the external environment. Therefore, sensor fault is characterized by a discrepancy between the actual value of the physical variable and its measured output. A sensor fault will be added to the system output, which misrepresents the system state and output information. Sensor faults can be characterized by offsets, drifts, degraded performance (reduced accuracy), saturation and calibration errors [1].

In addition to classifying faults according to their locations of occurrence, faults can also be classified according to their manifestations over time. It may change suddenly, slowly, or intermittently. Therefore, faults can be classified as abrupt fault, incipient fault and intermittent fault, as shown in Figure 2.2, where t_f denotes the fault occurrence time [125].

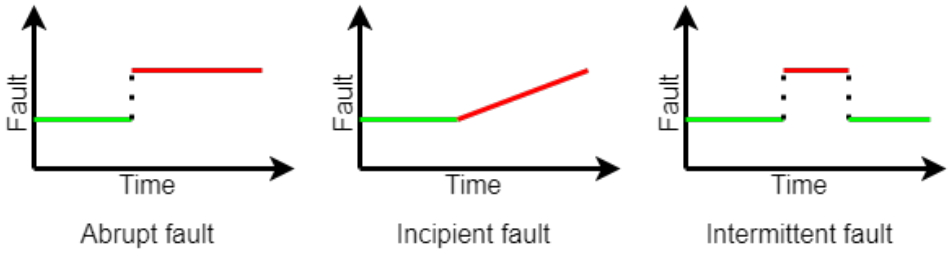

Figure 2.2: Fault classification with respect to time [121]

Abrupt fault: An abrupt fault is a fault that changes instantaneously, for example, a step change. The occurrence of such an abrupt fault may have a very serious impact on the system, but it is easy to detect.

Incipient fault: This is a slowly changing fault, a fault that accumulates as it develops over time. For example, the process of a valve being slowly blocked. Incipient faults can still cause degradation of system performance. Such faults are generally hard to detect unless they've accumulated to a certain level.

Intermittent fault: The fault appears only in some periods or certain operating conditions. It is not a permanent existence in the whole system.

From the angle of attribution, or considering about the model of fault, we have additive fault and multiplicative fault, see Figure 2.3. Additive faults influence a variable by the addition of the fault value, for instance, the sensor biased. On the other hand, multiplicative faults act by the product of another variable U with f, for example, a parameter change within the process [56].

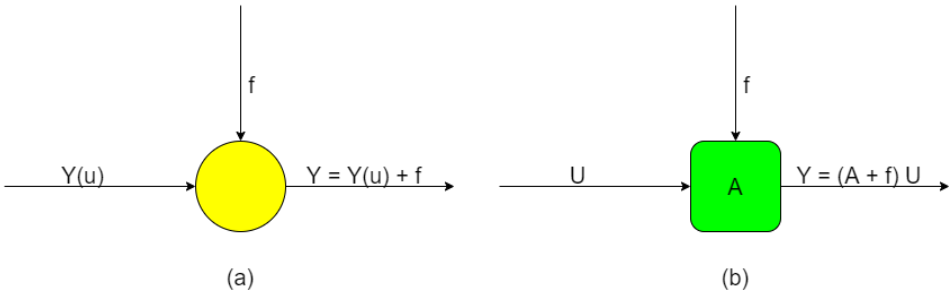

Figure 2.3: Basic models of faults: (a) additive fault; (b) multiplicative fault [4]

Besides that, some scholars classify the system fault as structural fault and parametric fault.

Structural fault: The fault which causes the topology change of the system. Its faulty parameter is defined as Boolean type.

Parametric fault: The fault which causes the performance degradation due to parameter changes. The faulty parameter is generally a continuous one.

The fault will degrade the system performance or even cause worse accident no mater which type it is. Therefore, it should be quickly detect the fault, isolate its location and identify its size. This is very meaningful to maintain the stability and security of the system.

2.2 Analytical model based fault diagnosis

Model-based fault diagnosis was proposed by Beard [14] in his PhD thesis in 1971, with the aim of replacing hardware redundancy with analytical redundancy. For this type of fault diagnosis technique, a mathematical model of the industrial process or system is essential, and the model can be obtained by using physical principles or system identification techniques. Analytical model-based fault diagnosis methods extract special features (e.g., parameters, state variables, or residuals) and compare the observed system characteristics with their nominal values by using a priori information in terms of mathematical models. The residual is constructed by comparing the actual measured values with their observed values of the system obtained according to the model. And then the occurrence of faults is detected by setting a fixed or variable envelope [96]. Afterwards, the residual is analyzed and evaluated to further determine the location and the magnitude of the fault.

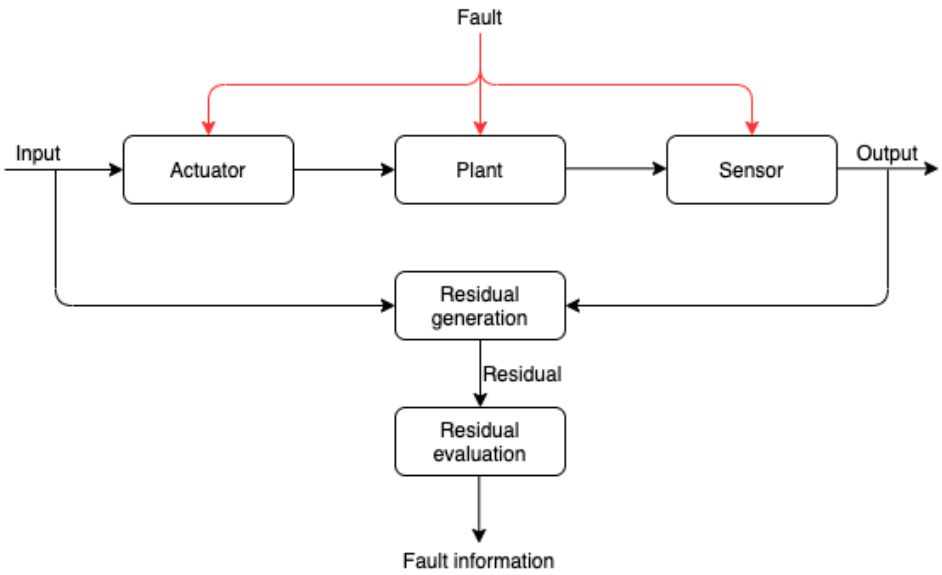

Figure 2.4: Fault diagnosis technology based on analytical model

Figure 2.4 gives the structure of fault diagnosis based on analytical model [36]. It is composed of two periods: residual generation and residual evaluation. This architecture was firstly proposed by Chow and Willsky in 1980 and is widely accepted by scholars [25]. Details are presented in the following paragraphs.

Residual generation: The purpose is using the measurable input and output signals of the system to generate a fault indication signal, residuals. When the system is operating under normal conditions and no faults occur, the residual should be zero or close to zero. However, when a fault occurs, the residual signal is no longer zero [112]. This means that the characteristics of the residual are independent of the input and output signals of the system [96]. The algorithm used to generate the residual is called the residual generator. Thus, residual generation is a process of extracting fault features from the system. Ideally, the residual signal carries only fault information. To ensure the reliability of fault diagnosis, the loss of fault information in the residual generation process should be as small as possible. Therefore, several residuals can be designed while each one is sensitive to specific fault occurring in different locations of the system. Afterwards, each residual is analyzed and once they exceed the threshold, we enter the fault isolation algorithm [96].

Residual evaluation: This phase aims at determining the generation of faults and extracting possible fault information from the generated residual signal. When the residual is clearly non-zero, the fault information can be extracted by a simple threshold test on the instantaneous or moving average value of the residual (geometric method). Or the residual can be evaluated by statistical methods such as generalized likelihood test or sequential probability ratio test.

There are many ways to generate residuals. According to the way of residual generation, analytical model based fault diagnosis techniques can be classified into the following three categories: state estimation method, parameter estimation method and parity space method [132]. The basic ideas of these methods are presented in the following sub-sections.

2.2.1 State estimation method

The main idea of the state estimation based fault diagnosis method is to construct observers or filters to estimate the internal states of the system. The observers use measurable input and output signals of the system to carry out the job. The residual is generated by comparing the real system output with the observer or filter output. Generally, a non-zero residual indicates the occurrence of a fault. However, it is worth

noting that when the system is disturbed by noises, the residual is also non-zero. Therefore, the ideal residual is sensitive only to the fault's occurrence and insensitive to the disturbances [125]. To prevent misjudgment from the non-fault signals such as disturbances, a threshold is usually set for the residual. Only when the threshold value is exceeded, the occurrence of a fault is determined. To further isolate and identify faults, a bank of state observers, each sensitive to only one type of fault and insensitive to others, can be set to handle the two tasks.

The construction of state observers is a hot research topic in fault diagnosis techniques all the time. The review literature [74][26][63] described the development of observer constructions for linear and nonlinear systems since the year 2000. Due to the diversity of observer design for nonlinear systems, the literature [74] divided the recent approaches on observer design for chemical process systems into six major categories, namely: Luenberger-based observers, Finite-dimensional system observer, Bayesian estimators, Disturbances and fault detection observers, Artificial intelligence based observers) and Hybrid observers. The literature [45] applied several typical nonlinear observers to a heat exchange reactor and compared the dynamic characteristics of their state estimations. The literature [68] creatively proposed a parameter space based observer that divides the operating range of system parameters into several intervals. It isolates and identifies faults by determining whether each interval contains information about the fault parameters. This method greatly reduces the time of fault isolation.

2.2.2 Parameter estimation method

The parameter estimation based fault diagnosis method is developed from the system identification techniques. Here a system fault is considered to be caused by a change in the system parameters. By using the input and output signals of the system, this method identifies the parameter information of the system online, and compares the estimated parameters with the nominal value. If the deviation is too large, it can be determined that a fault occurs in the system. This is a very straightforward fault diagnosis method, especially when there is a clear mapping relationship between the model parameters and the actual physical coefficients. Early review papers [54][55] provided a detailed description of this method. Recent developments and applications of this method can be found in the literature [3][130]. For the parameter estimation based fault diagnosis method, in some applications only one input and output signal is needed to estimate several parameters and thus to understand in detail the internal variables of the system [87]. In addition to this, the advantage of this method is that

the deviation values of the system parameters can be obtained directly, which is very useful for fault diagnosis.

The basic steps to implement this parameter estimation based fault diagnosis are as follows:

(1) Create the analytical model of the target system by using physical relations.

(2) Determine the mapping relationships of the system parameters to physical parameters.

(3) Identify and estimate parameters of the system on-line.

(4) Determine the nominal values of the physical parameters of the real system.

(5) Compare the estimated parameters with the nominal values. If the deviations exceed the threshold, a fault is believed to be appeared.

(6) Determine the location and size of the fault and its associated parameter change.

The parameter estimation based fault diagnosis method is very similar to the state estimation based one. It can directly reflect how the system parameter changes affect the overall system performance. So, the method has a high degree of flexibility and is more applicable to the detection, isolation and identification of multiple faults.

2.2.3 Parity space method

The main idea of this method is to determine the consistency between the analytic model and parity model of the system and thus generate the residual signal. The system parity model is obtained by transforming the system analytic model [125]. It rearranges the system analytic model so as to reflect the relationship between the static direct redundancies of the system output variables and the dynamic analytic redundancies of the input and output variables. Earlier literature [24] gave methods to obtain parity relations using the system analytical model. Recent studies on fault diagnosis methods based on parity space can be found in the literature [98][123]. The literature [123] extended the parity space approach from linear systems to nonlinear systems which are described by TS fuzzy models. The literature [98] performed diagnosis for actuator faults and sensor faults in satellite altitude control systems by combining the TS fuzzy model with the parity space method.

The parity space based fault diagnosis is closely related to the state estimation based fault diagnosis ,too. Although the design processes of the two approaches are different, the method can be structurally equivalent to the state estimation based method [125]. The method requires higher accuracy of the system model and is more suitable for the detection and isolation of additive faults.

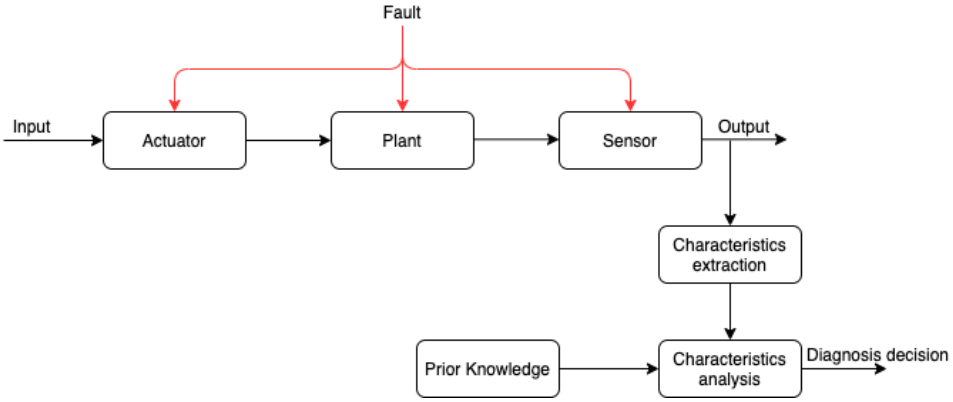

Figure 2.5: Structure of signal based fault diagnosis method

2.3 Signal based fault diagnosis

Signal processing based fault diagnosis method uses measured signals rather than explicit input-output models to perform fault diagnosis. Faults in the system are reflected in the measured signals. The method extracts the features of the measured signal and makes diagnostic decisions based on feature analysis and a priori knowledge of the fault-free system's characteristics. Signal based fault diagnosis has been widely used for real-time monitoring and diagnosis of induction motors, power converters, and mechanical components in systems. Figure 2.5 depicts a schematic diagram of signal processing based fault diagnosis.

Signal processing based fault diagnosis can be used in various industrial systems. The target signals used for characterization can be time-domain signals, such as mean, standard deviation, phase, slope and amplitude, or frequency-domain signals. Therefore, fault diagnosis techniques based on signal processing can be divided into Time-domain signal based methods, Frequency-domain signal based methods, and Time-frequency signal based methods. For example, in the literature [21], a fault diagnosis method for switched reluctance motor power converters was proposed by analyzing the variation of the root mean square current characteristics measured in the healthy state and in the single/dual transistor short-circuit or open-circuit cases. In the literature [118], the authors detected and separated the faults occurring in the bearing system based on statistical analysis and variation. They extracted the time-domain, frequency-domain and the mixed-domain features for each data set under different fault conditions.

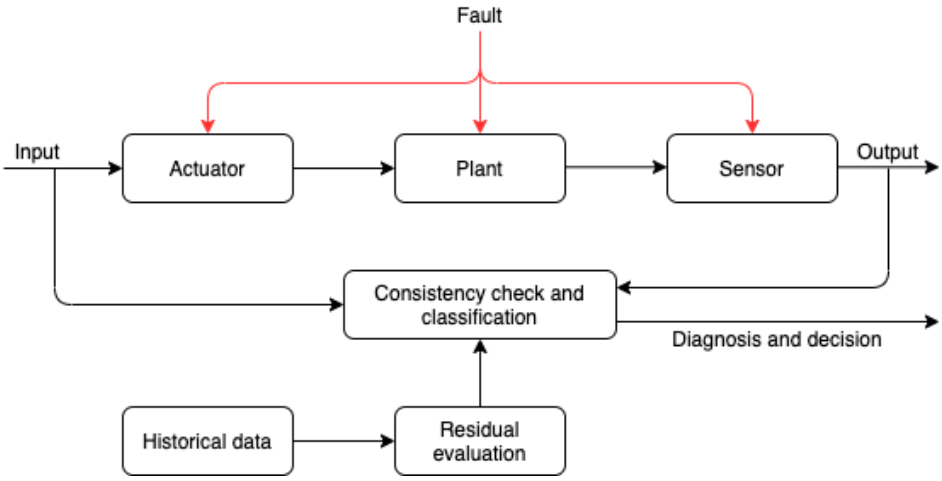

Figure 2.6: Structure of data-driven based fault diagnosis

2.4 data-driven fault diagnosis

Unlike the fault diagnosis techniques based on analytical models and those based on signal processing, data-driven fault diagnosis methods are built on the basis of obtaining a large amount of historical data. By applying various artificial intelligence techniques (symbolic intelligence or computational intelligence) to the historical data of industrial systems, the basic knowledge that can represent the interrelationships between system variables is extracted. Comparisons are then made between the measured signals of the system and the database. By checking the consistency between the two, fault diagnosis decisions are then made. It is worth noting that the analytical model based diagnostic approach, the signal processing based diagnostic approach, and the data-driven diagnostic algorithm must all utilize real-time data when performing online monitoring and fault diagnosis. However, only the data-driven diagnostic approach requires the use of a large amount of available historical data [39]. A schematic diagram of the data-driven fault diagnosis method is given in Figure 2.6.

Data-driven fault diagnosis can be divided into two categories: Qualitative data-driven fault diagnosis and Quantitative data-driven fault diagnosis

The commonly used qualitative data-driven methods are Expert system and Qualitative trend analysis (QTA). Expert system based fault diagnosis started in the 1980s [64]. It is based on a set of rules learned by human experts from past experiences to evaluate online monitoring data. Due to the advantages of easy development, transparent reasoning, the ability to do reasoning under uncertainties, and the ability to interpret the provided solutions, expert system based fault diagnosis methods are widely used in various fields, such as: energy systems [6], chemical industry [82], and so on. Qualita-

tive trend analysis based fault diagnosis method identifies and analyzes process trends from noisy and huge process data. It correlate the extracted trends with the fault trends in the database to determine the fault type and size. A comprehensive review of this method is presented in the literature [34]. Nowadays, QTA technique is widely used for fault diagnosis in complex industrial processes, especially in chemical production processes. Moreover, QTA can be integrated with other qualitative tools, such as the signed directed graphs (SDG) method, to achieve better results and compensate weaknesses. For example, an integrated SDG and QTA framework is proposed in the literature [37] for early fault diagnosis by combining the integrity of SDG and the high diagnostic resolution property of QTA.

The quantitative data-driven fault diagnosis is to formulate the solution of the diagnosis problem essentially as a pattern recognition problem. Quantitative information (or features) can be extracted using statistical or non-statistical methods. Therefore, the quantitative data-driven fault diagnosis can be approximately classified into two ways: fault diagnosis based on statistical analysis and fault diagnosis based on non-statistical analysis.

Under the framework of statistics, the quantitative data-driven fault diagnosis methods mainly use Principal component analysis (PCA), Partially least squares (PLS), Independent component analysis (ICA), statistical pattern classifiers, and the newly developed Support vector machine (SVM). All of these methods require a large amount of training data and use statistical analysis to capture the key features of the process. The most famous non-statistical analysis based fault diagnosis methods mainly use Neutral Network and Fuzzy logic (FL), where Neural Network is used to classify the extracted fault features and Fuzzy logic is a method to partition the feature space into fuzzy sets and use fuzzy rules for reasoning. Besides, the above methods can also be combined with each other to form a new hybrid class of fault diagnosis methods. Specific information can be found in the literature [39].

2.5 Fault tolerant control methods

The objective of fault-tolerant control is to design a control strategy that has the property of limiting or even eliminating the impact of faults on system performance. In the presence of less severe faults, a simple robust control can maintain the established performance of the system. This is a kind of passive fault-tolerant scheme. On the other hand, in the cases of severe faults, a fault detection and diagnosis strategy is

necessary to implement an active fault-tolerant strategy. In recent years, fault-tolerant control has been a hot research topic that is attractive to many scholars. Reviews of the literature [129][59][5] provided detailed descriptions of the development of fault-tolerant control methods and the commonly used ones. Therefore, the fault-tolerant control is usually classified into two categories: passive fault-tolerant control (PFTC) and active fault-tolerant control (AFTC). In this section, we briefly introduce these two types of fault-tolerant control methods.

2.5.1 Passive fault tolerant control

The PFTC approach does not require a fault diagnosis module or a controller reconfiguration strategy. Thus, the term "passive" indicates that the existing controller passively handles faults without requiring additional actions on the faults. As shown in Figure 2.7, PFTC is a control system which is designed by using system redundancy or robust controllers. It does not require any controller structure or parameter tuning to accommodate faults that occur in the system. According to the literature [131], PFTC techniques can be approximately classified into three types: reliable stabilization, integrity, and associative stabilization. Reliable stabilization focuses on controller faults. It uses multiple fault compensators to stabilize the same controlled object in parallel. The essence of the associative stabilization is to design a controller to stabilize multiple models of a dynamic system. It focuses on the faults that occur in the internal components of the controlled system. Integrity control is a fault-tolerant control mainly used for sensors and actuators. And there are state feedback based and parameter space based integrity controller designs.

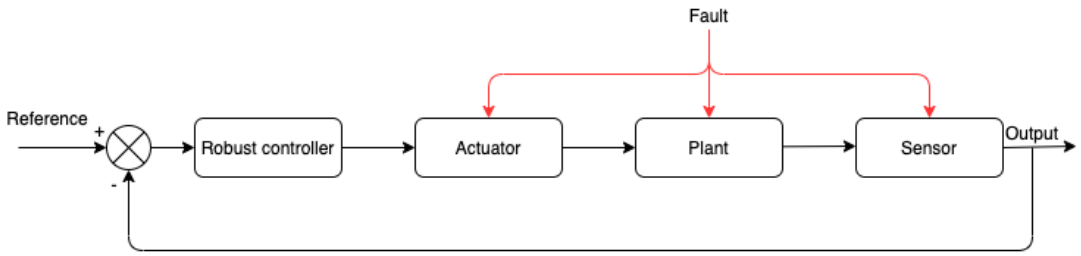

Figure 2.7: Structure of passive fault tolerant control[59]

2.5.2 Active fault tolerant control

AFTC first obtains real-time information about the fault through a fault diagnostic mechanism. It then re-configures the controller based on this information to respond

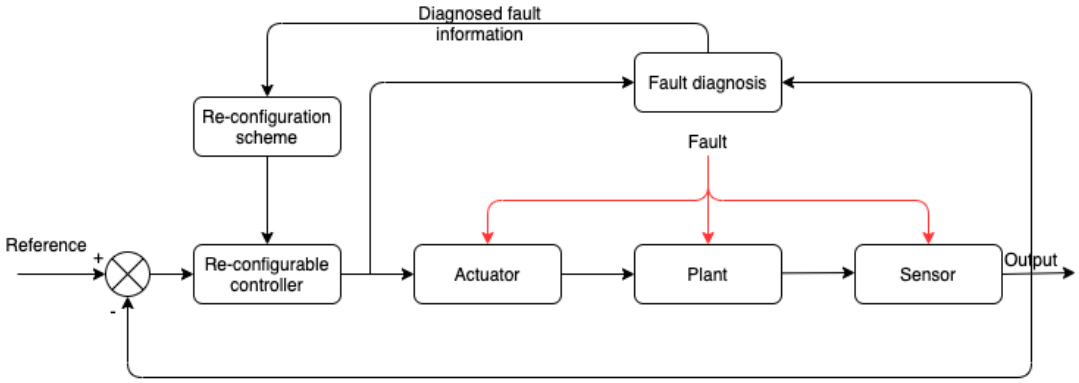

Figure 2.8: Structure of active fault tolerant control[59]

to the faults (including actuator faults, plant faults and sensor faults). The "active" indicates that the controller reconfiguration mechanism takes measures actively. It makes the whole system respond to the detected fault by adjusting the controller. As shown in Figure 2.8, AFTC typically consists of a fault diagnosis module, a re-configurable controller, and a controller reconfiguration mechanism. These three units must work in concert to accomplish successful FTC tasks. Based on this architecture, the design goals of an active fault-tolerant control system are: (1) Develop an effective FDD scheme that provides the accurate fault information in time, (2) Efficiently reconfigure the existing control scheme to achieve stable and acceptable performance of the closed-loop system, (3) Smoothly put the reconfigured controller into the system by minimizing potential switching transients [59]. Compared to PFTC, AFTC has broader implementations and can handle many types as well as more severe faults. Therefore, it draws more attentions to the researchers.

Commonly used AFTC strategies can be divided into two types: Controller reconfiguration and Controller reconstruction. The main idea of Reconfiguration is to achieve fault-tolerant control by adjusting the controller parameters online according to the severity of the fault and the available hardware redundancy. The controller parameters mentioned here are pre-set according to the possible faulty scenarios. In this case, when a fault is detected and diagnosed, it is only necessary to switch online to the appropriate controller parameters. This approach is fast, but also has significant limitations. In order to achieve better fault-tolerant control, all possible fault cases must be considered in advance and the corresponding controller parameters must be designed [73][131]. When the system cannot maintain its original performance, the entire control loop needs to be reconstructed. The main idea of controller reconstruction is to reconstruct the control law by using alternative input signals, output signals

or system component signals. When the actuator or sensor have faults, the controller reconstruction technique is often chosen to carry out FTC.

For linear systems, the commonly used AFTC methods are the Pseudo-Inverse Method (PIM) and the Eigen structure assignment method [85]. The pseudo-inverse method is to modify the feedback control law by minimizing a given criterion so that the dynamics of the faulty closed-loop system is approximately equal to the dynamics of the nominal closed-loop system [100]. The main idea of the eigen structure assignment method is to accurately assign the eigenvalues of the system matrix of the faulty closed-loop system such that the difference between its eigen vectors and those of the nominal closed-loop system is minimized [120].

For nonlinear systems, the commonly used AFTC methods are Model reference method, Multiple model control, Adaptive control, and Model predictive control [58]. The model reference method allows one to design a new control method so that the performance of the controlled faulty system is as close as possible to the performance of the reference model [100].Multiple model approach's main idea lies in decomposing the nonlinear system into several linearized regions around different operating points, and then it controls each linearized regions [48][49]. This approach will be described in detail in the following chapters. The adaptive control can automatically adjust the controller parameters according to the changes in the system and is therefore a very suitable basic control method to be combined with other strategies to handle AFTC design [113]. The model predictive control can also be used to construct AFTC strategy. It ensures that the faulty system is very close to the performance of the nominal model by online optimization and readjusting the control law in case of a fault [95].

2.6 Summary

This chapter provides a comprehensive description of fault diagnosis as well as fault-tolerant control approaches. First, the definitions related to fault diagnosis, such as fault and failure, are introduced. After that, the classification of faults is introduced in terms of its location, how they behave, and how they affect the system. When a fault appears in a system, our primary objective is to detect and get information about the fault as soon as possible. Therefore, the commonly used fault diagnosis methods are presented , such as: analytical model based methods, signal processing based methods, and data-driven methods. Finally, two types of fault-tolerant control methods (passive fault-tolerant control and active fault-tolerant control) are described.

Fault tolerant control ensures that the closed-loop system maintains its original or acceptable performance in the presence of faults. In contrast, with the help of the fault diagnosis module, active fault-tolerant control has a high degree of flexibility and is able to handle a wide range of faults. The following section will focus on the use of multiple model approach in active fault-tolerant control.

Chapter 3

Multi-dimension Multiple Model Structure Based Fault Tolerant Strategy

For real physical systems, it is essential to build accurate models in order to do characterizations in-depth or related design. In general, dynamic system modeling is divided into analytical and data-driven approaches. The analytical approach is based on the physical mechanism of the system and builds an analytical mathematical model. The data-driven modeling approach generally treats the system as a black box, and uses system identification or neural networks to obtain the numerical model. This process needs the input and output data of the targeting system.

3.1 Multiple Model Approach

Because of its ability to deal with complex systems with relatively simple logic, the multiple model approach has gained more and more attentions in engineering applications. Since its introduction by D. T. Magill in [71], it has been developed over a long period of time. In the book [76], main ideas of the approach are systematically described by several scholars. Generally, real industrial processes run between different operating points, which makes traditional modeling methods facing significant challenges. For this problem, the use of multiple model approach is the basis of most scholars' solutions [52]. One drawback of multiple model approach is the burden on the arithmetic power requirements brought by a large number of sub-models in parallel computation. However, with the rapid development of semiconductor and computer technologies, the computational ability of hardware has increased tremendously, making the drawback no longer be a problem in most applications. Currently, the multiple model approach has been widely used not only in controller design [75], but also in reliability areas such as fault diagnosis and fault-tolerant control [72]. The method avoids some nonlinear difficulties by its basic logic. However, the complexity still exists in the creation of the multiple model bank, in the determination of the parameters, and also in the overall controller design and the regulation of each sub-model pair.

3.1.1 The decomposition and synthesis problem of multiple model approach

The basic logic of the multiple model approach is to "divide and conquer" the target system. Where "divide" refers to the decomposition problem. Specifically, the target nonlinear system is decomposed into multiple sub-systems [115], and the operating space is divided into a limited number of sub-intervals. In this way one local model is determined for one sub-region. The decomposition of the operation space is usually the first step in initiating a multiple model approach and can be divided into two types: spatial decomposition based on prior knowledge [2] and spatial decomposition without prior knowledge [33].

The decomposition of the operation space is performed through the dynamic and static properties of the system when all or part of the system information is known. Decomposition methods based on a priori knowledge can be classified as linearized model sets based on operating points, velocity linearized model sets, sector nonlinear variations, and decomposition of the operating space from experimental data. Gener-

ally, they use mathematical models or experimental data containing priori knowledges. If there is no priori knowledge about the target system, taking full use of the I/O data becomes an effective way for the operation space decomposition. This is a data-driven method, which decomposes the operation space of a system while using input and output data to identify its parameters. The data-driven decomposition method requires little priori knowledge, and the mainstream methods here include orthogonal axis decomposition, oblique axis decomposition, and cluster decomposition [115].

Most of the methods described above are decomposition efforts based on open-loop performance metrics, and if carefully interrogated, we will find that the decomposition issues in the multiple model approach have a broader impact on both subsequent controller design and control performance. This leads to the issue of evaluating the decomposition of the operating space under closed-loop, such as closed-loop nonlinearity metrics and determining whether the controller meets the stability and control performance requirements. Literature [70] proposed to quantify the degree of nonlinearity using the minimum variance of lower bound ratio to determine whether a linear or nonlinear controller is required for nonlinear systems with different structures. Literature [99] proposed the concept of control-related nonlinearity degree and gave an optimal control structure based method to measure nonlinearity.

The decomposition problem is generally considered as a previous step to the synthesis problem. Most of the cases consider the closed-loop concept here only to find the variation of the nonlinear metric [29]. We know that for nonlinear systems, the introduction of feedback can greatly reduce the nonlinearity of the system [81], thus literature [115] proposed an operation space decomposition method based on the closed-loop performance of the controller design and the perspective of synthesis. It obtained the results relating to the dynamic characteristics of the system as well as the control input. This method solves the problem that the operation space decomposition may affect the control performance of the overall system in the synthesis process. It belongs to a decomposition method based on the closed-loop performance.

The synthesis problem of multiple model method is the problem of "handling". Once the decomposition is completed, the model set or controller set needs to be combined. Generally, there are two types of operations: switching and mixing.

Switching synthesis has distinct boundary for each sub-model, and the models are switched by scheduling variables. In this strategy, only one sub-model is selected to represent the target system at each moment. The selection of one or more scheduling variables has a criteria that the variables can completely characterize the behavior and the working conditions of the system [91]. It could be a state, an input, an output or

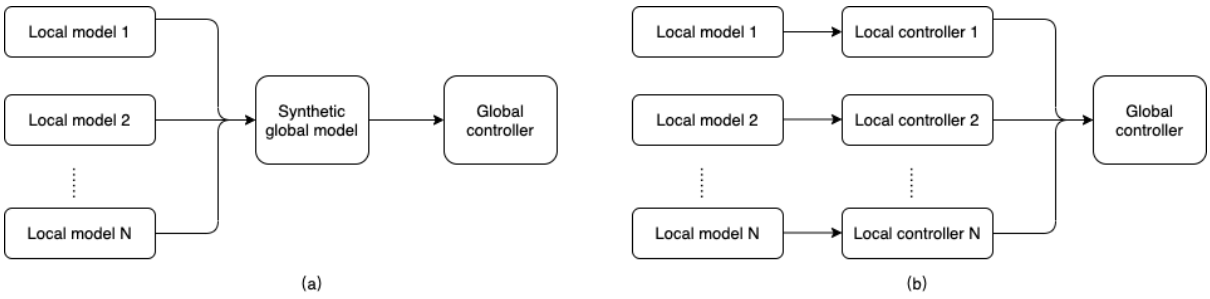

Figure 3.1: Global controller structure of multiple model method [115]

other relevant variables [92]. Switching strategies control the target system to obtain the desired closed-loop performance by selecting the linear sub-model whose switching conditions are the closest to those of the scheduling variables [10]. However, the existing methods have the possibility to cause problems such as oscillations during switching.

The mixing strategy, on the other hand, sets a weight function for each sub-model. It reflects the the affiliation degree of the sub-model to the real system, for example, in the T-S fuzzy system [102]. This strategy obtains the global model through the weighted sum of the sub-model bank. Obviously, the determination of the weight function is critical. The commonly used weight functions are Gaussian function [77], Bayesian network [11], Kernel function [32], and trapezoidal function [103]. The Gaussian function is again the most popular one.

According to the rules of multiple model synthesis, controller synthesis can also be divided into two categories: global controllers and local controllers. Global controllers are designed by global models or sub-model sets to achieve control of the whole system under the condition that performance metrics and constraints are satisfied [77][28]. The global controller is divided into two ways, the first one is based on a synthetic global model design after some combination of linear models, see Figure 3.1(a), and the second one is made by some combination of local controller set corresponding to linear models, see Figure 3.1(b).

The local controllers synthesis, on the other hand, is similar to the structure in Figure 3.1(b). By scheduling in the local controller bank, it selects an optimal one to represent the output of the overall controller pool by means of appropriate switching rules. It is not like the fusion strategy in the global mode. The risk of this strategy is that if the switching rule fails to grasp the dynamic characteristics of the whole system from the global perspective, it may result in low control accuracy or cause system instability. The structure is schematically shown in Figure 3.2.

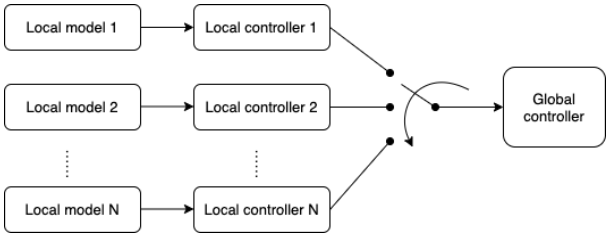

Figure 3.2: Local controller structure of multiple model method

3.1.2 The construction problem of multiple model approach

According to previous studies, there are many ways to build a multiple model set of the target system. In the former section we mentioned two possible methods, sector nonlinear variation and operational space decomposition of experimental data. Besides that, local model set can also be obtained by intelligent algorithms such as artificial neural networks. Here, the thesis presents the two most commonly used methods.

(1) Multiple model bank construction through system identification

When representing a nonlinear system in a multiple model form, the problem of identifying the target system is reduced to the identification of the subsystem defined by the local linear model and its activation function. After determining the structure of the local linear model and the activation function, numerical optimization methods can be used to obtain their parameters.

Generally, the multiple model approach describes the nonlinear system in the time domain in the following form:

$$x(t) = \sum_{i=1}^{N} \mu_i(\xi(t))(A_i x(t) + B_i u(t)) \tag{3.1}$$

where $\xi(t) \in \mathbb{R}^q$ is the scheduling variable, $\mu_i(\cdot)$, $i = 1, 2, \cdots, N$ is the activation function of i^{th} local model, namely weight.

The construction of a multiple model bank from the input/output data requires the following items before [85]: definition of the structure of the multiple model set, definition of the attribution function, parameters estimation of the local models and their activation function , and performance evaluation of the multiple model set.

For the parameter estimation, numerical optimization methods based on a priori knowledge can be used. It is generally obtained by minimizing a performance function that reflects the deviation of the estimated output of the multiple model $y_m(t)$ from the measured output of the system $y(t)$. The variance between the two outputs is

commonly used to do the evaluation.

$$J(\theta) = \frac{1}{2}\sum_{t=1}^{N_p}\epsilon(t,\theta) = \frac{1}{2}\sum_{t=1}^{N_p}(y_m(t) - y(t))^2 \tag{3.2}$$

where N_p is the observation width, θ is the parameter vector of local model and its activation function.

The method of minimizing the performance function $J(\theta)$ is usually by iterating it step by step around a specific parameter vector θ. θ is updated in the following form:

$$\theta(k+1) = \theta(k) - \eta D(k) \tag{3.3}$$

where η adjusts the converge speed and $D(k)$ denotes the search direction.

The calculation of $D(k)$ often based on some optimization algorithms, such as Levenberg-Marquardt algorithm, gradient method, Newton's algorithm and Gauss-Newton algorithm.

(2) Multiple model bank construction through linearization

If an analytic form of the target physical process's nonlinear model is available, suitable set of working points can be selected for local linearization to obtain a local linear model bank. Consider a nonlinear system of the following form:

$$\begin{cases} \dot{x}(t) = F(x(t), u(t)) \\ y(t) = G(x(t), u(t)) \end{cases} \tag{3.4}$$

where $(F, G) \in \mathbb{R}^{2n}$ are nonlinear functions, $x(t) \in \mathbb{R}^n$, $u(t) \in \mathbb{R}^m$ are state vector and input vector respectively.

Thus multiple model representation of nonlinear system 3.4 can be in the following form [40][76]:

$$\begin{cases} \dot{x}_m(t) = \sum_{i=1}^{N}\mu_i(\xi(t))(A_i x_m(t) + B_i u(t) + E_i) \\ y_m(t) = \sum_{i=1}^{N}\mu_i(\xi(t))(C_i x_m(t) + D_i u(t) + R_i) \end{cases} \tag{3.5}$$

Eq. 3.5 stands for the local model bank obtained through linearization of the target system in several working points $(x_i, u_i) \in \mathbb{R}^n \times \mathbb{R}^m$. Parameters of the local models are given by the following equations:

$$A_i = \left.\frac{\partial F(x,u)}{\partial x}\right|_{\substack{x=x_i \\ u=u_i}} \tag{3.6}$$

$$B_i = \left.\frac{\partial F(x,u)}{\partial u}\right|_{\substack{x=x_i \\ u=u_i}} \tag{3.7}$$

$$C_i = \left.\frac{\partial G(x,u)}{\partial x}\right|_{\substack{x=x_i \\ u=u_i}} \tag{3.8}$$

$$D_i = \left.\frac{\partial G(x,u)}{\partial u}\right|_{\substack{x=x_i \\ u=u_i}} \tag{3.9}$$

$$E_i = F(x,u) - A_i x - B_i u \tag{3.10}$$

$$R_i = G(x,u) - C_i x - D_i u \tag{3.11}$$

The number of local models N depends on the required modeling accuracy, the complexity of the nonlinear system, and the chosen activation function structure. The activation functions (weight functions) generally satisfy the following properties:

$$\begin{cases} \sum_{i=1}^{N} \mu_i(\xi(t)) = 1 \\ 0 \leq \mu_i(\xi(t)) \leq 1 \end{cases} \tag{3.12}$$

3.1.3 The stability problem of multiple model approach

The structural features of multiple model methods make it necessary to discuss about stability from not only the sub-model but also the global perspective. Most of the stability discussions of multiple model approaches in the literature are still based on Lyapunov's second stability theorem [86][117]. The goal is to find a positive definite symmetric matrix and thus a quadratic Lyapunov function in the form of linear matrix inequality (LMI) satisfying specific conditions. Here we give a brief description of state feedback stabilization as an example.

The stabilization of multiple model set is often performed by a parallel distributed compensation controller (PDC) [104]. Using the same weight function $\mu_i(z(t))$ as in the model bank Eq. 3.1 and with fixed gain K_i, we have:

$$u(t) = -\sum_{i=1}^{N} \mu_i(z(t)) K_i x(t) \tag{3.13}$$

By applying the control law to multiple model bank Eq. 3.1, the following close-loop could be obtained:

$$\dot{x}(t) = \sum_{i=1}^{N}\sum_{j=1}^{N} \mu_i(z(t))(A_i - B_i K_j)x(t) \tag{3.14}$$

Thus, the stability condition of the closed-loop system 3.14 is to find suitable control gain, making the Lyapunov function 3.15 has a negative derivative 3.16:

$$V(t) = x(t)^T P x(t), P > 0 \tag{3.15}$$

$$\dot{V}(t) = \sum_{i=1}^{N}\sum_{j=1}^{N} \mu_i(z(t))\mu_j(z(t))x(t)^T((A_i - B_iK_j)^T P + P(A_i - B_iK_j))x(t) < 0 \quad (3.16)$$

Assume $G_{ij} = (A_i - B_iK_j)$, then there is a theorem:

Theorem 1 [117][85]

Multiple model closed-loop 3.14 is asymptotically stable if, for all $i, j = 1, 2, \cdots, N$ (except the (i, j) pair making $\mu_i(z(t))\mu_j(z(t)) = 0$), there exist a symmetric matrix $P > 0$ and matrices Q_{ij} ($Q_{ij} = Q_{ji}^T$ for $i \neq j$ and Q_{ii} symmetric):

$$G_{ii}^T P + PG_{ii} + Q_{ii} < 0 \quad (3.17)$$

$$\left(\frac{G_{ij} + G_{ji}}{2}\right)^T P + P\left(\frac{G_{ij} + G_{ji}}{2}\right) + Q_{ij} + Q_{ij}^T \leq 0, i < j \quad (3.18)$$

$$\begin{pmatrix} Q_{11} & \cdots & Q_{1N} \\ \vdots & \ddots & \vdots \\ Q_{N1} & \cdots & Q_{NN} \end{pmatrix} > 0 \quad (3.19)$$

□

The determination of PDC gain $K_j, (j = 1, 2, \cdots, N)$ needs to transform the condition of the theorem to the equivalent LMI problem. In this way, it could be solved by available convex optimization tools [85]. This transformation corresponds to simple bijective changes of variables $X = P^{-1}$, $K_i = M_iP^{-1}$ and the use of a congruence (multiplication on the right by a given matrix and on the left by its transpose) to the inequalities in the theorem. Thus, the following LMI expressions can be determined by the variables X, M_i, S_ij:

$$A_iX + XA_i - B_iM_i - M_i^T B_i^T + S_{ii} < 0 \quad (3.20)$$

$$A_iX + XA_i + A_jX + XA_j - B_iM_j - M_j^T B_i^T - B_jM_i - M_i^T B_j^T + S_{ij} + S_{ij}^T \leq 0, i < j \quad (3.21)$$

$$\begin{pmatrix} S_{11} & \cdots & S_{1N} \\ \vdots & \ddots & \vdots \\ S_{N1} & \cdots & S_{NN} \end{pmatrix} > 0 \quad (3.22)$$

The number of conditions which need to be verified is $N(N + 1)/2$. Therefore, the number of local model is one of the reasons why the result given by the three conditions of the theorem is conservative. To reduce the conservatism brought by the selection of quadratic Lyapunov function, some scholars proposed non-quadratic Lyapunov function, see [60][19][44]. Other discussions about the stability issues of multiple model approach concerns about output feedback stabilization, robust stabilization of uncertain multiple model set and observer based stabilization through a multiple H_∞ controller, see [62][117].

3.2 The multiple model approach based fault tolerant control

3.2.1 The multi-dimensional multiple model structure concerning faults

The main purpose of this thesis is to complete the design of fault-tolerant control for complex industrial systems. The multiple model approach is used to do the model matching of the target system. For the fault-tolerance purpose, it is necessary to match the faulty system as well. When using the multiple model approach for practical applications to systems, previous literature whether considered only the use of multiple model identification and representation of nonlinear complex systems for the controller design [84][22], or constructed only a simple set of sub-models for the fault case without considering the variation of operating point [89]. In order to unify the two objectives, the concept of multi-dimensional multiple model structure is proposed so that a complete representation of the system can be given by considering operating points and faulty parameters at the same time.

For the nonlinear system 3.4, when considering the faulty parameters, it has the following form:

$$\begin{cases} \dot{x}(t) = F(x(t), u(t), \theta_{j,f}) \\ y(t) = G(x(t), u(t), \theta_{j,f}) \end{cases} \tag{3.23}$$

where $\theta_{j,f} \in \mathbb{R}^{P \times Q}$ represents the parameter considering the j^{th} faulty value in the f^{th} fault, ($j = 1, 2, \cdots, Q$ and $f = 1, 2, \cdots, P$).

Eq.3.23 considers the type of fault as well as its severe degree and thus it could be seen as a hyper system. If we represent system 3.4 by multiple model approach, it's local model like this:

$$M_i : \begin{cases} \dot{x}_m(t) = A_i x_m(t) + B_i u(t) + E_i \\ y_m(t) = C_i x_m(t) + D_i u(t) + R_i \end{cases} \tag{3.24}$$

where $i = 1, 2, \cdots, N$ is the index of the considered operating points.

Therefore, the hyper system 3.23 has a structure as shown below:

$$M_i \triangleq [M_1, M_2, \cdots, M_N] \tag{3.25}$$

$$M_{ij} \triangleq [M_{i,1}, M_{i,2}, \cdots, Mi, Q] \tag{3.26}$$

$$M_{ijf} \triangleq [M_{i,j,1}, M_{i,j,2}, \cdots, Mi, j, P] \tag{3.27}$$

Eq.3.25 to Eq.3.27 are the multiple model description of system 3.23 after considering operating point, faulty parameter value and fault type. In this process, the dimension of the model bank increases gradually. The final model set 3.27 has three dimensions while each one concerns a considering variable. During the process, we can refer to parameter interval method in [66] to assure the interval monotonicity of local model.

The main reason for using the multiple model approach is that the nonlinear system has multiple operating points, which are difficult to be approximated and adapted by a single simple model. The multi-dimensional multiple model framework enables the subsequent fault-tolerant strategy to narrow down the fault parameter interval in the shortest period, and then make the optimal matching to it. Like this the controller mapping can be completed by the model matching information, and the predefined optimal controller can be applied to the faulty system to achieve the fault-tolerance goal. The offline optimization of the controller bank based on the multiple model set is designed to shorten the transient process of the faulty system by quickly switching to the corresponding controller once the model matching is completed during the implementation of FTC.

It is actually a probabilistic optimal process to match the multiple model framework to the real system. No matter which strategy is selected, its goal is to minimize the parameter error between the actual system and the model bank.

3.2.2 Control problem under multi-dimensional multiple model structure

After deconstructing the nonlinear system from the above multi-dimensional multiple model framework in the normal and fault cases respectively, its corresponding controller design in the sub-interval can be equated to a robust control problem.

After completing the construction of the multi-dimensional multiple model set for the target nonlinear system Eq.3.4, its equivalent linear model at any moment will fall into the predefined model space regardless of the operating point and the presence of faults. But its parameters are still unknown. The equivalent model may be equal to a local model in the model set, or it is in the domain that is composed of several models. Therefore, it has a parameter uncertainty that can be expressed as:

$$M_{eq} : \dot{x} = [A + \Delta A] + [B + \Delta B]u \tag{3.28}$$

where perturbation matrices ΔA and ΔB denote the model deviation.

Obviously, the maximum model deviation is determined by the neighbouring local models in the model space which is created by the multi-dimensional multiple model set Eq.3.24. Since this model bank is set offline and the maximum model deviation can be adjusted in advance. Therefore, the following condition concerns the perturbation matrices can be hold:

$$[\Delta A, \Delta B] = E\Sigma(t)[F_a, F_b] \tag{3.29}$$

where $E \in R^{n\times r}$, $F_a, F_b \in R^{q\times m}$ are known time-invariant matrices. $\Sigma(t) \in R^{r\times q}$ are unknown function matrix which belongs to set Ω:

$$\Omega = \{\Sigma(t) | \Sigma^T(t)\Sigma(t) \leq I, \forall t\} \tag{3.30}$$

After the fault interval being diagnosed, the following theorem is given for the fault tolerant control design:

Theorem 3

For the nonlinear system Eq.3.4, during the design of its multi-dimensional multiple model set, the maximum model deviation meets the condition described in Eq.3.29. To the equivalent model M_{eq} of the real process described by Eq.3.28, which is located between local models, if the following Riccati inequality:

$$A^TP + PA + PEE^TP + F_a^TF_a - (PB + F_b^TF_b)(F_b^TF_b)^{-1}(B^TP + F_b^TF_a) < 0 \tag{3.31}$$

has positive-definite solution matrix P, then there exist the following state-feedback control that can assure Lyapunov stability of the equivalent model of the real system which has parameter uncertainty:

$$u = Kx \tag{3.32}$$

where the control gain K is given by:

$$K = -(F_b^TF_b)^{-1}(B^TP + F_b^TF_a) \tag{3.33}$$

□

Proof: To the equivalent model M_{eq} of the real system which has parameter uncertainty and described by Eq.3.28, the state-feedback control Eq.3.32 is designed and the closed-loop system is described as:

$$\dot{x} = [A + \Delta A] + [B + \Delta B]Kx \tag{3.34}$$

substitute the considered condition Eq3.29 during the offline design of model set, we have:

$$\dot{x} = [A + BK + E\Sigma(t)(F_a + F_bK)]x \tag{3.35}$$

According to the Theorem 4.4.1 in [94], the necessary and sufficient condition that the closed-loop system Eq.3.35 is Lyapunov stable is $A + BK$ stable and:

$$\|(F_a + F_bK)(sI - A - BK)^{-1}E\|_\infty < 1 \tag{3.36}$$

The calculation of the control gain K is equivalent to the standard design of the following augmented system:

$$G(s) = \begin{bmatrix} A & E & B \\ F_a & O & F_b \\ I & O & O \end{bmatrix} \tag{3.37}$$

The closed-loop system constructed of the augmented system and state-feedback controller is described as:

$$\begin{cases} \dot{x} = [A + BK]x + E\omega \\ z = (F_a + F_bK)x \end{cases} \tag{3.38}$$

where ω denotes the perturbation input.

The inner stability of system Eq.3.38 equivalent to $A + BK$ stability. According to Theorem 2.4.1 in [94], the necessary and sufficient condition which meets the requirements that $A + BK$ is stable and the transfer function of perturbation ω to the system respects:

$$\|T_\omega(s)\|_\infty < 1 \tag{3.39}$$

is there exist a positive-definite matrix $P > 0$ that makes:

$$P(A + BK) + (A + BK)^T P + PEE^T P + (F_a + F_bK)^T(F_a + F_bK) < 0 \tag{3.40}$$

After arrangement, it is described as:

$$PA + A^T P + PEE^T P + F_a^T F_a - (PB + F_a^T F_a)(F_b^T F_b)^{-1}(B^T P + F_b^T F_a) + N_K^T N_K < 0 \tag{3.41}$$

where $N_K = F_b[K + (F_b^T F_b)^{-1}(B^T P + F_b^T F_a)]$.

If there exist a feedback matrix K that makes $A + BK$ to be stable and lets Eq.3.39 being satisfied, therefore, Eq.3.40 has positive-definite solution. And then, according to Eq.3.41, it can be deduced that the positive-definite solution satisfies the Riccati inequality Eq.3.31.

On the contrary, if Eq.3.31 has positive-definite solution P and K is given by Eq.3.33, it make Eq.3.41 to be satisfied. And then, Eq.3.40 holds, which indicates that $A + BK$ is stable and Eq.3.39 is satisfied. □

3.2.3 Basic concepts and FTC ideas

Before discussing the multi-model approach based fault tolerant control , we make several definitions as follows.

Model bank (model set): a collection of local models obtained according to a certain rule.

Model space: a virtual space which contains all the local models seen as elements to the target system.

Model matching: The process of finding the equivalent or closest model to the current state of the given target system in the model space.

Full information analysis: The overall analysis and utilization of the systematic and non-systematic information of the target system obtained from the relevant links in the implementation of fault tolerant strategy. The main response is to maximize the use of existing information when the diagnosis result is not clear and the acquired fault information is not sufficient, in order to obtain the best possible fault tolerant control effect.

Since most of the real systems are nonlinear, the multiple model approach can simplify the process of designing their controllers and avoid some difficulties. After obtaining the multiple model set of the target system, sub-controllers can be designed for the sub-models separately, so the set composed of sub-controllers is the controller bank corresponding to the model set. The fault tolerant control of the target system can be transformed into an optimization problem in the controller parameter space. When the target system has a fault, it deviates from the nominal state. Come to the model space, we say that the range of model uncertainty becomes larger. Correspondingly, the feasible domain in the controller parameter space decreases. Specifically, for the system Eq.3.4, assume that its multiple model representation Eq.3.5 constitutes a model space Γ, and the design of the controller for each equivalent sub-model of the real plant in the model space is done off-line. Assuming that the controller structure is homogeneous, for a performance index, such as stability requirements, the sub-controller parameters corresponding to each equivalent model of the actual plant have a range of values (feasible domain) ϕ, and the real plant is in a model space Γ which composed of N sub-models, the controller parameter space can be expressed as:

$$\Phi = \phi_1 \cup \phi_2 \cup \cdots \cup \phi_i \cup \cdots \cup \phi_N \tag{3.42}$$

When the system is in the normal case, the parameters are determined and the equivalent model is explicit. The feasible domain of controller parameters equal to

that of the equivalent model ϕ_i. When the system is faulty, its equivalent model has uncertainty if the fault diagnosis is on-going. If we assume that the equivalent model of the real process is between M_{i-m} and M_{i+n} in the model space, then the controller feasible domain that satisfies the required performance index is:

$$\Phi_f(\Theta) = \phi_{i-m} \cap \phi_{i-m+1} \cap \cdots \cap \phi_{i+n-1} \cap \phi_{i+n} \tag{3.43}$$

where subscript f denotes faulty situation, $\Theta \subseteq \Omega$ is the parameter uncertainty domain. $\Phi_f(\Theta)$ will change with the model parameter domain. Its maximum $\Phi_{max}(\Theta)$ is defined as the biggest feasible domain of controller parameters. The situation discussed here is actually a discretization extension of the insufficient fault information based fault tolerant control in [67].

Obviously, the controller feasible domain $\Phi_f(\Theta) \subseteq \Phi$ under model uncertainty, and $\Phi_f(\Theta) \leq \phi_i$. The specific control parameters are determined as a result of optimizing the performance index in the controller feasible domain by minimizing $J(\Theta, \varphi)$ (where φ denotes the controller parameters). Suppose φ_m and φ_n are the controller parameters optimized in the feasible domain $\Phi_m(\Theta)$ and $\Phi_n(\Theta)$ respectively, and if $\Phi_n(\Theta) \subseteq \Phi_m(\Theta)$, it follows from Lemma 2 of the literature [67] that $min(J_m) \leq min(J_n)$ holds.

If we define the goal of resetting the controller parameter is to satisfy the following two formulas:

$$min(J(\Theta, \varphi)) \tag{3.44}$$

$$p_i(\Theta, \varphi) \in \Omega_i, \forall i = 1, 2, \cdots, v \tag{3.45}$$

where p_i denotes v constraints of the target system, Ω_i is a domain in the complex plane.

Thus, to reach a better control, we have the following theorem:

Theorem 2

For a system Eq.3.4 whose equivalent linear model is in the model space given by a multi-dimensional multiple model set Eq.3.24, to achieve the objective of control parameter selection described in (3.44) and Eq.3.45, the control parameter vector is optimized in the maximum feasible domain $\Phi_{max}(\Theta)$.

Proof: Assume the optimization domain of control parameter vector is Φ, to meet the constrains of Eq.3.45, Φ is a sub-set of $\Phi_{max}(\Theta)$, i.e. $\Phi \subseteq \Phi_{max}(\Theta)$. According to Lemma 2 in [67], we have $min(J(\Phi)) \leq min(J(\Phi_{max}(\Theta)))$. In this way, to achieve the objective, Eq.3.44, it should let $\Phi = \Phi_{max}(\Theta)$. □

That is to say, the larger the controller parameter feasible domain the optimization is performed in, the better the control performance will be obtained. As a corollary,

when using the multiple model approach for fault tolerant control problems, the model matching operation can be performed in the model space for the actual faulty system to minimize the uncertainty range of the equivalent model. Thereby, under the fault scenario, a larger controller feasible domain could be achieved and the optimization of control parameter is carried out according to the predefined objectives. The newly obtained parameters are used to perform the fault tolerant control. In particular, full information analysis during model matching process helps to reduce the uncertainty range of the equivalent model. Although it may not be possible to determine the equivalent model in just one step, it helps the acquisition of better control parameters.

The model bank is constructed by offline optimization. One benefit is that it avoids the time consumption of online optimization and is possible to do fast switching during real-time operation. In this way it satisfies the need for speed in active fault tolerant control.

3.3 The FTC method based on multi-dimensional multiple model structure and model matching strategy

3.3.1 FTC strategy through direct multiple model matching

The creation of multi-dimensional multiple model structure presents convenience for controller design. The multi-dimensional multiple model set contains considerations for specific fault and its parameters. Thus controllers for that fault can be designed in advance and used as a priori knowledge, or specific design rules can be developed to enable fast switching or reconstructing control law in case of fault. As shown in Figure 3.1 and Figure 3.2, the controller design based on multi-dimensional multiple model set has two ways, too. Either it can be designed according to the global model which is the combination of the local models, or it is designed based on each local model and combined later as the global control.

Taking the two-dimensional multiple model set as an example, when the target system considers different levels of a single fault, a two-layer multiple model structure with two dimensions can be constructed. Then the corresponding controller library can be designed based on the two-layer multiple model set with a homogeneous structure. Since the second layer of the model set involves faulty scenarios, the corresponding controller library has the ability to maintain the system performance under the considered situations. The FTC architecture with direct model set matching is shown in

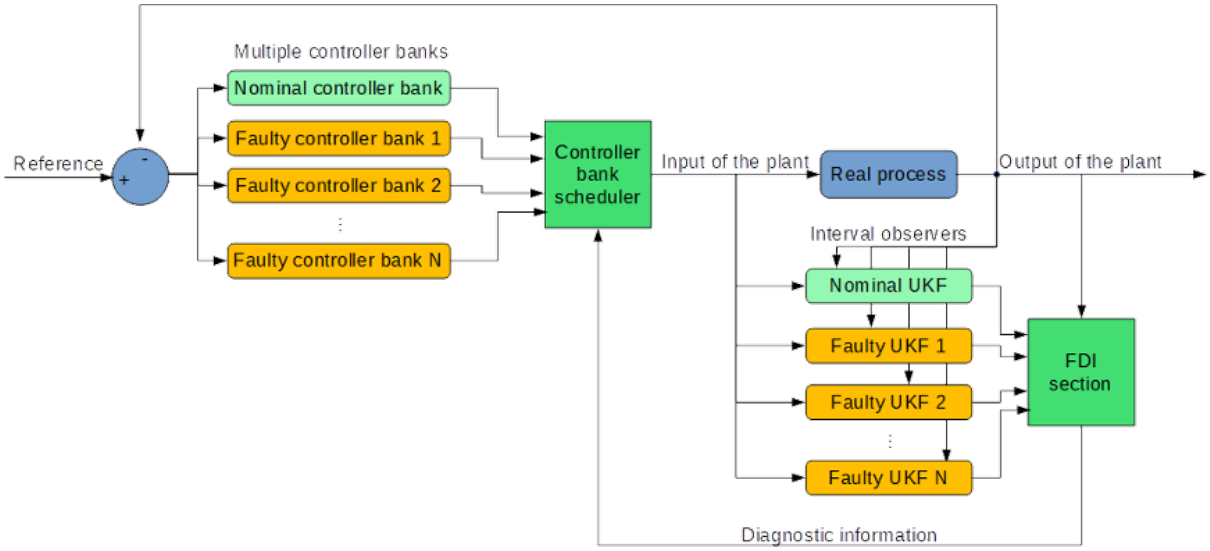

Figure 3.3: FTC strategy using two-layer multiple model structure [48]

Figure 3.3.

In this strategy, the FDI part uses the estimates given by the interval observer to monitor the actual process. It then generates diagnostic information to guide the controller bank scheduling to finish the work. When a fault is detected and isolated, there are two possible scenarios: the fault is within the set interval or beyond the boundaries of the interval. Depending on the design purpose, the first scenario should cover most cases. For example, in the simulation results in **Figure 5.6**, the fault is located between the second and third interval. At this point, in order to compensate the fault and achieve fault tolerance, the two corresponding controller banks can be selected to give the weighted control output of the faulty system, i.e., direct matching. The weighting values can be determined by specific criteria or calculated by a simple linear fusion using residuals:

$$\begin{cases} \mu_i & = 1 - \dfrac{|e_i|}{|e_i| + |e_{i+1}|} \\ \mu_{i+1} & = 1 - \dfrac{|e_{i+1}|}{|e_i| + |e_{i+1}|} \end{cases} \tag{3.46}$$

$$u = u_i \mu_i + u_{i+1} \mu_{i+1} \tag{3.47}$$

where μ indicates the weight the controller bank, i is the index of the second layer controller bank, and u denotes the control output.

One special case in this "Within-interval" situation is the one when $e_i \cdot e_{i+1} = 0$. It means the current system behaves exactly the same as one assumed faulty situa-

tion. Using 3.46 and 3.47 to calculate new control signal is also valid because the corresponding weight will equal to 1 to have suitable assignment.

For the "Beyond-interval" situation, the term $e_i \cdot e_{i+1} \leq 0$ is not hold, meaning the faulty system behaves beyond the worst situation. It is very rare and one can only activate the controller bank of the closest assumed faulty case to compensate the fault in some extend.

3.3.2 FTC strategy through multiple adaptive model matching

The direct matching FTC strategy has the advantage of simple design and rapid switching. However, the disadvantage is also obvious, i.e., the faulty parameter values cannot be accurately determined, especially when the considered faulty parameter also shows nonlinearity, i.e., the parameter values are nonlinearly varying in the interval. In this case, a multiple adaptive model matching strategy is proposed.

The basic idea is firstly to construct a multi-dimensional multiple model set based on the former section to design the fault detection module. It determines the vertex model that surrounds the current system from the parameter space by analyzing the actual system output and the model set output. In this way the uncertainty range of the faulty system can be quickly reduced. Secondly, it uses the parameter of the vertex model to initiate the adaptation process and achieves an accurate approximation of the actual system. At the same time, the strategy designs a controller for the reference model, and uses its output as the reference input to the adaptive process. Thus it indirectly enabling the unknown parameter system to be matched accurately while ensuring that the output follows the original reference. When a fault occurs, it can be equated to a relatively large parameter change in the actual system. The fault diagnosis module first gives the fault interval, and the fault-tolerant strategy restarts the adaptation process in that interval. Then it completes the fault-tolerant control of the faulty system. Taking the single-fault case as an example, the process is shown in Figure 3.4.

In general, FTC requires a higher time limit for the actual system approximation than basic adaptive control, so the fault-tolerant strategy shown in Figure 3.4 is designed in this thesis. Compared with previous studies, the proposed strategy can jump to a smaller range of fault intervals as soon as the system encounters a fault due to the introduce of a multi-dimensional multiple model set. And the adaptation process also ensures an accurate matching to the faulty system, which results in a more accurate control effect. The specific implementation is described in Chapter 6.

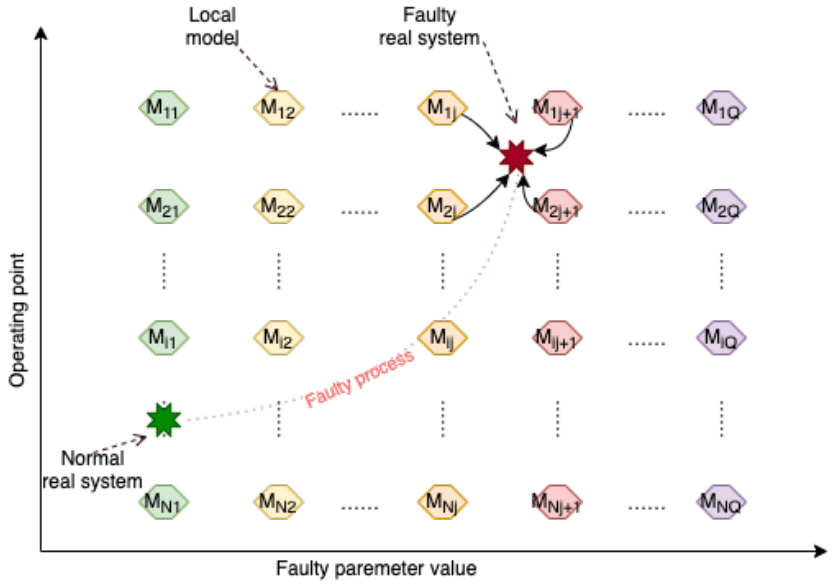

Figure 3.4: Two-layer multiple model structure based multiple adaptive model matching FTC [48]

3.4 Summary

This chapter reviewed the multiple model approach, and briefly discussed the decomposition and synthesis problem, the model set construction problem, and the stability problem of this approach. Then, the concept of multi-dimensional multiple model structure is proposed for the exploration of fault diagnosis and fault-tolerant control. This structure is designed for the complete representation of a nonlinear system in the whole workspace as well as the faulty parameter space. In this way, it formed a new hyper multiple model bank. Finally, based on this model set, three ideas of fault-tolerant strategy were proposed and discussed.

Chapter 4

Development of the Nominal Model of the Heat-exchanger/Reactor

This chapter presents the modeling process of an intensified chemical reactor which is designed by our collaborate laboratory LGC and their partner enterprise. It is an innovative object designed under the popular trend of process intensification in chemical engineering. This reactor combines high heat transfer ability and chemical performances, which would have a very bright prospect. The modeling is also based on the previous researches and experiments of this reactor.

Although some previous researches of our team have already concerned about control design or fault diagnosis problems about this HEX/reactor, they were considered in simple situations and limited to heat exchange only. In this chapter, the modeling process is described in detail and physical structure is considered also. More importantly, a typical chemical reaction is introduced and modeled to simulate the real working state of the reactor. The developed nominal model is validated to be accurate. It has a very good consistency to the real reactor and could be a base for further researches in the domain of automatic control of this kind of chemical reactor. Since the proposed FTC will be evaluated by this nonlinear chemical reactor in the future, modeling process is a key section in this thesis.

4.1 Background

Recent years, there is an increasing interest in process intensification[42][51][31], which aims at replacing the traditional batch chemical processes by novel ones combining two or more traditional operations in one hybrid unit. The technological limitations of discontinuous reactors, which may result in safety and productivity constraints, mainly come from their poor heat exchanging performances. These disadvantages excited research teams to design and develop new devices based on the coupling of high heat transfer behavior and good mixing performances[88][101]. As a consequence, intensified heat-exchanger/reactors (HEX/reactor), which are well-known for their thermal and hydrodynamic performances[7], are widely studied for highly exothermic reactions[16]. By combining heat-exchanger and plug-flow reactor in only one unit, the HEX/reactor not only meets the demand of miniaturization and low cost of the chemical plant, but also improves the ability of heat and mass transfer. Recent works in the field of dynamic characterization and optimization[12][9], predictive control[108][83] and fault diagnosis and isolation [30][127][126] have illustrated that it is important to utilize adequate and computationally efficient dynamic HEX/reactor models.

In the application of FDI, many authors have confined their work to a simplified model in which chemical reaction is not included as well, see [65][13]. However, there are many parameters which should be taken into consideration when a chemical reaction is introduced. It is an essential step to completely understand the dynamic characteristics of a new equipment in terms of process safety[12][13] and further control. Like most of the cases, a cell-based model is used in this paper, i.e. each cell is modeled by means of energy and mass balances[124][107][18]. The aim of this paper is to implement the concept of general modeling and validate it on a particular intensified HEX/reactor which is already studied at LGC[105]. During modeling, thermal and hydrodynamic performances of the pilot under the condition of chemical reaction which brings highly non-linear features are investigated. Once the detailed nominal model is set up and validated, further researches like optimal control, adaptive control, fault diagnosis, and fault tolerant control would be carried out on it.

The first part of this paper gives a brief description of the specific intensified HEX/reactor. After that, mathematical equations, as well as model structure, are presented according to different parts of the pilot. In addition, parameters which are used to identify heat transfer coefficient are searched using genetic algorithm with part of experimental data. Simulations have been carried out in order to investigate the performance of the model. Considering different aspects involved in the model (hydro-

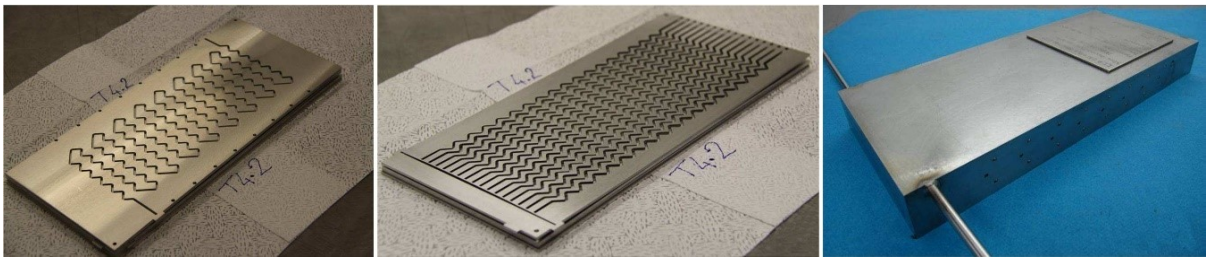

Figure 4.1: Details of the heat exchanger/reactor: (a) Process channel; (b) utility channel; (c) the heat exchanger/reactor after assembly [9]

dynamic, heat transfer and reaction), the validation study has been conducted in two parts: experiments with water and experiments with the highly exothermic reaction of sodium thiosulfate oxidation. Finally, results of simulations and real experiments have been compared in order to demonstrate the relevance and precision of the developed model.

4.2 Physical structure of the reactor

To show the validity of the general model presented in this paper, it has been applied to a specific intensified HEX/reactor with well-characterized performances. This reactor is based on the concept of plate heat exchanger in a modular block. It exhibits a plug-flow behavior and is designed in such a way that reaction and heat transfer take place in plate walls. The pilot consists of three process plates sandwiched between four utility plates. The process plates, as well as the utility plates, have been engraved by laser machining to obtain 2 mm square cross-section channels. Process and utility channels are presented in Figure 4.1 (a) and (b). The process fluid circulates in a single channel in order to offer the longest possible residence time for reactants while the utility fluid flows in parallel zigzag-type channels so as to bring in or take reaction heat away as soon as possible. The characteristics of the pilot are detailed in Table 1. The flow configuration of the two different fluids is shown in Figure 4.2.

The reactor is manufactured in 316L stainless steel and different plates are assembled by hot isostatic pressing (HIP)[8][106], which makes it a very compact one with 32 cm height, 14 cm width, 3.26 cm thickness and a mass of 10.84 kg. In order to find compromises between heat transfer and mixing performances, the pumping power, the compactness and the manufacturing costs, the process channel design has been optimized in the frame of the RAPIC project[8]. Geometrical parameters such as curvature radius, straight length between two bends, aspect ratio and bend angle,

Table 4.1: Geometrical properties of the heat-exchanger/reactor [105]

Item	Process Stream	Utility Stream
Number of parallel channels	1	1
Number of plates for each stream	3	4
Individual channel width $L_{width}(mm)$	2.0	2.0
Individual channel depth $L_{depth}(mm)$	2.0	2.0
Total channel length $L_{total}(mm)$	6.7×10^3	2.8525×10^4
Hydraulic diameter $D_h(mm)$	2.0	2.0
Total fluid volume (mm^3)	2.68×10^4	1.141×10^5
Metal thickness between streams (mm)	2.0	2.0

which have a great impact on the thermal performances, residence time and pressure drop distribution, have been studied at lab-scale. More details are described in a previous paper dedicated to the experimental study of the reactor[9].

4.3 Modeling

4.3.1 General Modeling of the Reactor

A realistic description based on a modular structure of the HEX/reactor is presented in Figure 4.2. Two (or several) feeding lines, the main feeding line (R1) and a secondary feeding line (R2), ensure that reactants could be introduced in the reactor. Two loops, process fluid and utility fluid, are in charge of reacting and cooling/heating, respectively. Arrows indicate the inner flow directions of the process fluid and utility fluid. It is obvious that there are three types of plates, which are denoted as a (utility plate), b (process plate), and c (plate wall) in Figure 4.2.

The pilot operates as a plug-flow reactor. Flow modeling is therefore based on the same hypothesis as the one used for the modeling of real continuous reactors[20]. The reactor is then represented by a series of perfectly stirred tank reactors (called cells). Generally, the number of cells could be defined according to the requirement of accuracy in concrete situations. To make a balance between model accuracy and calculation cost, and according to the geometry and the physical structure of the process channel, the reactor is divided into 17 computing units (see Figure 4.3), as there are 17 horizontal lines in each process plate. Based on previous investigations [9][127], 17 can be considered an adequate number of units for a detailed model here. Each unit

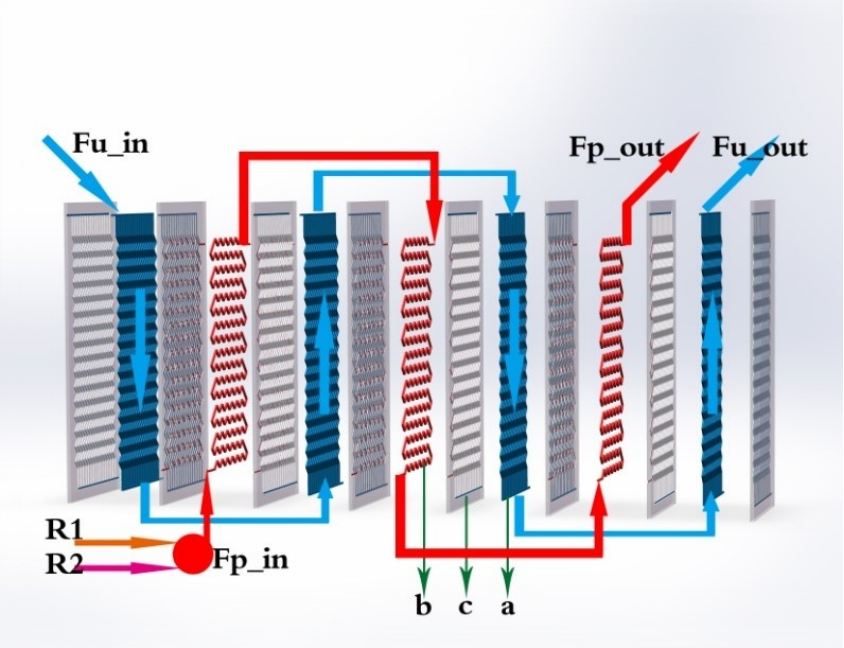

Figure 4.2: Block modeling description, showing (a) utility plate, (b) process plate, and (c) plate wall

contains 15 cells (see Figure 4.4): 3 process cells, 4 utility cells, and 8 plate wall cells. Therefore, the HEX/reactor considered in this paper was divided into 255 cells in total. The far-right plate wall, as well as the far-left one, was covered by low heat transfer materials, so they are called adiabatic plates, i.e., there is no heat exchange between the reactor and environment. Thus, each process cell is a mini-reactor. It is obvious that convective heat exchange (see bi-directional arrows in Figure 4.4) mainly takes place between neighboring cells in the horizontal direction inside one computing unit. The flows of fluids are the connections between neighboring units.

Such description makes it very easy to represent all possible flow configurations of the reactor (co-current, counter-current). In fact, it implies that the behavior of a cell only depends on the inlet streams and phenomena taking place inside: reaction, heat transfer, etc. Since the inlets of a given cell are generally the outlets of the preceding one, any configuration of flows may be represented by correct discretization. It can also be noticed that it is easy to generalize the model to any HEX/reactor by applying the number of plates and the number of cells in the plate to the actual configuration of the reactor.

The modeling of a cell is based on the expression of mass and energy balance and constraint equations. The constraint equations aim to consider the geometric characteristics of the reactor and the physical properties of the medium mentioned. The

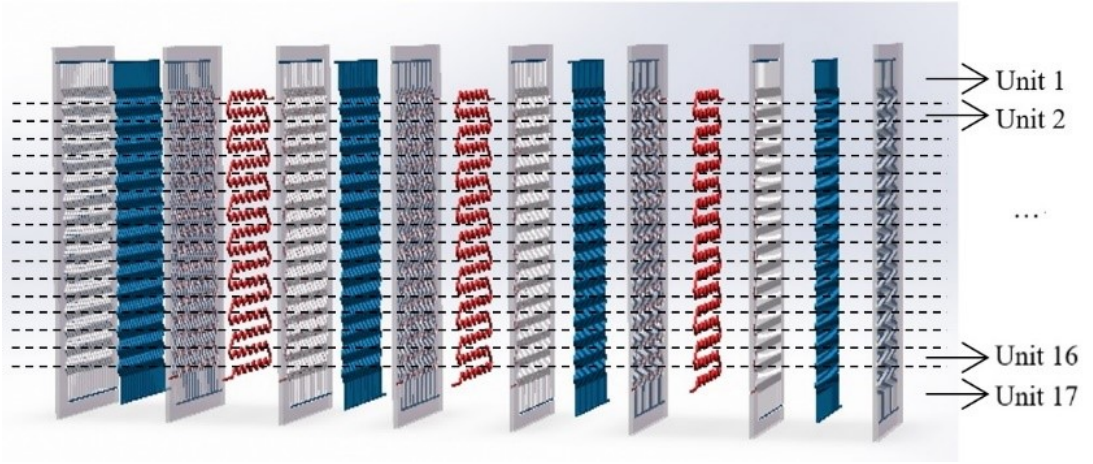

Figure 4.3: Description of units dividing

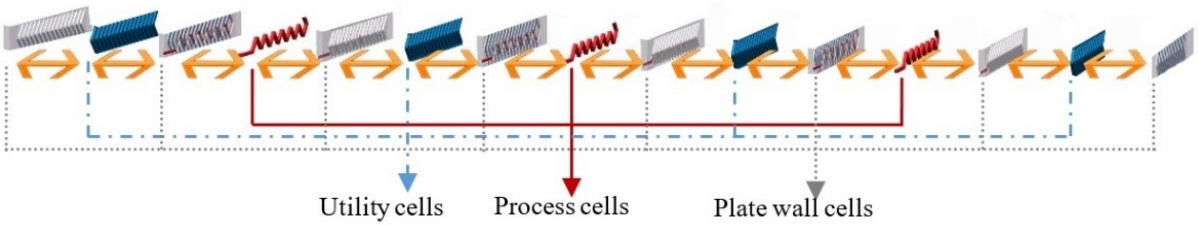

Figure 4.4: Internal description of one computing unit and convective heat exchange

balances are used to describe the relations of the characteristic values: temperature, mass composition, etc. according to the following formula:

$$\left\{ \begin{matrix} Accumulation \\ flow \end{matrix} \right\} = \left\{ Inlet \right\} - \left\{ Outlet \right\} + \left\{ \begin{matrix} Production \\ flow \end{matrix} \right\} \tag{4.1}$$

Given the specific geometry of the reactor, three main parts are distinguished. The first one is the process plate, where complex hydrodynamics coupled with reactions and heat transfers are found. The second one is the utility plate, where hydrodynamic and heat transfers are involved. The third one is the plate wall, which is only concerned with the heat transfer aspect.

4.3.2 Modeling of the Process Plate

It was considered that the process plate is sandwiched between two plate walls (right and left). Moreover, the cells representing the process plate (see Figure 4.5) are filled with a perfectly stirred homogeneous medium which has the following characteristics:

Homogeneity of characteristic values (temperature, flow rate, composition, etc.).

Homogeneity of physical properties (density, viscosity, etc.).

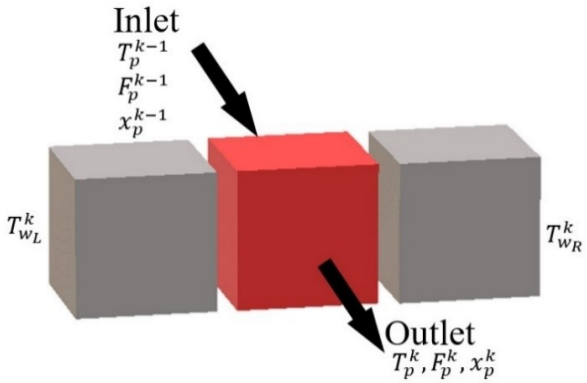

Figure 4.5: Representation of a cell k of process plate

Homogeneity of chemical phenomena (mixing, reaction, etc.).

Invariable volume linked to the mixture of fluids (reactants).

The state and evolution of the homogeneous medium circulation inside a given cell k are then described by the following balance and constraint equations: Global mass balance ($mol \cdot s^{-1}$):

$$\frac{du_p^k}{dt} = f_p^{k-1} - f_p^k + \Delta n_p^k \times V_p^k \tag{4.2}$$

where $u_p^k(mol)$ denotes molar hold-up in process plate cell k; f_p^k $(mol \cdot s^{-1})$ represents molar flow rate in process plate cell k; $\Delta n_p^k(mol \cdot m^{-3} \cdot s^{-1})$ is production rate of the reactions; and $V_p^k(m^3)$ is volume of process plate cell k.

Mass balance of component i $(mol \cdot s^{-1})$:

$$\frac{du_p^k \times x_{p,i}^k}{dt} = f_p^{k-1} x_{p,i}^{k-1} - f_p^k x_{p,i}^k + \Delta n_{p,i}^k \times V_p^k \tag{4.3}$$

where $x_{p,i}^k$ represents molar fraction of component i in process plate cell k.

Process energy balance (W):

$$\rho_p^k V_p^k Cp_p^k \frac{dT_p^k}{dt} = F_p^k \rho_p^k Cp_p^k (T_p^{k-1} - T_p^k) + \Delta q_p^k \times V_p^k + h_{pw}^k A_{pw}^k (T_{wL}^k - T_p^k) + h_{pw}^k A_{pw}^k (T_{wR}^k - T_p^k) \tag{4.4}$$

where $\rho_p^k(kg \cdot m^{-3})$ and $Cp_p^k(J \cdot kg^{-1} \cdot K^{-1})$ are density and specific heat of material in process plate cell k, respectively; $F_p^k(m^3 \cdot s^{-1})$ is volume flow rate in process plate cell k; $T_p^k(K)$ is temperature in process plate cell k; $\Delta q_p^k(W \cdot m^{-3})$ denotes heat generated by the reactions in process plate cell k; $h_{pw}^k(W \cdot m^{-2} \cdot K^{-2})$ and $A_{pw}^k(m^2)$ represent heat transfer coefficient and area between process plate and plate wall for cell k, respectively; and $T_{wL}^k(K)$ and $T_{wR}^k(K)$ are temperatures of left and right plate wall cells of the targeting cell k.

Volume constraint (m^3):

$$V_p^k = V_{cell}^k \tag{4.5}$$

where $V_{cell}^k(m^3)$ denotes maximum volume of cell k.

Due to the fact that the process plates are channels embedded in plate walls in reality, for one process plate cell, which is assumed to be a cuboid, the surface connected between process cell and plate wall cell is the four-lateral area of that cuboid. Therefore, the heat transfer area between one process cell and one plate wall cell (A_{pw}^k) actually equals half of the four-lateral area. According to the principle of cell partition, each plate has 17 cells. As the targeting HEX/reactor has three process plates, the total number of process cells is 51.

Thus, heat transfer area between process plate and plate wall for cell k is (m^2):

$$A_{pw}^k = \frac{\frac{1}{2}A_{pLateral}}{51} \tag{4.6}$$

where $A_{pLateral}$ is four-sided lateral area of process channel and is computed as follows (m^2):

$$A_{pLateral} \approx L_{pTotal} \times (2 \times L_{pWidth} + 2 \times L_{pDepth}) \tag{4.7}$$

where L_{pTotal}, L_{pWidth}, and $L_{pDepth}(m)$ are length, width, and depth of process channel respectively.

The volume of process cell k is (m^3):

$$V_p^k = \frac{V_{pTotal}}{51} \tag{4.8}$$

where V_{pTotal} is total fluid volume of process channel and is computed as follows (m^3):

$$V_{pTotal} \approx L_{pTotal} \times L_{pWidth} \times L_{pDepth} \tag{4.9}$$

4.3.3 Modeling of the Utility Plate and Plate Wall

To represent the reactor structure precisely, all the different heat transfer zones must be considered. Therefore, elements involved in the heat balance described by the model are as follows:

Utility fluid plates

Plate walls (right and left)

Adiabatic plates

A utility plate (see Figure 4.6) is sandwiched between two plate walls (right and left), and the description of heat transfer is as follows:

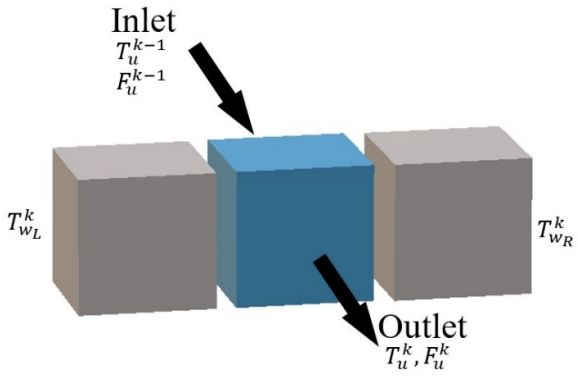

Figure 4.6: Representation of a cell k of utility plate

Energy balance on the utility fluid (W):

$$\rho_u^k V_u^k Cp_u^k \frac{dT_u^k}{dt} = F_u^k \rho_u^k Cp_u^k (T_u^{k-1} - T_u^k) + h_{wu}^k A_{wu}^k (T_{wL}^k - T_u^k) + h_{wu}^k A_{wu}^k (T_{wR}^k - T_u^k) \quad (4.10)$$

where $\rho_u^k (kg \cdot m^{-3})$, $V_u^k (m^3)$ and $Cp_u^k (J \cdot kg^{-1} \cdot K^{-1})$ are density, volume, and specific heat of material in utility plate cell k respectively; $F_u^k (m^3 \cdot s^{-1})$ is volume flow rate in utility plate cell k; $T_u^k (K)$ is temperature in utility plate cell k; $h_{wu}^k (W \cdot m^{-2} \cdot K^{-1})$ and $A_{wu}^k (m^2)$ represent heat transfer coefficient and area between utility plate and plate wall for cell k, respectively.

In the same way, utility plates are also channels embedded in plate walls. As the targeting HEX/reactor has four utility plates, the total quantity of utility cells is 68. Therefore, heat transfer area between utility plate and plate wall for cell $k(m^2)$ is calculated by:

$$A_{wu}^k = \frac{\frac{1}{2} A_{uLateral}}{68} \quad (4.11)$$

where $A_{u_lateral}$ is the four-sided lateral area of the utility channel and is computed as follows (m^2):

$$A_{uLateral} \approx L_{uTotal} \times (2 \times L_{uWidth} + 2 \times L_{uDepth}) \quad (4.12)$$

where L_{u_total}, L_{u_width}, and $L_{u_depth} (m)$ are length, width, and depth of the process channel, respectively.

The volume of utility cell $k(m^3)$ is given by:

$$V_u^k = \frac{V_{uTotal}}{68} \quad (4.13)$$

where V_{u_total} is total fluid volume of the utility channel and is computed as follows (m^3):

$$V_{uTotal} \approx L_{uTotal} \times L_{uWidth} \times L_{uDepth} \quad (4.14)$$

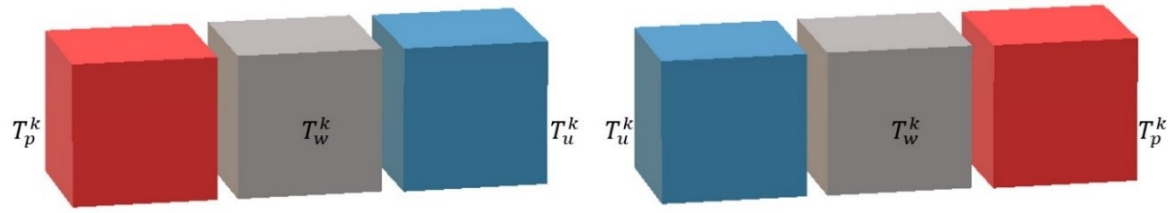

Figure 4.7: (a) Representation of a cell k of plate wall with process plate in the left and utility plate in the right; (b) Representation of a cell k of plate wall with process plate in the right and utility plate in the left

A plate wall (see Figure 4.7) is always sandwiched between a process plate and a utility plate, between which heat transfer is considered.

Energy balance on the plate wall (W):

$$\rho_w^k V_w^k Cp_w^k \frac{dT_w^k}{dt} = h_{pw}^k A_{pw}^k (T_p^k - T_w^k) + h_{wu}^k A_{wu}^k (T_u^k - T_w^k) \tag{4.15}$$

where $\rho_w^k (kg \cdot m^{-3})$, $V_w^k (m^3)$ and $Cp_w^k (J \cdot kg^{-1} \cdot K^{-1})$ are density, volume, and specific heat of plate wall cell k respectively; $T_w^k (K)$ is temperature of plate wall cell k.

Adiabatic plates assembled in both sides of HEX/reactor are special plate walls, for which heat transfer is taking place between utility plate and environment. In this paper, it is assumed that the adiabatic plates are heat-insulated, i.e., that there is no heat transfer between adiabatic plates and the environment.

Energy balance on the adiabatic plate (W):

$$\rho_w^k V_w^k Cp_w^k \frac{dT_w^k}{dt} = h_{wu}^k A_{wu}^k (T_u^k - T_w^k) \tag{4.16}$$

In fact, the plate wall cell cannot be assumed to be a cuboid, owing to the embedded channels. The exact value of the volume is obtained by its mass and density under the assumption of uniform distribution of the material. According to the dividing rules, the plant has 17 units, and each unit contains 8 plate wall cells. Thus, there are 136 plate wall cells in total.

The volume of plate wall cell $k (m^3)$ is calculated as:

$$V_w^k = \frac{\frac{M_r}{\rho_r}}{136} \tag{4.17}$$

where $M_r (kg)$ and $\rho_r (kg \cdot m^{-3})$ are mass and material density of the HEX/reactor.

4.3.4 Calculation of Heat Transfer Coefficient

As mentioned in Figure 4.7, the heat transfer process is divided into two parts: one is the convective heat exchange between the process channel and the plate wall, the other is between the utility channel and the plate wall. Therefore, the heat transfer ability, which is denoted by multiplying the overall heat transfer coefficient (U) and the overall heat transfer area (A), can be calculated by the convective heat transfer coefficient of the process fluid side to plate wall (h_{pw}) and heat transfer coefficient of plate wall to utility fluid side (h_{wu}), which is generally defined by the following equation [127]:

$$\frac{1}{UA} = \frac{1}{h_{pw}A_{pw}} + \frac{1}{h_{wu}A_{wu}} + R_f \tag{4.18}$$

where $R_f(W^{-1} \cdot K)$ is thermal resistance or fouling parameter in channels. For a clean HEX/reactor, R_f is considered to be negligible.

For calculation of the overall heat transfer coefficient through pipes and channels, the Nusselt number, which represents the ratio of convective to conductive heat transfer, is an important dimensionless number. In the case of this paper, fluids inside the channels are all assumed to have the same thermal characters as water and there is no phase change. Thus, for this given HEX/reactor (i.e., size, structure, and material fixed), the Reynolds number is the dominant variable in the equation of calculating Nu. Besides, when computing the Reynolds number, the flow rate of the fluid becomes the key variable, because other parameters will have very small changes. Therefore, it can be assumed that the convective heat transfer coefficients are functions of mass flow rate and physical properties of both fluids (process and utility). For simplicity, they could be defined as linear functions in the normal operation domain, as follows:

$$h_{pw} = \alpha \dot{M}_p \tag{4.19}$$

$$h_{wu} = \beta \dot{M}_u \tag{4.20}$$

where α and β are two scalar factors; and $\dot{M}_p$ and $\dot{M}_u(kg \cdot h^{-1})$ are mass flow rates in process and utility plate, respectively. Substitute Equations (19) and (20) into (18), then:

$$UA = (\frac{1}{\alpha \dot{M}_p A_{pw}} + \frac{1}{\beta \dot{M}_u A_{wu}} + R_f)^{-1} \tag{4.21}$$

Experimental data concerning the HEX/reactor considered in this work (see Table 4.2) are available, and some of them have been reported in a previous paper [105]. Using the same calculation method as in [105], several values of UA could then be obtained. As heat transfer area A_{pw} and A_{wu} are fixed according to the geometrical

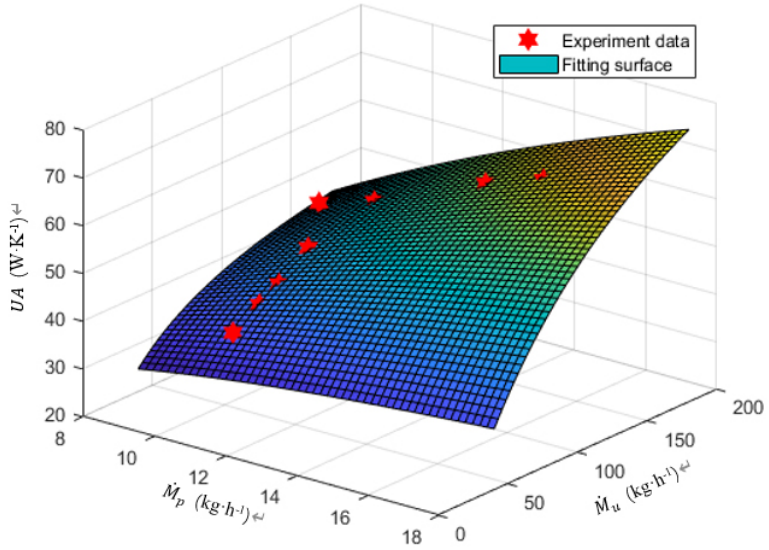

Figure 4.8: The matched UA as a function of $\dot{M}_p$ and $\dot{M}_u$ (hexagonal stars are computed from experimental data)

properties of the HEX/reactor, a genetic algorithm was introduced to search a group of optimal value for α, β and R_f. The fitness function of the genetic algorithm is defined below:

$$J = \sum_i \left| UA(i) - \left(\frac{1}{\alpha \dot{M}_p(i) A_{pw}} + \frac{1}{\beta \dot{M}_u(i) A_{wu}} + R_f\right)^{-1} \right| \tag{4.22}$$

where $UA(i)$ is the value of UA calculated from data of i^{th} experiment, and $\dot{M}_p(i)$ and $\dot{M}_u(i)$ are mass flow rates of process and utility channels in the i^{th} experiment.

The fitness function guides the genetic algorithm to find a relatively minimal total error of Equation (21) towards experimental data. When the goal is achieved, the targeting values of α, β, and R_f are found. For all the experimental data available in Table 4.2, we randomly reserved Experiment 5 and Experiment 8 for validation of the heat exchange simulations in Section 4. Other data of experiments in Table 4.2 were used here for searching relatively optimal parameters mentioned above. To prevent the algorithm dropping to a local optimal too early, the number of individuals in one generation and the number of evolutionary generations were set to 5000 and 1000 respectively. Satisfactory results were searched out, and the fitting surface is presents in Figure 4.8. Corresponding parity plot is shown in Figure 4.9.

Parameters searched by genetic algorithm are $\alpha = 777.33\ W \cdot m^{-2} \cdot K^{-1} \cdot kg^{-1} \cdot h$, $\beta = 9.77\ W \cdot m^{-2} \cdot K^{-1} \cdot kg^{-1} \cdot h$, $R_f = 0\ W^{-1} \cdot K$. As mentioned before, R_f is negligible. The confidence intervals depend mainly on the temperature difference between the process fluid and utility fluid. Generally, this varies from 10% to 15% of the nominal

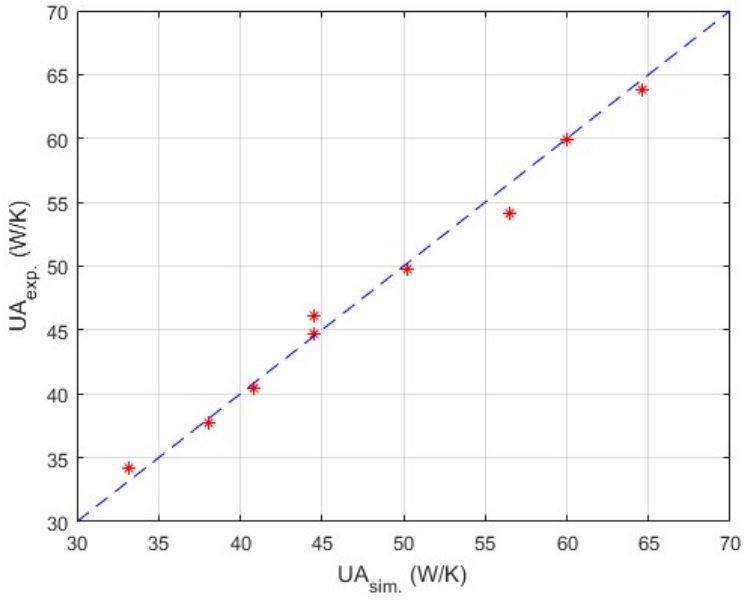

Figure 4.9: Parity plot of UA calculated from experimental data against those given by Equation (21) using the searched values of α, β, and R_f

value. Thus, h_{pw} and h_{wu} were obtained in satisfactory accuracy with Equations (19) and (20).

4.3.5 Reaction Modeling

In order to demonstrate the advantages of the HEX/reactor, experiments were carried out step by step in [105]. To validate the model, the preliminary step concerned experiments with water to verify the thermal description of the reactor and the behavior of related thermal correlations. In the second step, experiments with the reaction of sodium thiosulfate oxidation by hydrogen peroxide carried out in the reactor were considered.

$$2Na_2S_2O_3 + 4H_2O_2 \rightarrow Na_2S_3O_6 + Na_2SO_4 + 4H_2O$$

The reaction takes place in a homogeneous liquid phase and shows the following characteristics: irreversibility, fast kinetics, and very strong exothermicity. These features make it an ideal example for validation of the thermal and kinetic aspects of the HEX/reactor and its model.

The speed of the reaction is determined by the concentration decrease of the reactants over time. As the reaction goes, the concentrations of the reactants (C_i^k) gradually decrease.

Knowing the speed of a reaction makes it possible to estimate the rate of production

for a given constituent (Δn_i^k), the total production rate (Δn^k), and the heat generated (Δq^k). These estimations, which are used within the mass and energy balance of the cell, are based on the following relations: The production rate of constituent i:

$$\Delta n_i^k = \sum_j \tau_{i,j} r_j^k \tag{4.23}$$

where $\tau_(i,j)$ represents stoichiometric coefficient of constituent i in reaction j.

Total production rate:

$$\Delta n^k = \sum_i \Delta n_i^k \tag{4.24}$$

Heat generated:

$$\Delta q^k = \sum_j (\Delta H r_j \times r_j^k) \tag{4.25}$$

where $\Delta H r_j$ is the heat of reaction $j (J \cdot mol^{-1})$. For the reaction of sodium thiosulfate oxidation by hydrogen peroxide, $\Delta H r_j$ is [105]:

$$\Delta H r = -5.86 \times 10^5 J \cdot mol^{-1}$$

In this paper, the kinetic constant of reaction was assumed to be governed by an Arrhenius law, which made it possible to estimate the evolution of the constant as a function of temperature:

$$k_j = k_j^0 exp(-\frac{(E_j^a}{RT}) \tag{4.26}$$

where $k_j^0 (m^3 \cdot mol^{-1} \cdot s^{-1})$ is the pre-exponential factor of the reaction j; $E_j^a (J \cdot mol^{-1})$ is activation energy of reaction j ; and R $(J \cdot mol^{-1} \cdot K^{-1})$ is the perfect gas constant. The following values, given in Reference [6], were implemented in the model:

$$k_j^0 = 8.13 \times 10^8 \ m^3 \cdot mol^{-1} \cdot s^{-1}$$
$$E_j^a = 7.6123 \times 10^4 \ J \cdot mol^{-1}$$
$$R = 8.314 \ J \cdot mol^{-1} \cdot K^{-1}$$

Considering the stoichiometric scheme of the reactions and Equations (23) to (26), the concentration of each reactant in a cell behaves according to the following relationships:

$$\frac{dC_{Na_2S_2O_3}^k}{dt} = \frac{F_{Na_2S_2O_3} + F_{H_2O_2}}{V_p^k} C_{Na_2S_2O_3}^{k-1} - \frac{F_{Na_2S_2O_3} + F_{H_2O_2}}{V_p^k} C_{Na_2S_2O_3}^k - 2r_j^k \tag{4.27}$$

$$\frac{dC_{H_2O_2}^k}{dt} = \frac{F_{Na_2S_2O_3} + F_{H_2O_2}}{V_p^k} C_{H_2O_2}^{k-1} - \frac{F_{Na_2S_2O_3} + F_{H_2O_2}}{V_p^k} C_{H_2O_2}^k - 4r_j^k \tag{4.28}$$

where $C_{Na_2S_2O_3}^k$ and $C_{H_2O_2}^k$ $(mol \cdot m^{-3})$ are the concentrations of $Na_2S_2O_3$ and H_2O_2 in process cell k, respectively; and r_j^k is the speed of a reaction j taking place in cell k. It is expressed as a function of the concentrations of the reactants, as follows:

$$r_j^k = k_j C_{Na_2S_2O_3}^k C_{H_2O_2}^k \tag{4.29}$$

where $k_j(m^3 \cdot mol^{-1} \cdot s^{-1})$ is the kinetic constant of the reaction and is given in Equation (26).

4.3.6 Calculating the Model in Matlab/Simulink

The formulation of the model leads to a hybrid differential and algebraic equations (DAE) system. Ordinary differential equations (ODE) (Equations (4.2), (4.3), (4.10), (4.15), (4.16)) contain mass and energy balances. Algebraic equations (AE) (Equations (4.5), (4.19) to (4.21)) consist of the reactor constraints and physical properties estimation equations. This DAE system presents a strongly nonlinear nature, mainly resulting from the modeling of the chemical reaction.

The system was modeled and simulated in Matlab/Simulink. One unit consisted of three process plate cells, four utility plate cells, and eight plate wall cells. Each cell here was called a calculating module. For process plate cells, both mass and energy balance equations were introduced in the module to take into account the evolution of the temperature and the concentrations of the components due to heat transfer and to the reaction. For utility plate and plate wall cells, only energy balance equations were considered.

Therefore, the complete pilot was represented by the connection of 17 units. For each unit, multiple inputs and outputs concerning cells in other units were elicited to connect to associate ports. As shown in Figure 4.2 and Figure 4.3, for utility fluid, the temperature output of utility plate cell 1 in unit 1 would be connected to the temperature input of utility plate cell 1 in unit 2. For that of unit 17, it is different; the temperature output of utility plate cell 1 in unit 17 would be connected to the temperature input of utility plate cell 2 in unit 17 itself.

For process fluid, the fluid was injected at process plate cell 1 in unit 17 due to the opposite flow direction between process fluid and utility fluid. Afterward, the temperature input of process plate cell 1 in unit 16 came from the temperature output of process plate cell 1 in unit 17. The temperature output of process plate cell 1 in unit 1 was linked to process cell 2 in unit 1. Therefore, in accordance with the general scheme of the reactor presented in Figure 4.2, outputs of process fluid corresponded to data of cell 3 of unit 1, and outputs of utility fluid to these of cell 4 of unit 1.

These connections maximized the heat transfer efficiency, thus, the heat generated by reactions was rapidly taken away by utility fluid. According to the manner of the connection, heat exchange mostly took place horizontally, i.e., between different kinds of cells inside a unit, due to the thin plate structure of the reactor. As a consequence,

15 cells of different plates were packed in one unit, and the heat exchange was dealt inside while the fluid flow was handled outside the unit.

4.4 Simulation of the Model

4.4.1 Initial States of the Simulations

Simulations were planned to correspond to the same situations as in experiments. In the reaction-free section, process channel and utility channel were pumped with water at different target temperatures, and flow rates of the two channels were considered as variables separately. It is natural to suppose that both the channels of the process plate and the utility plate were empty at the very beginning. The liquid was injected into the tubes only when the experiment or simulation started. Thus, for these process or utility cells, as they were considered to be connected in series, the initial condition of one cell was just the output state of the former one. The initial state of the first cell was the input state, which was the input temperature. Cells of plate wall had other initial states. Since plate wall cells are considered to form the solid reactor, their initial states were just the environment temperature, because it can be assumed that the temperature of the reactor was in equilibrium with the environment before starting the experiments. However, these initial states only affected the dynamic process. The balance states were in relation to inputs and the structure of the reactor.

4.4.2 Simulation Results of Heat Exchange Procedure

Operating conditions for the first part are given in Table 4.2. These experiments mainly focused on the inner temperature distribution of the HEX/reactor under different flow rates.

Experimental data were collected from eight thermocouples. Four of them were in the first half of the process plate, which is shown in Figure 4.10. Two sensors were implemented at the entrance of the other two process plates, while the other two were used to detect the input temperature of the first process plate and the output temperature of the third process plate. It is obvious that all the internal sensors were located at the connecting area of two horizontal process channels. However, according to the partition rules, the output temperature of each process cell was actually the average value of that cell. Thus, after simulation, a linear interpolation between two neighboring process cells was introduced to get a more accurate calculation of sensor

Table 4.2: Experimental conditions for simulating the heat exchange experiments [105]

Experiment No.	Utility Stream		Process Stream	
	$(kg \cdot h^{-1})$	(°C)	$(kg \cdot h^{-1})$	(°C)
1	57.0			
2	75.2			
3	87.8	≈ 15.6	≈ 10.0	≈ 77.0
4	111.3			
5	127.0			
6	151.0			
7			2.4	
8			5.5	
9	≈ 152.0	≈ 15.6	8.7	≈ 77.0
10			12.2	
11			15.0	

outputs.

Simulations were run with the same operating conditions as the experiments. After that, data from simulations were compared with those from experiments. Figure 4.11 shows the simulation results of experiments 1 to 4 and 6 (corresponding to different utility flow rates), and Figure 4.12 presents those of experiments 7 and 9 to 11 (corresponding to different process flow rates). These two figures could be compared with Figure 4.13 and Figure 4.14, presented in [105] to see the general behavior of the developed model. The HEX/reactor was very efficient from heat transfer aspect, as the heat exchange process was almost completed at the first plate. When the flow rate of the process channel was fixed in Figure 4.11, more heat was taken away by the utility fluid as its flow rate increased. As expected, output temperature would be lower with a higher utility flow rate. This trend was opposite when the utility flow-rate was fixed in Figure 4.12. Output temperature would be higher if the process fluid ran more quickly. Features of these simulation results were consistent with the natural fact and the experiments reported in [105]. More detailed validations were carried out using the reserved data. The computing time varied according to the performance of the computer. Generally, it took about $90s$ to simulate a process of $300s$ in real time on an i7-5500U platform.

There was an interesting phenomenon that nearly all the simulations had a minimal temperature at 0.33 L_{sensor}/L_{total}. In fact, the sensor located there was just at the

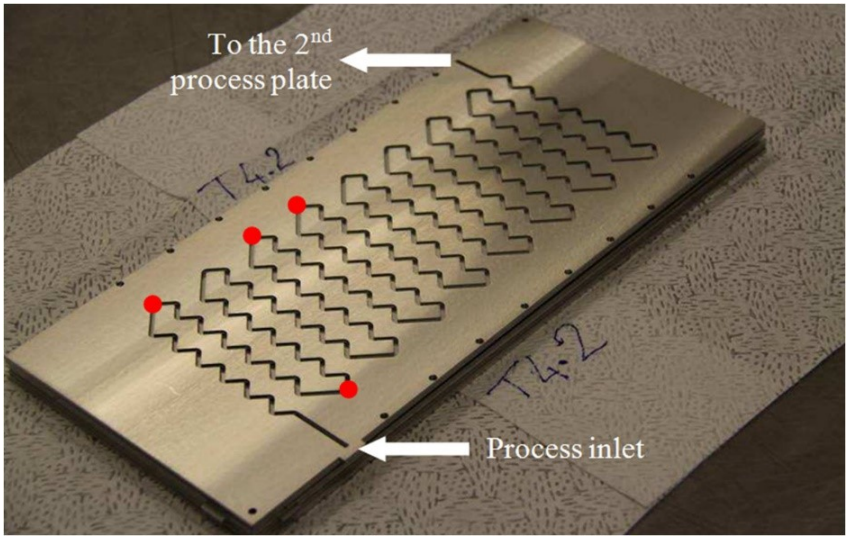

Figure 4.10: Localization of five thermocouples in the first process plate [105]

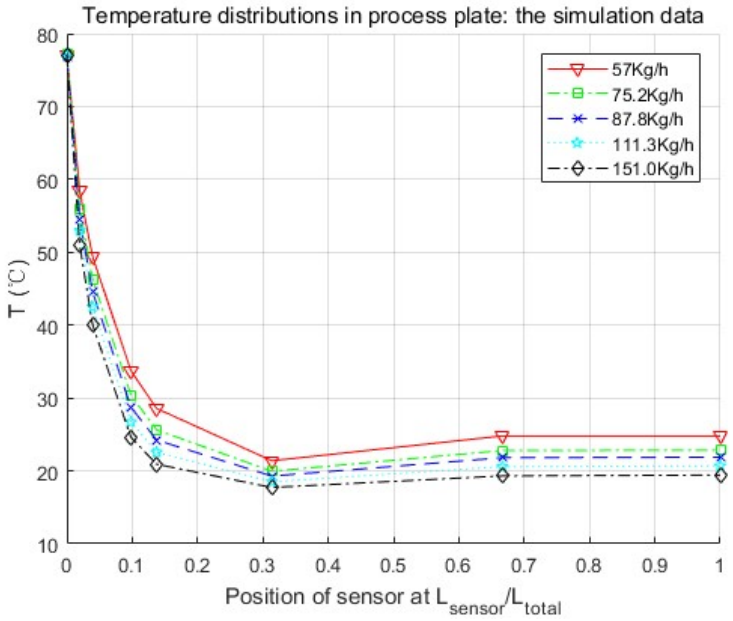

Figure 4.11: Simulation results of the process fluid temperature along the process channel for different utility flow rates, with $\dot{M}_p = 10kg \cdot h^{-1}$ and $T_{p-in} = 77°C$

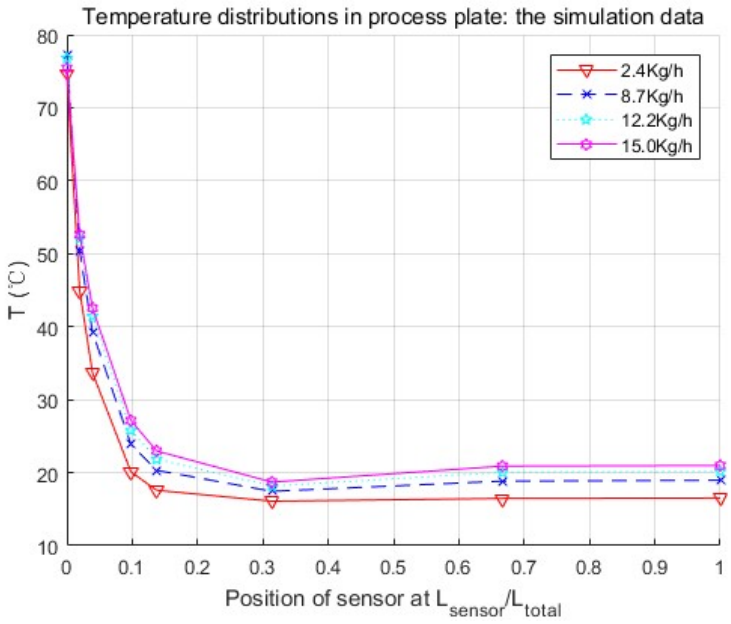

Figure 4.12: Simulation results of the process fluid temperature along the channel for different process flow rates, with $\dot{M}_u = 152kg \cdot h^{-1}$ and $T_{u-in} = 15.6°C$

entrance of the second process plate, and it was directly connected to the exit of the first process plate. As can be seen in Figure 4.2, we had opposite directions for the two injected fluids. For the simulation results presented in Figures 10 and 11, the utility fluid had a lower temperature than the process fluid. When the process fluid started its journey in the HEX/reactor, it started cooling down. When it came to the end of the first process plate, the process fluid was facing the newly injected utility fluid nearby. As, in this area, the utility fluid had the lowest temperature, it absorbed the heat through the plate wall and generated a minimal temperature for the process fluid. This was measured by the neighboring sensor at the beginning of the second process plate and presented in the figures mentioned above. Experiments presented in Reference [105] showed the same behavior.

4.5 Validation

To validate the accuracy and the relevance of the model and make comparisons with experiments, simulations were performed in two parts, as were the experiments. The first one concerned the heat exchange behaviors between process and utility fluid without chemical reaction. The second part introduced an exothermic chemical reaction to test the validity of the complete model. As data of Experiment 5 and Experiment

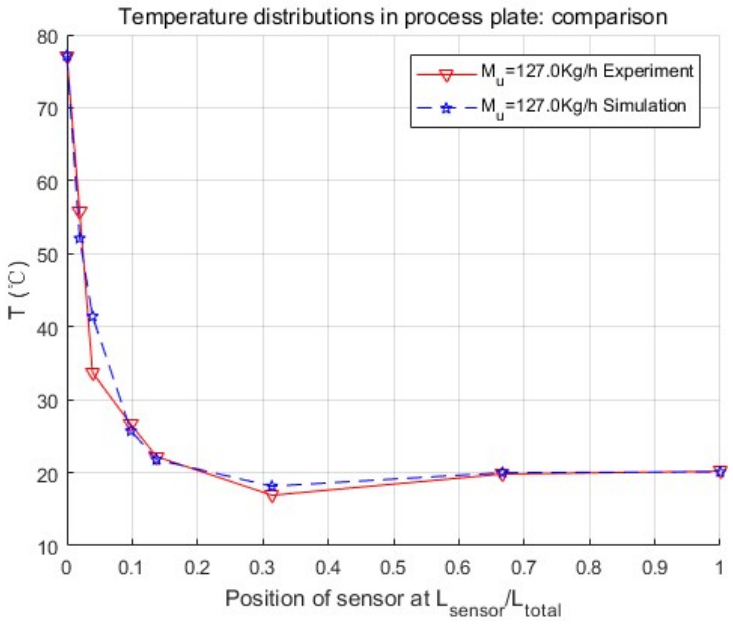

Figure 4.13: Comparison of inner temperature distribution of Experiment 5 with $\dot{M}_p = 10kg \cdot h^{-1}$ and $T_{p-in} = 77°C$

8 in Table 4.2 were not involved in parameter searching, simulations of these two experiments were used for the validation of the heat exchange part.

4.5.1 Validation of Heat Exchange Procedure

Simulations of Experiment 5 and Experiment 8 are compared with experimental data here in Figure 4.13 and Figure 4.14. Because these two groups of data were not used before in the parameter searching section, they could be used to verify if the searched parameters worked well or not.

According to Figure 4.13 and Figure 4.14, not only did temperatures obtained in simulations and experiments vary in the same manners, but their inner distributions were also close. Errors of the simulation results of the third sensor were relatively big.However, all other spots worked very well, in that they were quite close to the experimental values. Furthermore, output temperatures were identical, even though there was a little difference in the first process plate.

Based on these comparisons, the performance of the model developed in this paper in the calculation of heat exchange was acceptable. Results were highly consistent with the experiments.

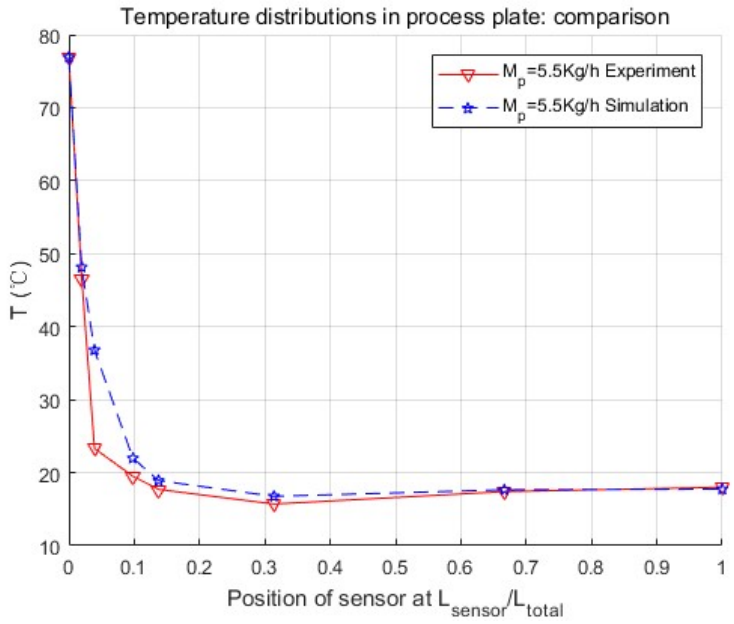

Figure 4.14: Comparison of inner temperature distribution of Experiment 8 with $\dot{M}_u = 152kg \cdot h^{-1}$ and $T_{u-in} = 15.6°C$

4.5.2 Simulation Results of Heat Exchange with Reaction

In this part, concentrations of sodium thiosulfate $Na_2S_2O_3$ and hydrogen peroxide H_2O_2 were both set to 9% in mass. Generally, it takes approximately $100s$ for the reactor to reach a balance state for the heat exchange procedure without reaction. Then reactants were introduced at time $t = 150s$, and the reaction began. Five simulations were launched in this part[105]. Table 4.3 gives the details of operating conditions, output temperatures, and conversion rates, which were counted in different ways.

As the concentrations were both set to 9% in mass, hydrogen peroxide H_2O_2 was

Table 4.3: Comparisons of experiment and simulation data with reaction

Data Source	Operating Condition					Output Temperature		Conversion Rate (%)		
	F_{p1}[*1] $(L \cdot h^{-1})$	F_{p2}[*2] $(L \cdot h^{-1})$	T_{p-in} $(°C)$	$\dot{M}_u$ $(kg \cdot h^{-1})$	T_{u-in} $(°C)$	T_{p-out} $(°C)$	T_{u-out} $(°C)$	Reactor	Dewar	C[*3] $(Na_2S_2O_3)$
Experiment 1	9.3	4.7	17.6	113.0	39.7	43.9	39.9	60	59	–
Simulation 1						39.4	39.2	–	–	67
Experiment 2	3.3	1.7	19.3	113.5	39.7	41.4	40.4	82	94	–
Simulation 2						39.9	39.8	–	–	90
Experiment 3	4.7	2.3	20	113.0	39.7	43.4	41.1	88	91	–
Simulation 3						39.9	39.8	–	–	83
Experiment 4	4.7	2.3	20.7	112.0	49.6	51	50.7	93	100	–
Simulation 4						49.4	49.4	–	–	94
Experiment 5	4.7	2.3	21.1	112.5	59.4	59.2	60.1	95	100	–
Simulation 5						58.7	58.7	–	–	99

[*1] The flow-rate of reactant $Na_2S_2O_3$

[*2] The flow-rate of reactant H_2O_2

[*3] C($Na_2S_2O_3$) denotes that conversion rates below are calculated by the concentration loss of $Na_2S_2O_3$

in excess during the reaction. Therefore, the conversion rate in the simulation was calculated regarding the concentration loss of thiosulfate $Na_2S_2O_3$. By contrast, in the experiments, two methods were used to calculate the conversion rates, which were based for the first on the thermal balance in the reactor, and for the second, on the use of thermal balance in a Dewar vessel after the output of the reactor (see [105]).

Data in Table 4.3 show the interesting fact that the temperature gap between the outlets of process channel and utility channel grew smaller as the conversion rate rose. It is true that, when the conversion rate was low, the reaction took place all along the reactor till the last minute. That means materials in process channel kept generating heat, and some could not be taken away immediately in the end. Thus, the temperature gap was relatively large. While there was a higher conversion rate, the reaction mostly took place in the first plate, which left enough time for heat exchanging. Thus, the temperature gap was smaller in the end.

Figure 4.15 shows the dynamic procedure of the simulation with reaction. The steady state was reached at about $100s$. During this period, the process channel was fed with water at the same temperature as the reactants. The time it took to reach a steady state differed in the function of the operating conditions for the different experiments. Conservatively, reactants were introduced at time $t = 150s$. After a residence time around $7s$, the output temperature started to change. A new steady state was reached after about $100s$. Simulations of other experiments with reaction had similar trends.

It could be noticed that the kinetic parameters of the reaction are those given by [7] and have not been fitted to the experimental data. These parameters could be renewed if there is a more accurate research about this reaction. Parameters of other reactions could also be used here to investigate the performance of the targeting HEX/reactor under these reactions. For the conversion rate, experimental data calculated from the thermal balance method have errors because concentrations of products are difficult to detect precisely in mixtures. This model presents an ideal way to simulate and calculate it.

Overall, from the comparisons between experiments and simulations, it could be deduced that the model proposed in this paper is generally valid to the HEX/reactor for both the heat exchange and reaction parts.

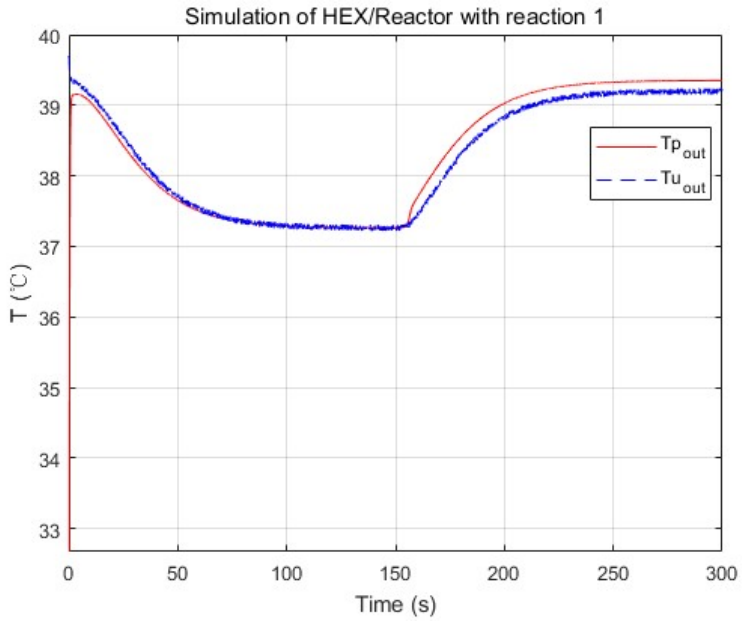

Figure 4.15: Simulated temperature profiles for experiment 1 (reaction was introduced at $150s$)

4.6 Summary

In this paper, the modeling process of an intensified HEX/reactor is presented in detail, which is different from previous studies in the introducing of the chemical reaction, the modeling platform, and the combination of the physical structure and thermal features of the model. At first, the physical structure was studied, and the continuous process was discretized into cells. Consequently, the representative equations of each cell were given under the consideration of heat exchange, fluid movements, and chemical reaction. These differential equations were introduced in the general simulation platform, Matlab/Simulink. After that, three parameters concerning the heat transfer coefficient were searched by genetic algorithm, and a non-linear model of 255 basic calculating modules was developed. Finally, several simulations were launched in different working conditions to make comparisons with the experimental data.

Simulation results were quite consistent with the experiments. For the heat exchange part, this model had very accurate inner temperature distributions toward the HEX/reactor. For the reaction part, this model also performed well, in that it generated good dynamic curves, as the physical one did. Furthermore, conversion rate, which is a crucial parameter to a chemical reactor, could be easily and precisely computed from the concentration loss of reactants in the model. Thus, it could be concluded that the nominal model obtained in this paper is accurate and equivalent to the real

HEX/reactor. One thing should be mentioned is that the modeling methodology implemented in this paper is not restricted, and could also be used for other reactions and other sizes of HEX/reactors by replacing parameters to specific reactions or reactor size. The cell number could also be optimized to meet the requirements of accuracy, calculation consumption, or consistency to the physical reactor.

The purpose of modeling the HEX/reactor is for further control use. With the model developed in this paper, internal states, as well as conversion rates, were easily achieved while simulating. Algorithms like model-based observers could be designed and validated conveniently on this model. These algorithms can then be used for developing approaches like fault detection, isolation, identification, and fault-tolerant control, which could be implemented on real plants to improve the performance of HEX/reactors on safety, efficiency, and productivity.

Chapter 5

FTC Strategy through Direct Multiple Model Matching and Its Application to the HEX/Reactor

Based on the nominal model of the heat exchange reactor developed in the previous chapter, this chapter focuses on the fault-tolerant control application for it. To avoid the difficulties and strong nonlinearities that may be encountered in designing a fault-tolerant scheme for this reactor, especially after the introduction of chemical reactions, this chapter designs the FTC scheme according to the two-layer multiple model structure proposed before. The first layer is dedicated to represent the nonlinear system through a set of local linear models, while the second layer uses a multiple model bank to deal with fault situations. Here, a model set consisting of simple linear local models is obtained by system identification, and Model Predictive Control (MPC) is used to design the corresponding controller bank. Afterwards, the Unscented Kalman Filter (UKF) is introduced to estimate the states and form the fault detection and diagnosis (FDD) module. Finally, simulations were performed under two fault assumptions, heat transfer coefficient fault and input utility fluid temperature fault, to verify the performance of the proposed fault tolerant strategy. The two-layer multiple model structure provides a general framework for fault-tolerant control design of complex and highly nonlinear systems such as heat transfer reactors whose mathematical models have been created. It also implements the design process in a unconventional way that is worth trying in other cases as well.

5.1 Two-layer multiple model bank construction

5.1.1 Mathematical model of the HEX/Reactor

The nominal model construction of the target heat exchange reactor was conducted from the physical structure as well as the chemical and thermodynamic directions in the previous chapter. The nominal model is obtained under the consideration of a strong exothermic reaction of sodium thiosulfate with hydrogen peroxide.

$$2Na_2S_2O_3 + 4H_2O_2 \rightarrow Na_2S_3O_6 + Na_2SO_4 + 4H_2O \tag{5.1}$$

The entire model is made up of 17 units and within each unit there are 15 basic cells. Therefore, the total cell number is 255. It is somehow too complex to begin with. For this reason, we start from a typical group of three basic cells to skip the complexity first. The relationship between the cell/unit number and the precision of the model has also been discussed before [125]. Thus,basic dynamics of the HEX reactor with reaction could be given [49]:

$$\begin{cases} \dot{T}_p = \dfrac{F_{p1}+F_{p2}}{V_p}(T_{pin}-T_p) + \dfrac{h_pA_p}{\rho_pV_pC_p}(T_w-T_p) + \dfrac{\Delta H}{\rho_pC_p}k^0 exp(-\dfrac{E_a}{R(T_p+273.15)})C_1C_2 \\ \dot{T}_u = \dfrac{F_u}{V_u}(T_{uin}-T_u) + \dfrac{h_uA_u}{\rho_uV_uC_u}(T_w-T_u) \\ \dot{T}_w = \dfrac{h_pA_p}{\rho_wV_wC_w}(T_p-T_w) + \dfrac{h_uA_u}{\rho_wV_wC_w}(T_u-T_w) \\ \dot{C}_1 = \dfrac{F_{p1}+F_{p2}}{V_p}(C_{1in}-C_1) - 2k^0 exp(-\dfrac{E_a}{R(T_p+273.15)})C_1C_2 \\ \dot{C}_2 = \dfrac{F_{p1}+F_{p2}}{V_p}(C_{2in}-C_2) - 4k^0 exp(-\dfrac{E_a}{R(T_p+273.15)})C_1C_2 \end{cases} \tag{5.2}$$

where T_p, T_u, T_w, C_1, C_2 are temperature of process channel, temperature of utility channel, temperature of plate-wall, concentration of $Na_2S_2O_3$ and concentration of H_2O_2 respectively. F_{p1}, F_{p2} and F_u are the input flow rate of process and utility channels. V, A, h, ρ and C stand for volume, heat exchange area, heat transfer coefficient, density and specific heat capacity. k^0 is a pre-exponential factor of the reaction; E_a is the activation energy; R is the perfect gas constant and ΔH is the unit heat generated by the reaction. Detailed values of these parameters could be found in [50].

Apparently, researches on fault detection, isolation, and identification for the HEX reactor is the prerequisite for further implementations. An FTC system is able to

recover and continue to operate as in normal conditions or to maintain the stability to the desired level when a fault occurs. Developing suitable FTC strategies becomes a must to ensure the reliability.

For simplicity, we set the flow-rate of utility fluid F_u as the only input and the temperature of process channel T_p as the only output of the system to start from a SISO case. This hypothesis is consistent with the reality that the inputs of reactants would generally have a fixed optimal proportion while no restrictions would be set on utility flow-rate. As for the output, temperature of the reactants is always an important index of the reaction. Thus, F_u and T_p in (5.2) are suitable to set as the input and output of the system.

5.1.2 Construction of the first layer multiple model

The two-layer multiple model structure proposed here is generally an expansion of the classical multiple model approach. As is known, multiple model approaches use the divide-and-conquer strategy to deal with complexity in engineering systems [76]. For a complex nonlinear system, local models, which are valid for certain ranges of workspace, are combined to describe the complete workspace.

Since the original nonlinear model (5.2) is available, virtual experiments could be done by simulations to generate enough data for local model identification. As the HEX reactor is considered as a SISO system first, the input F_u could be a suitable candidate of decision variable [84] which indicates the validity of local models.

The first layer of multiple models is then created using system identification method. For the given HEX reactor, assume that the input F_u ranges from 0 to 200 L/h. First, interval inputs could be generated by adding white noises on base signals (see Figure 5.1: Fu).

By applying the interval inputs on model (5.2) one by one, corresponding outputs could be generated (see Figure 5.1: Tp). Thus, several sets of IO data are prepared and we come to the second step: local model identification. The following ARX structure is chosen for local models.

$$x_j(k+1) = a_{1j}x_j(k) + a_{2j}x_j(k-1)\cdots + b_{1j}u(k-d) + b_{2j}u(k-d-1)\cdots + c_j \quad (5.3)$$

where j denotes the number of local models; a_{ij}, b_{ij} are parameters of the regressors; c_j is an offset and d is the time delay.

After investigating, the residence time of process fluid would be a key parameter for estimating the time delay. In this work, we suppose that F_{p1} and F_{p2} equal to $4.7L/h$

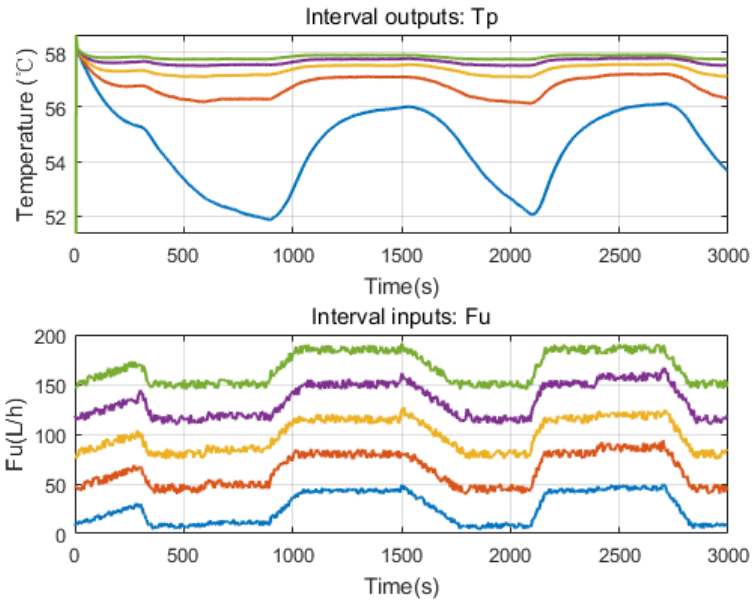

Figure 5.1: The interval inputs and outputs from virtual experiments (The color indicates the IO pair).

and $2.3L/h$ respectively. The residence time is then around 10 seconds. Thus, the time delay is 2 steps when sample time is set to 5 seconds. Orders of the local model could be found using a modified Lipschitz-quotient method proposed in [17].

When local models are identified by the classical least square approach, they are combined by a switching function to generate an overall output according to current input. A multiple model bank in the first layer is given by:

$$\begin{cases} x_j(k+1) = a_{1j}x_j(k) + a_{2j}x_j(k-1)\cdots + b_{1j}u(k-d) + b_{2j}u(k-d-1)\cdots + c_j \\ y(k) = f(u(k), x_j(k)) \end{cases} \tag{5.4}$$

where y is the overall estimation of T_p given by the model bank; f is a switching function whose decision variable and candidate outputs are the input u and outputs of local models x_j respectively; u is F_u in (5.2).

For verifying the accuracy , a set of input signal, which vibrates in a big range, are send to both the original nonlinear model and the first layer model bank (see Figure 3).

According to Figure 5.2, the behavior of the nonlinear system is well captured by the model bank with 5 local models. It also shows that the switching strategy is used and different local model is activated when input F_u goes into its corresponding interval. The number of local models is a parameter which should be investigated. Figure 5.3

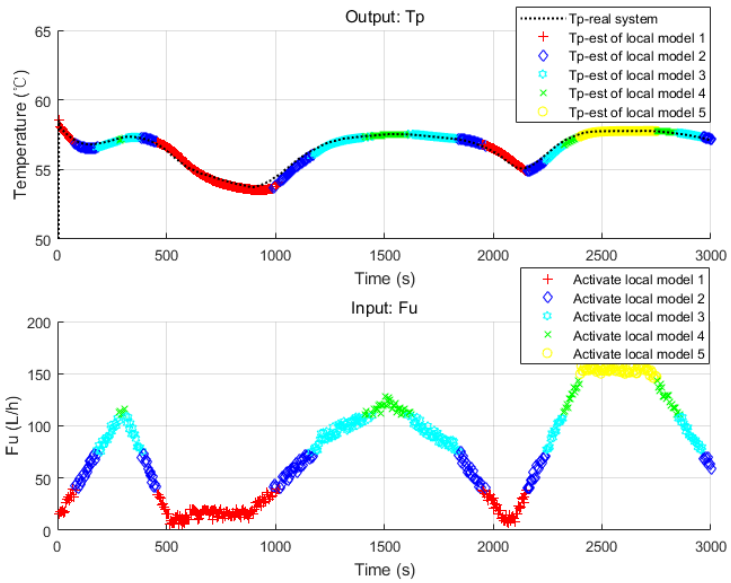

Figure 5.2: Verification of the first layer model bank using inputs of integral range.

shows the accuracy of model banks with different quantity of local models. Apparently, for the case of our HEX reactor, 5 local models are enough to constitute a model bank to describe the original system in a high economic and accurate way.

5.1.3 Construction of the second layer model bank

The construction of the second layer, which concerns about faults, would be a simple extension of the same steps to the second dimension. In this paper, we mainly focus on dynamic faults, i.e. the change of plant parameters. For simplicity, single fault is considered here. Thus, as defined in biographies, a fault would be caused by the deviation of a parameter from its nominal value [73]. When the reactor works, there is a possibility that materials in the fluids may stay at the inner surface of the channels, which affects the performance of the heat exchange process. It is a typical fault of this reactor and could be considered as the change of heat transfer coefficient h. Therefore, the value of this parameter is chosen to set faulty intervals for the construction of the second layer model banks. Virtual experiments could be carried out to generate I/O data with these intervals. We set four faulty situations (80%h, 60%h, 40%h, 20%h) along with one nominal case (100%h). By repeating the identification process of the first layer model bank, a two-dimension multiple model matrix is given (see Figure 5.4).

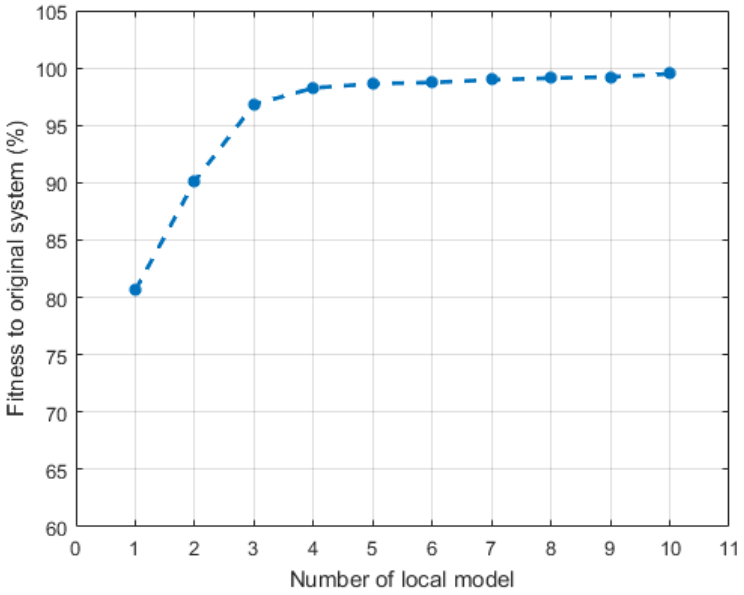

Figure 5.3: The accuracies of multiple model bank with different total number of local models.

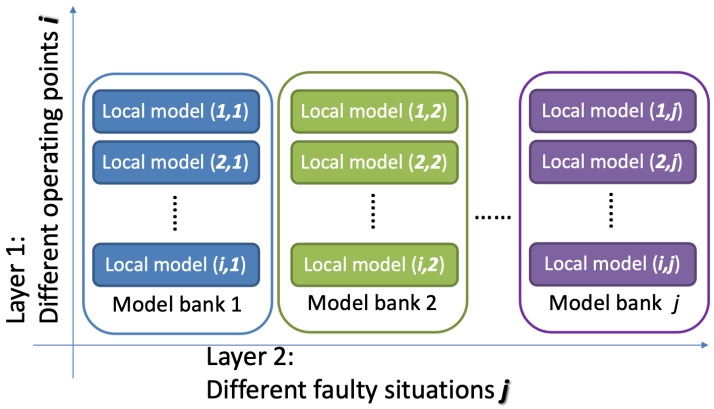

Figure 5.4: Two-layer multiple models.

5.2 Two-layer controller bank design

Controller design for the complex HEX reactor is easy now because the highly nonlinear system is described by equivalent model banks using linear local models. The task becomes designing controllers for these homogeneous local linear models where nearly all kinds of controllers can competent. Thus, several controller banks, which are considered at the second layer, are constructed according to the model banks. Inside each controller bank, multiple controllers are defined as in the first layer.

5.2.1 Controller bank design

Model predictive control [114][116], for its popularity and capability of handling hard constraints in the process control domain, is chosen here for constructing the corresponding controller banks. To achieve that, some transformations should be done on the local models. First, we transform them from ARX (5.3) to state-space-like form by defining a new state vector and input vector in the following way:

$$\boldsymbol{x}_{mj}(k) = \begin{bmatrix} x_j(k) \\ x_j(k-1) \\ \vdots \end{bmatrix} \tag{5.5}$$

$$\boldsymbol{u}_j(k) = \begin{bmatrix} u(k-d) \\ u(k-d-1) \\ \vdots \end{bmatrix} \tag{5.6}$$

where $u(k)$ and $x_j(k)$ stand for the input and the local estimation of state at step k. The lengths of the two vectors are dependent on the order and time delay of the local model.

In this way, the following state-space-like model is given:

$$\begin{cases} \begin{bmatrix} x_j(k+1) \\ x_j(k) \\ \vdots \end{bmatrix} = A_{mj} \begin{bmatrix} x_j(k) \\ x_j(k-1) \\ \vdots \end{bmatrix} + Bmj \begin{bmatrix} u(k-d) \\ u(k-d-1) \\ \vdots \end{bmatrix} + \begin{bmatrix} c_j \\ 0 \\ \vdots \end{bmatrix} \\ \hat{y}_j(k) = \begin{bmatrix} 1 & 0 & \cdots \end{bmatrix} \begin{bmatrix} x_j(k) \\ x_j(k-1) \\ \vdots \end{bmatrix} \end{cases} \tag{5.7}$$

where A_m, B_m are matrices calculated from the transformation of ARX model and the item containing c_j concerns about the offset in (5.3). Model (5.7) could be written in

(5.8) for short:

$$\begin{cases} \boldsymbol{x}_{mj}(k+1) = A_{mj}\boldsymbol{x}_{mj}(k) + B_{mj}\boldsymbol{u}_j(k) + \boldsymbol{c}_j \\ \hat{y}_j(k) = C_{mj}\boldsymbol{x}_{mj}(k) \end{cases} \tag{5.8}$$

By making a difference on state and input vectors, offset vector $\boldsymbol{c}_j$ could be eliminated:

$$\Delta\boldsymbol{x}_{mj}(k+1) = \boldsymbol{x}_{mj}(k+1) - \boldsymbol{x}_{mj}(k) \tag{5.9}$$

$$\Delta\boldsymbol{u}_j(k) = \boldsymbol{u}_j(k) - \boldsymbol{u}_j(k-1) \tag{5.10}$$

Define a new state vector:

$$\boldsymbol{x}_j(k) = \begin{bmatrix} \Delta\boldsymbol{x}_{mj}(k) & \hat{y}_j(k) \end{bmatrix}^T \tag{5.11}$$

Then, an augmented system is given by combining from (5.7) to (5.10):

$$\begin{cases} \boldsymbol{x}_j(k+1) = \begin{bmatrix} A_{mj} & o \\ C_{mj}A_{mj} & 1 \end{bmatrix} \begin{bmatrix} \Delta\boldsymbol{x}_{mj}(k) \\ \hat{y}_j(k) \end{bmatrix} + \begin{bmatrix} B_{mj} \\ C_{mj}B_{mj} \end{bmatrix} \Delta\boldsymbol{u}_j(k) \\ \hat{y}_j(k) = \begin{bmatrix} o & 1 \end{bmatrix} \begin{bmatrix} \Delta\boldsymbol{x}_{mj}(k) \\ \hat{y}_j(k) \end{bmatrix} \end{cases} \tag{5.12}$$

And (12) is written in (13) for short:

$$\begin{cases} \boldsymbol{x}_j(k+1) = A_j\boldsymbol{x}_j(k) + B_j\Delta\boldsymbol{u}_j(k) \\ \hat{y}_j(k) = C_j\boldsymbol{x}_j(k) \end{cases} \tag{5.13}$$

Therefore, a standard MPC design [114] is carried out in the following steps based on (5.13). First, we assume that the future control signal is known. Then, the future states and outputs are predicted according to current data in step k:

$$Y_j(k) = F_jX_j(k) + \phi_j\Delta U_j \tag{5.14}$$

where $Y_j(k)$, $X_j(k)$ are predictions of states and outputs computed at step k; ΔU_j is the future incremental control inputs. Elements in (5.14) are constructed in the following way:

$$Y_j(k) = \begin{bmatrix} \hat{y}_j(k+1|k) \\ \hat{y}_j(k+2|k) \\ \vdots \\ \hat{y}_j(k+N_p|k) \end{bmatrix} \tag{5.15}$$

$$X_j(k) = \begin{bmatrix} \boldsymbol{x}_j(k+1|k) \\ \boldsymbol{x}_j(k+2|k) \\ \vdots \\ \boldsymbol{x}_j(k+N_p|k) \end{bmatrix} \tag{5.16}$$

$$\Delta U_j = \begin{bmatrix} \Delta \boldsymbol{u}_j(k) \\ \Delta \boldsymbol{u}_j(k+1) \\ \vdots \\ \Delta \boldsymbol{u}_j(k+N_c-1) \end{bmatrix} \tag{5.17}$$

$$F_j = \begin{bmatrix} C_j A_j \\ C_j A_j^2 \\ \vdots \\ C_j A_j^{N_p} \end{bmatrix} \tag{5.18}$$

$$\Phi_j = \begin{bmatrix} C_j B_j & 0 & \cdots & 0 \\ C_j A_j B_j & C_j B_j & \cdots & 0 \\ \vdots & \vdots & \ddots & \vdots \\ C_j A_j^{N_p-1} B_j & C_j A_j^{N_p-2} B_j & \cdots & C_j A_j^{N_p-N_c} B_j \end{bmatrix} \tag{5.19}$$

where N_p and N_c are prediction horizon and control horizon respectively.

For a given reference signal R_s, prediction error can be defined:

$$E_j = R_s - Y_j \tag{5.20}$$

The following cost function is given based on the prediction error:

$$J_j = E_j^T E_j + \Delta U_j^T \bar{R} \Delta U_j \tag{5.21}$$

where $\bar{R}$ is a positive penalty parameter concerning about the magnitude of control input.

By letting the first derivative of J_j (5.22) equal to zero, optimal control value (5.23) could be calculated:

$$\frac{\partial J_j}{\partial \Delta U_j} = -2\Phi_j^T (R_s - F_j X_j(k)) + 2(\Phi_j^T \Phi_j + \bar{R}) \Delta U_j \tag{5.22}$$

$$\Delta U_j = (\Phi_j^T \Phi_j + \bar{R})^{-1} \Phi_j^T (R_s - F_j X_j(k)) \tag{5.23}$$

For each calculation step, only the first element of ΔU_j will be implemented. Calculations would be done again for the next step to carry out the dynamic optimization strategy of MPC.

All local controllers could be created in the same way according to their corresponding local models. A similar switching strategy using input as the decision variable is implemented to manage the controllers to give out an overall output of the controller bank. In this way, controller design of the complex nonlinear system is solved by designing sub-controllers for simple linear local models. Controller design for the second layer is carried out the same way using the information of the second layer model banks.

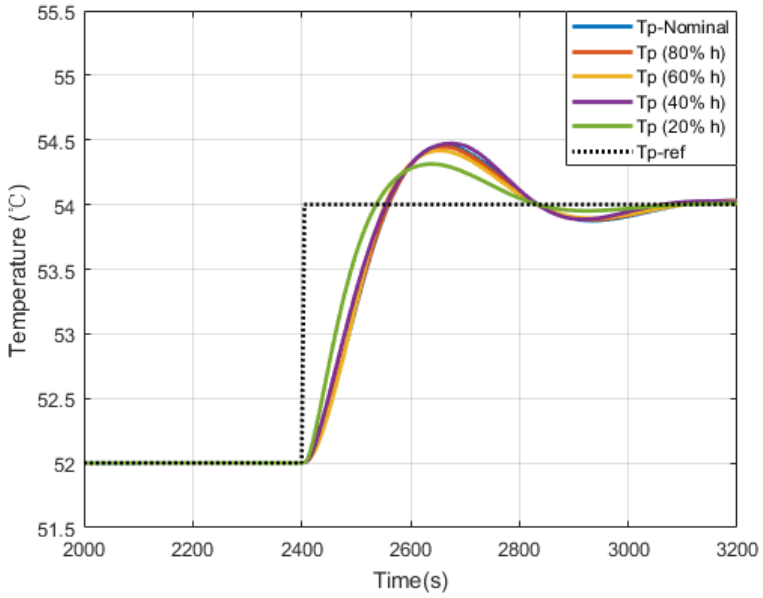

Figure 5.5: Performances of controller banks under the same reference Tp-ref after tuning.

5.2.2 Tuning of the second layer controller banks

The key problem is that the performances of all the controller banks should be tuned to be similar. Only in this way can the FTC strategy behave well when the controller bank is switched during faulty situations.

Among the three parameters which could be adjusted in MPC, penalty $\bar{R}$ is the most sensitive one. After setting a standard performance in the nominal controller bank, other controller banks could achieve similar performances by adjusting $\bar{R}$. Here we choose the convergence time as the index, and introduce binary search to finish the job to have a result as shown in Figure 5.5. The corresponding vector for $\bar{R}$ of each controller bank in Figure 6 is $\begin{bmatrix} 0.0300 & 0.0149 & 0.1453 & 0.0755 & 0.0093 \end{bmatrix}$.

After the tuning procedure, it is obvious in Figure 5.5 that the performances of each controller bank are getting similar toward the same step reference. This implies that the two-layer controller bank is obtained.

5.3 Fault detection and isolation section

5.3.1 The Unscented Kalman Filter

The Unscented Kalman Filter was proposed by Julier and Uhlman in in the context of state-estimation for nonlinear systems [61]. To avoid the linearization process in the famous Extended Kalman Filter(EKF), a finite set of weighed sigma points will be generated by the UKF to compute the predicted states and measurements and the associated covariance matrices [93]. Generally, the UKF estimates the states of nonlinear systems according the flowing steps.

Step 1: determine the set of sigma points and calculate the corresponding weights.

$$\hat{x}^a_{k-1|k-1} = \begin{bmatrix} \hat{x}_{k-1|k-1} \\ \mathbf{0} \\ \mathbf{0} \end{bmatrix} \tag{5.24}$$

$$P^a_{k-1|k-1} = \begin{bmatrix} P_{k-1|k-1} & \mathbf{0}^{L\times q} & \mathbf{0}^{L\times r} \\ \mathbf{0} & Q_{k-1} & \mathbf{0} \\ \mathbf{0} & \mathbf{0} & R_{k-1} \end{bmatrix} \tag{5.25}$$

$$\chi^a_{k-1} = \hat{X}^a_{k-1|k-1} + \begin{bmatrix} \mathbf{0} & \sqrt{(L^a+\lambda)P^a_{k-1|k-1}} & -\sqrt{(L^a+\lambda)P^a_{k-1|k-1}} \end{bmatrix} \tag{5.26}$$

$$W_i = \begin{cases} \dfrac{\lambda}{2(L^a+\lambda)}, & i = 1 \\ \dfrac{1}{2(L^a+\lambda)}, & otherwise \end{cases} \tag{5.27}$$

where L is the dimension of state vector of the original system, Q and R are tuning parameters of the filter, λ is the scaling factor denoting the distance for choosing sigma points, W is the weight.

Step 2: prediction.

$$\chi^x_k = f(\chi^x_{k-1}, \chi^w_{k-1}, u_{k-1}) \tag{5.28}$$

$$\gamma_k = h(\chi^x_k, \chi^v_{k-1}, u_k) \tag{5.29}$$

$$\hat{x}_{k|k-1} = \sum_{i=1}^{2L^a+1} W_i \chi^x_{i,k} \tag{5.30}$$

$$\hat{y}_k = \sum_{i=1}^{2L^a+1} W_i \gamma_{i,k} \tag{5.31}$$

where $f(\cdot)$ and $h(\cdot)$ are nonlinear system function and output function respectively.

Step 3: update.

$$P_{k|k-1} = \sum_{i=1}^{2L^a+1} W_i [\chi^x_{i,k} - \hat{x}_{k|k-1}][\chi^x_{i,k} - \hat{x}_{k|k-1}]^T \tag{5.32}$$

$$P_{y,k} = \sum_{i=1}^{2L^a+1} W_i[\gamma_{i,k} - \hat{y}_k][\gamma_{i,k} - \hat{y}_k]^T \tag{5.33}$$

$$P_{xy,k} = \sum_{i=1}^{2L^a+1} W_i[\chi^x_{i,k} - \hat{x}_{k|k-1}][\gamma_{i,k} - \hat{y}_k]^T \tag{5.34}$$

$$K_k = P_{xy,k} P_{y,k}^{-1} \tag{5.35}$$

$$P_{k|k} = P_{k|k-1} - K_k P_{y,k} K_k^{-1} \tag{5.36}$$

$$\hat{x}_{k|k} = \hat{x}_{k|k-1} - K_k(y_k - \hat{y}_k) \tag{5.37}$$

5.3.2 UKF based fault detection and isolation

Since the nonlinear system function is available in this paper, state estimation using UKF is easy to apply by giving the parameters of noise. To detect the fault, one can simply define the residual e as the difference between the system output and the estimated output and check if it exceeds a certain threshold.

To achieve the FTC using the proposed two-layer multiple model structure, a bank of Unscented Kalman Filters could be created to form a set of interval observers, which has the ability to isolate the fault and determine the faulty interval by checking the corresponding residuals.

$$\begin{cases} \hat{x}_{k,i} = UKF(f_{\theta i}, \hat{x}_{k-1}, u_k) \\ \hat{y}_{k,i} = h(\hat{x}_{k,i}) \end{cases} \tag{5.38}$$

$$e_{k,i} = y_k - \hat{y}_{k,i} \tag{5.39}$$

where UKF denotes the Unscented Kalman Filter and $f_{\theta i}$ is a system function with the faulty parameter θ_i.

One thing should be noticed is that the isolation of the fault should be carried out when the effect of the fault is getting relatively stable. Otherwise, the result given in the transient period may not be trustful. For this reason, one defines an index z which equals to the absolute value of the derivative of residuals to determine if it is the time to do interval checking.

$$z_i \triangleq |diff(e_i)| \tag{5.40}$$

The FDI strategy would be implemented first by checking elements of $z_{k,i}$ to see if at least one of them exceeds the detection threshold. If it holds, a fault is detected happening. Then, checking z_i step by step when all of its elements are not higher than the fault isolation threshold, which means estimations are stable and it's the time to

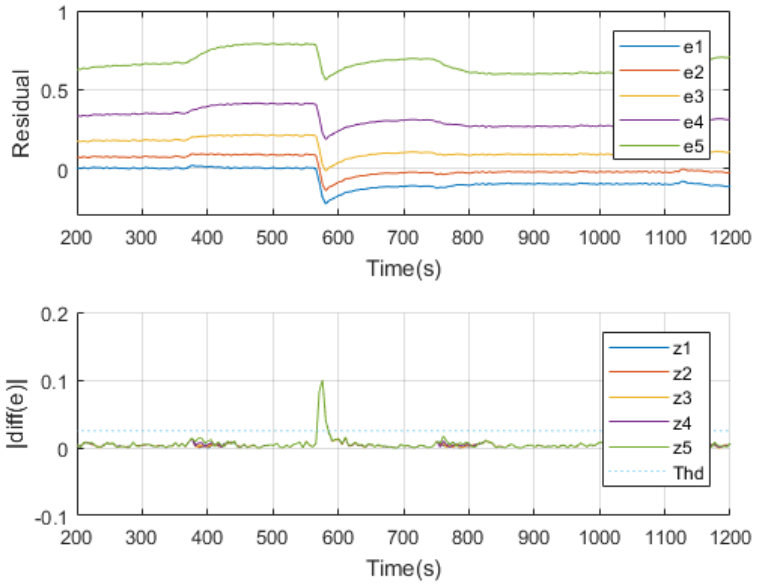

Figure 5.6: FDI process using interval unscented Kalman filters

determine the fault interval. At this moment, residuals e_k would behave with interval features. It is easy to find the two filters who hold the zero residual by checking if $e_{k,i} \cdot e_{k,i+1} \leq 0$.

As is illustrated in Figure 5.6, a fault is introduced at 560s. It is detected several seconds when one of z_i beyonds the threshold. After about 20 seconds, all of z_i reduced and below the threshold. At this moment, behaviors of the residuals get stable and it is easy to see that e_2 and e_3 cover the zero axis, indicating the fault value is in the assumed second interval. Thus the fault is isolated.

5.4 FTC simulation and analysis of the HEX/Reactor

The FTC strategies described in the former sections are simulated here. Key information about the HEX reactor, exothermic reaction, and initial states of the simulation are listed in Table 1. Besides, concentrations of sodium the two reactants are both set to 9% in mass just as the experiments did.

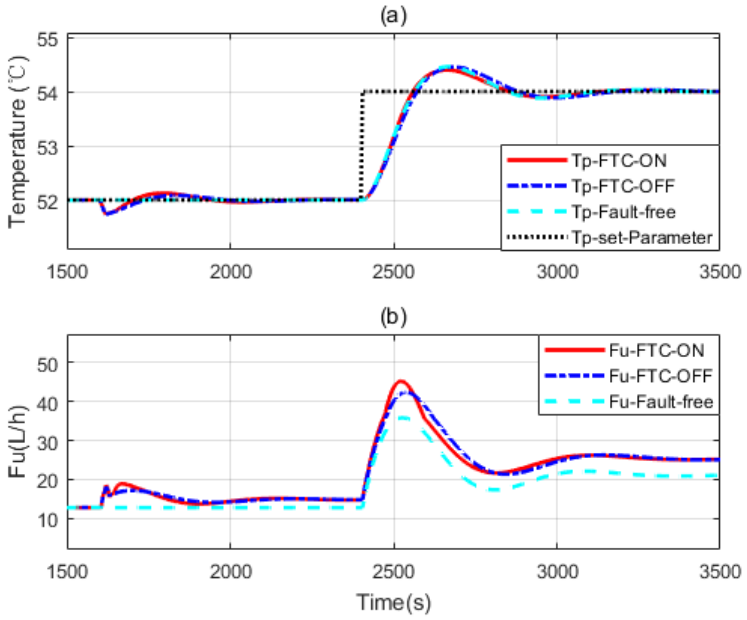

Figure 5.7: The simulation considering faulty parameter drops to 65% of its nominal value

Table 5.1: Key information about the simulation

Notation	Description	Value
M_w	Mass of the HEX reactor	10.84 kg
A_p	Heat exchange area of process channel	2.68×10^4 mm^2
A_u	Heat exchange area of utility channel	4.56×10^5 mm^2
E_a	The activation energy	7.61×10^4 $J \cdot mol^{-1}$
k_j^0	Pre-exponential factor of the reaction	$8.13 \times 10^1 1$ $L \cdot mol^{-1} \cdot s^{-1}$
F_{p1}	Flow-rate of $Na_2S_2O_3$	4.7 $L \cdot h^{-1}$
F_{p2}	Flow-rate of H_2O_2	2.3 $L \cdot h^{-1}$
T_{pin}	The input temperature of process fluid	21.1 $^\circ C$
T_{uin}	The input temperature of utility fluid	59.4 $^\circ C$

5.4.1 FTC simulation for heat exchange fault

Figure 5.7, Figure 5.8 and Figure 5.9 give the system dynamics under different faulty conditions. The heat exchange fault is introduced at 1600s. Heat transfer coefficient drops to 65%, 45% and 18% of its nominal value, respectively. The control reference has a step change at 2400s. This is used to test the behavior of the designed FTC strategy and its tracking ability to the reference in the faulty situation.

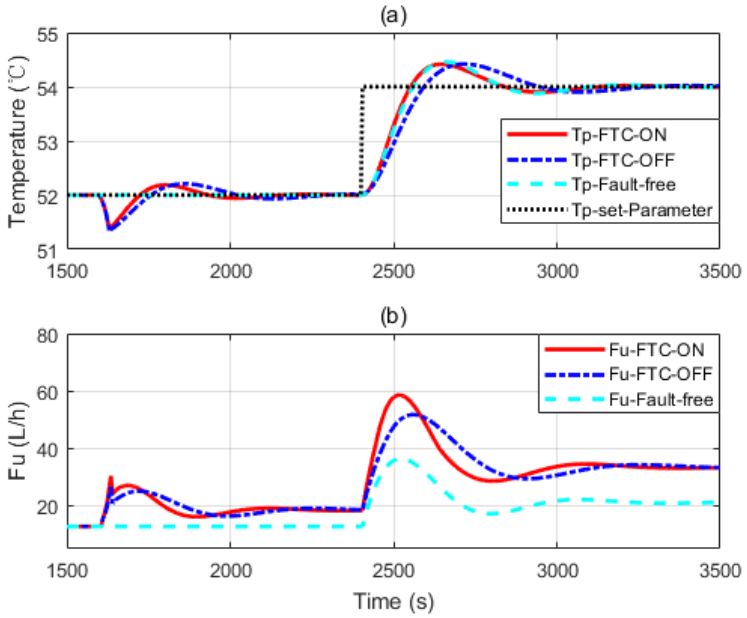

Figure 5.8: The simulation considering faulty parameter drops to 45% of its nominal value

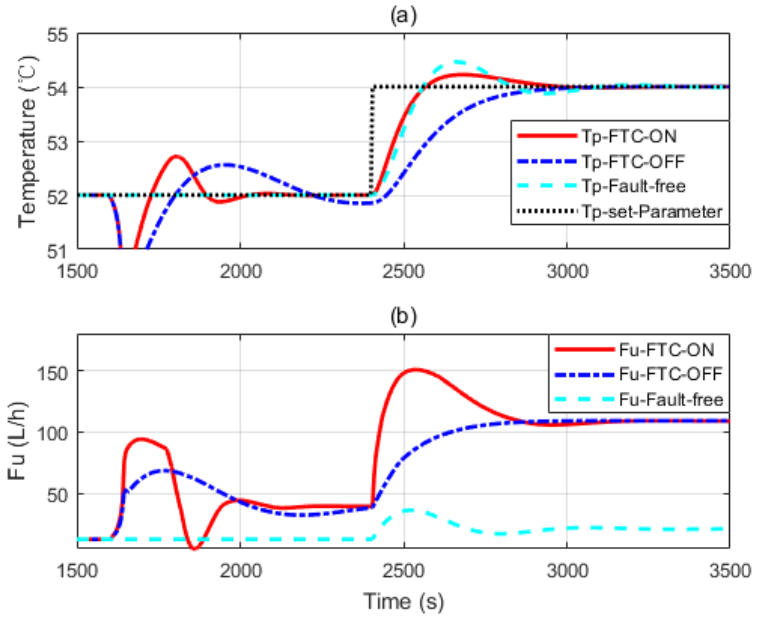

Figure 5.9: The simulation considering faulty parameter drops to 18% of its nominal value

Figure 5.7(a), Figure 5.8(a) and Figure 5.9(a) showed three independent simulation outputs of the HEX reactor, FTC ON, FTC OFF, and fault free cases. Figure 5.7(b), Figure 5.8(b) and Figure 5.9(b) presented corresponding control signals given by the controller banks. It can be seen from Figure 5.7 that when the fault occurs, no matter the FTC strategy is turned on or off, controller banks could bring the faulty system to the desired output. However, it performs slightly better when the FTC strategy is turned on. When the reference changes at $2400s$, all the controller banks reacted to that. The one in which FTC is turned on also behaves a little bit better than that when FTC is turned off. It is really close to the performance of the controller bank corresponding to the fault-free situation. That means the FTC strategy works and has proper compensation to the faulty system. To demonstrate the effectiveness of the proposed design strategy, simulations with serious faults are presented. More obvious results are shown in Figure 5.8 and Figure 5.9. One thing should be noticed is that the faulty values are chosen randomly. They are used to do simulations to show that the proposed design strategy should work as soon as the faulty range is covered by the two-layer multiple model structure.

From Figure 5.8 and Figure 5.9, we can see that more aggressive controls are given by the controller banks under the FTC strategy. It helps the faulty system to recover fast. Figure 5.9 belongs to the third case of the former section that the fault is severe and the faulty system behaves beyond the interval of the second layer model banks. Therefore, when the fault is detected, controller banks corresponding to the model bank with a preset-fault at $20\%h$ is activated to handle the problem. Though it may not be the perfect FTC strategy, it is the optimal one under all the assumptions.

Figure 5.10 presents a simulation result considering measurement noise for the case in Figure 5.8. It shows that the proposed FTC strategy also works well in noisy situation. Other cases have the similar results under measurement noise.

5.4.2 FTC simulation for the utility input temperature fault

Another simulation about the faults affecting the temperature of utility input is done the same way as the former sub-section. According to previous assumptions, we measure only T_p and manipulate only F_u of the system. Other parameters are seen as constants. In this case, we consider that there's a fault, for instance, the failure of heater in utility source tank or the damage of the insulation material of that tank, which would affect the temperature of utility input.

In this simulation, we keep all the conditions as in Table 5.1. for the targeting

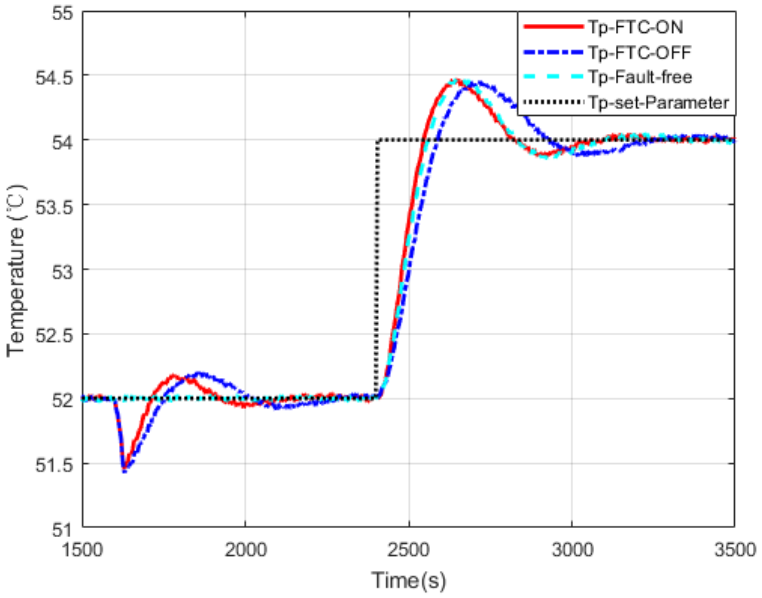

Figure 5.10: The simulation of $45\%h$ fault case considering measurement noise

parameter T_{uin}, besides its nominal value $59.4^{\circ}C$, four faulty situations are set at $(57.2^{\circ}C, 55.0^{\circ}C, 52.8^{\circ}C, 50.6^{\circ}C)$. A fault, the temperature of the utility input drops from nominal value to 93% of that value$(55.2^{\circ}C)$, is introduced at $3200s$.

Simulation results are presented below. In Figure 5.11, interval residuals calculated from UKF estimations show us the state of the system at each time point. It is clear that before the fault occurs at $3200s$, residuals of UKF1 are around zero, which means the system is in normal state. When the fault comes, all UKFs have reactions. After the transient period, the intervals become stable and it is easy to see that residuals corresponding to UKF2 and UKF3 cover the zero axis, indicating the fault is in this interval. One thing interesting is that there are big fluctuations around $5000s$. Though their magnitudes are much higher than the changes before, the interval covering the zero axis stays unchanged before and after. This is because they are not caused by a fault, but the controller effect from a change in the reference input, see Figure 5.12.

Like the case in Figure 5.9 and Figure 5.10, the controller bank of the nominal model has the ability to maintain the system in faulty situation in some extend. However, when the FTC strategy is applied, it switches to suitable controller bank in faulty situations and presents better performance than the case when FTC strategy is turned off, which also illustrates the effectiveness of the proposed method.

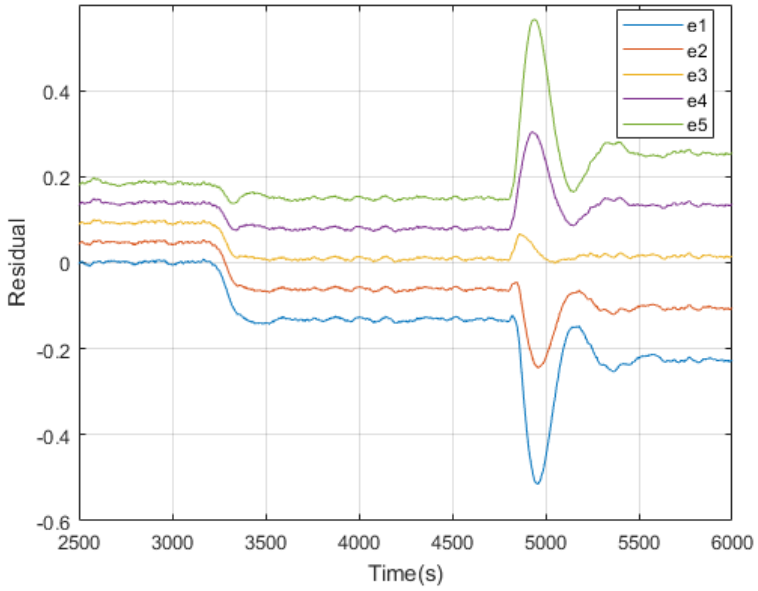

Figure 5.11: The simulation of interval residuals of T_{uin} fault

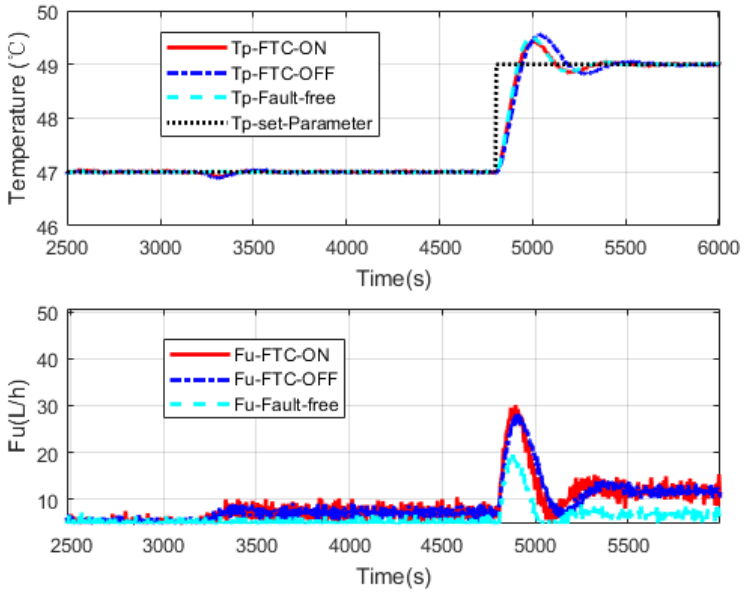

Figure 5.12: FTC simulation of T_{uin} fault

5.5 Summary

In this chapter, a fault tolerant control strategy using two-layer multiple model structure and direct model matching is proposed for an intensified heat-exchanger/reactor.

The HEX reactor points out a new direction for the development of classical batch reactors. However, its dynamics under chemical reactions are complex and of highly nonlinear. Traditional methods for its controller design are complicated and difficult. It will be even more difficult when considering FTC applications. To handle this problem, multiple model approach and its divide-and-conquer strategy are used to construct a two-layer multiple model structure. Among this structure, the first layer considers a simple description of the nonlinear system and the second layer concerns about faults. As the mathematical model is already available, virtual experiments could be done to generate enough IO data for the creation of multiple model banks by using system identification method. And then, model predictive control approach is used to design controllers by using the information of model banks. A switching strategy combines local models and local controllers to give out unified outputs of each model bank and controller bank respectively. The FDI section uses Unscented Kalman Filter to estimate the states of the reactor and forms index to tell the interval of faults. For the FTC implementation, both switching and linear merging schemes are used according to the faulty situations. After the tuning of controller banks, fault tolerant control of the HEX reactor is simulated in two kinds of faults. Simulation results prove the validity of the proposed FTC strategy. Complexity of handling the FTC design for the nonlinear systems is greatly reduced under the proposed method. However, accurate nominal model of the system is still a pre-condition for applying it.

Chapter 6

FTC Strategy through Multiple Adaptive Model Matching

Adaptive control theory [79] [41], on the other hand, is very classic and has been studied since the 1960s form dealing with the control of linear time-invariant (LTI) systems with unknown parameters[47]. Classical adaptive control assures both stability and robustness when parametric errors of the considered system are small. When they are large, oscillations would appear in the transient response of adaptive systems. To overcome this, numerous and tremendous of efforts have been made. Among these efforts, combination with other theories is one of the popular direction. The concept and theoretical works propose in [46] are interesting combinations of multiple model approach and adaptive control. It also showed great improvements in solving the control problem of the system with unknown parameters.

Inspired by the concept and method of adaptive model in [78]. This chapter proposed a strategy for FTC design by introducing the multiple adaptive models concept into the multi-dimensional multiple model structure which was presented before. During this process, multiple model approach is applied in two dimensions to form a two-layer multiple model structure for precise system representation in both nominal and the considered faulty situations. These two-layer multiple banks will then be used as a prior knowledge for the FTC implementation. By online checking the outputs of the first layer model banks and the real plant, faulty regime could be located. Decision variables would give the indication of current working point. In this way a group of local simple models could be confirmed and their parameters could be used to initiate the multiple adaptive models which will finally identify the faulty plant. Model Predictive Control is selected to design a controller for the reference model to achieve the overall control goal by chasing the reference inputs.

6.1 The concept of multiple adaptive models

This part of theoretical work was originally presented in [46]. The concept and main idea is introduced here and combined with the two-layer multiple model structure for dealing the FTC problem.

6.1.1 Adaptive control problem and identification model

Generally, sub-models obtained in the previous section are simple and easy to use. We assume these local models are linear time-invariant ones and their state variables are accessible. The real system at every moment could be described by the state equation that has the same structure as the local model in the model banks. For simplicity, we assume it has a special form:

$$\dot{x}_p(t) = A_p x_p(t) + bu(t) \tag{6.1}$$

where $A_p \in \mathbb{R}^{n\times n}$ and $b \in \mathbb{R}^n$ are in companion form. The last row of A_p are $[a_{p(1)}, a_{p(2)}, ..., a_{p(n)}] = \theta_p^T$ and are assumed to be unknown. $b = [0, ..., 0, 1]^T$.

A reference model will have the following description:

$$\dot{x}_m(t) = A_m x_m(t) + br(t) \tag{6.2}$$

where $r(\cdot) : \mathbb{R}^+ \to \mathbb{R}$ is a bounded piece-wise continuous reference signal to assure the adaptive process satisfy the overall control goal. It will be discussed later. A_m is also in companion form and has the last row θ_m^T.

The reference model is generally stable and its parameters are known. It stands for the real plant in the situation which we expected. Thus, the objective of adaptive control is to calculate the input $u(\cdot)$ to the real plant such that:

$$lim_{t\to\infty}[x_p(t) - x_m(t)] = 0 \tag{6.3}$$

To achieve this, the following identification model is set up:

$$\dot{x}_I(t) = A_m x_I(t) + [A_I(t) - A_m]x_p(t) + bu(t) \tag{6.4}$$

where $A_I(t)$ is a matrix in companion form and its last row $\theta_I^T(t) = [a_{I(1)}, a_{I(2)}, ..., a_{I(n)}]$ contains the identified parameters and is adaptable.

Defining the identification error of states as:

$$e_I(t) \triangleq x_I(t) - x_p(t) \tag{6.5}$$

The following feedback control is used to assure the stability of the plant:

$$u(t) = -k^T(t)x_p(t) + r(t) \tag{6.6}$$

where $k(t) = \theta_I(t) - \theta_m$.

And the parameter renew law is:

$$\dot{\theta}_I(t) = -e_I^T(t)Pbx_p(t) \tag{6.7}$$

where P is the positive definite matrix solution of the Lyapunov equation:

$$A_m^T P + PA_m = -Q, Q = Q^T > 0. \tag{6.8}$$

Proof: Define parameter identification error as:

$$\tilde{\theta}_I(t) \triangleq \theta_I(t) - \theta_p \tag{6.9}$$

Assume the parameter change of the target system is ignorable during the adaptation process, then:

$$\dot{\tilde{\theta}}_I(t) = \dot{\theta}_I(t) \tag{6.10}$$

Using the following Lyapunov function:

$$V(e_I, \tilde{\theta}_I) = \tilde{\theta}_I^T\tilde{\theta}_I + e_I^T Pe_I \tag{6.11}$$

And its derivative is expressed as:

$$\dot{V}(e_I, \tilde{\theta}_I) = \tilde{\theta}_I^T\dot{\tilde{\theta}}_I + e_I^T P\dot{e}_I + \tilde{\theta}_I + \dot{\tilde{\theta}}_I^T\tilde{\theta}_I + \dot{e}_I^T Pe_I \tag{6.12}$$

Substitute (6.1) and (6.4) into (6.5), we have:

$$\dot{e}_I(t) = A_m e_I(t) + b\tilde{\theta}_I^T(t)x_p(t) \tag{6.13}$$

Substitute (6.13) into (6.12), we have:

$$\dot{V}(e_I, \tilde{\theta}_I) = e_I^T(A_m^T e_I + x_p^T\tilde{\theta}_I b^T)P + \dot{\tilde{\theta}}_I^T\tilde{\theta}_I + e_I^T P(A_m e_I + b\tilde{\theta}_I^T x_p) + \tilde{\theta}_I^T\dot{\tilde{\theta}}_I \tag{6.14}$$

Substitute (6.10) and the adaptive law (6.7) into (6.14), the complex item $b\tilde{\theta}_I^T x_p$ could be eliminated:

$$\dot{V}(e_I, \tilde{\theta}_I) = e_I^T A_m^T Pe_I + e_I^T PA_m e_I \tag{6.15}$$

Therefore, combining with (6.8), we have:

$$\dot{V}(e_I, \tilde{\theta}_I) = -e_I^T Qe_I < 0 \tag{6.16}$$

Thus, the error system based on the adaptation process (6.7) is stable. The convergence and identification to the unknown real system is then reached. □

6.1.2 Multiple adaptive model

The previous sub-section discussed how adaptive law is used to create an adaptive model for identifying the unknown system. When simultaneously running the two-layer multiple banks, the real system will always be surrounded by several local models in the two-dimension netted space. Information of these models are useful because they are close to the real situation and can help launching a fast search. In adaptive control domain, it is allowed to use any number of models to identify the system but only one control signal can be applied. Thus, we do an extension of (6.4) and introduce all the N surrounding local models into the identification process.

$$\begin{cases} \dot{x}_l(t) = A_m x_l(t) + [A_l(t) - A_m] x_p(t) + bu(t) \\ x_l(t_0) = x_p(t_0) \end{cases} \tag{6.17}$$

where $l \in [1, N]$ indicates l^{th} identification model.

Since we assume the states of the original system are available, the adaptation process is initiated through them. The introduction of multiple model requires the parameter renew of each sub-identification model. The adaptation law can be extended from (6.7):

$$\dot{\theta}_l(t) = -e_l^T(t) P b x_p(t) \tag{6.18}$$

where $e_l(t) = x_l(t) - x_p(t)$.

Through there are several identification models involved in the adaptation process, control calculation is dependent on just one of them. Therefore, a simple strategy is used to organize them: the one who owns the minimum estimation error wins and the control calculation will be based on its information. Some extra consideration, like the memory item, can be added, too. So the new control signal would still be given by 6.6 but the calculation of $k(t)$ will be different and is given here to realize the optimal procedure:

$$k_z(t) = \theta_z(t) - \theta_m \tag{6.19}$$

where $\theta_z(t)$ is defined as the parameters of the identification model who has the minimum state error $e_l(t)$.

When considering the approximation of the multiple adaptive model to the real system, it is necessary to study of its convex hull property. It means the adaptation process which starts from the interval vertex models should ensure that the real system be surrounded by the multiple identification models during the iteration. According to the theorem in literature [46], if at t_0, the real system lies inside the convex hull formed by the multiple adaptive model (6.17) on the parameter space, then (6.17) can

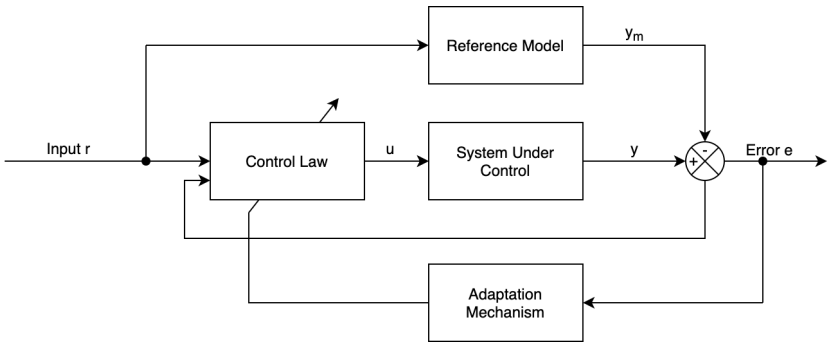

Figure 6.1: Model reference adaptive control

guarantee that the real system always lies inside the convex hull it forms by using the parameter renew law (6.18).

6.1.3 Controller Design for Reference Model

The former sub-sections discussed how to use the adaptive method to build one or more adaptive models to identify and approximate an unknown target system. The calculated control signal is applied on the system and force it approaching the states and outputs of the reference model. As we described before, a known reference signal is needed here and it is set as the input of both the reference model and the adaptive controller, as is shown in Figure 6.1.

To complete the control goal, a controller can be set to give the input $r(t)$ to the reference model. The input of this controller is then set to the original control objective, such as the states that the adaptive system needs to follow or be stabilized. In general, the reference model can be set to a more familiar form or linear one, so its controller design is relatively easy. In this section, we use a model predictive controller to complete this closed loop, and its structure is shown in Figure 6.2 below.

From the discussion in the previous two subsections, it is clear that the adaptive process discussed in this chapter uses only the parameter error between the identification model and the reference model. Generally the reference model stays constant, so the block diagram shown in Figure 6.2 resembles an open-loop structure in the adaptation part. Under the proposed architecture, the adaptive law focuses on identifying the real system and approximating the reference model, while the MPC controller ensures that the reference model follows the original reference input. Thus, the strategy achieves two levels of tracking, allowing the adaptive process to accurately identify the real system parameters while indirectly chasing the original reference input. This control goal is achieved with the help of the reference model controller.

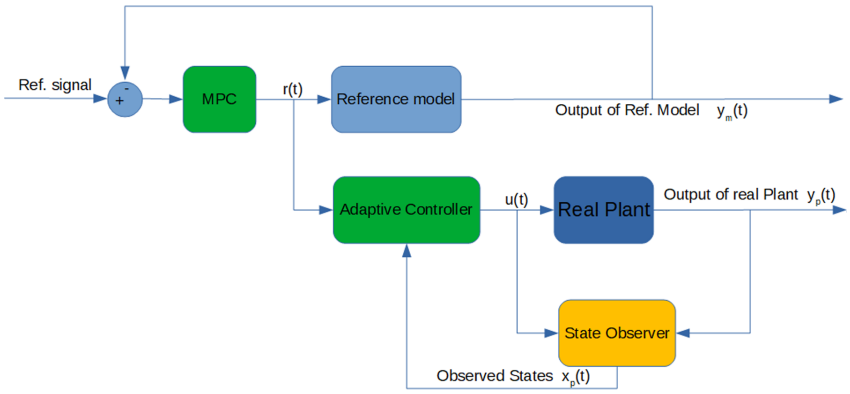

Figure 6.2: Introduction of MPC for reference model

For the reference model (6.2), the control output is calculated according to classical MPC logic [114]:

$$r(t) = \int_0^t \dot{u}_{mpc}(\tau)d\tau \tag{6.20}$$

where $\dot{u}_{mpc}$ is given by:

$$\dot{u}_{mpc}(t) = \begin{bmatrix} K_x & K_y \end{bmatrix} \begin{bmatrix} \dot{x}_m(t) \\ y_m(t) - r_{in}(t) \end{bmatrix} \tag{6.21}$$

where $\begin{bmatrix} K_x & K_y \end{bmatrix} = K_{mpc}$ is the MPC gain. $x_m(t)$ and $y_m(t)$ are the state and output of the reference model. $r_{in}(t)$ is the initial reference input.

6.2 Multiple adaptive model based FTC stategy

Here we combine the concept of multiple adaptive models with a two-layer multiple model architecture to propose the structure as illustrated in Figure 3.4 for fast and accurate implementation of fault-tolerant control. In Figure 3.4, each point represents a sub-model and each column represents a multiple model set under one considered parameter value. The red dashed lines represent the possible locations and trajectories of the real system in case of a fault. From this, a fault diagnosis module can be designed to determine the current fault class and fault interval of the system, and to discriminate multiple models that surround the target system from the dimensions of both operating point and faulty parameter. The parameters of the surround models are used to initialize the adaptive process to achieve an accurate approximation of the actual system. At the same time, when a fault is detected and the system deviates from the current workspace, the fault diagnosis module can quickly locate the probable

interval of the current faulty system by comparing it with the model banks that run in parallel. This module then gives out the index of the surround models. Therefore, multiple identification models are initialized with the parameters of new surrounding models. A new adaptive process is then launched to accurately approximate the faulty system. While giving the fault parameters, the fault system is forced to follow the original reference indirectly. The control goal and the purpose of fault-tolerant control are achieved by using the synergy of the reference model controller and the adaptive process.

Before implementing the fault-tolerant control strategy, the following preparations need to be completed:

- The construction of the target system's analytical mathematical model
- Obtaining sufficient I/O data of the target system in both nominal and faulty conditions
- The construction of the two-layer multiple model set through priory knowledge:

$$\begin{cases} \dot{x}_{ij(t)} = A_{ij}x_{ij(t)} + B_{ij}u(t) \\ y_{ij(t)} = C_{ij}x_{ij(t)} \\ y_j(t) = \sum_{i=1}^{L} \mu_{ij(t)} y_{ij(t)} \end{cases} \tag{6.22}$$

  where i denotes the operating point and j indicates the considered faulty situation. μ_{ij} is the weight of the basic sub-model. A_{ij}, B_{ij} and C_{ij} are the system matrix, input matrix and output matrix of each sub-model respectively.
- Determine the parameters of the reference model (6.2).
- Design and calculate the MPC parameter of the reference model according to (6.20) and (6.21)

After that, the FTC strategy is implemented as shown in Figure 6.3.

It should be noticed here that the exact number of identification models involved in the adaptation process needs to be determined by the practical situations. Usually, the number of unknown parameters determines the dimension of the space where this adaptive process is located. In order to complete the adaptive process quickly and accurately, the more the unknown parameters are, the stronger the need for the minimization of search space is. The more surrounding models and identification models are involved in this process, the smaller the scope in which the adaptive process can be started. And, naturally, the shorter the time is consumed to obtain the desired results.

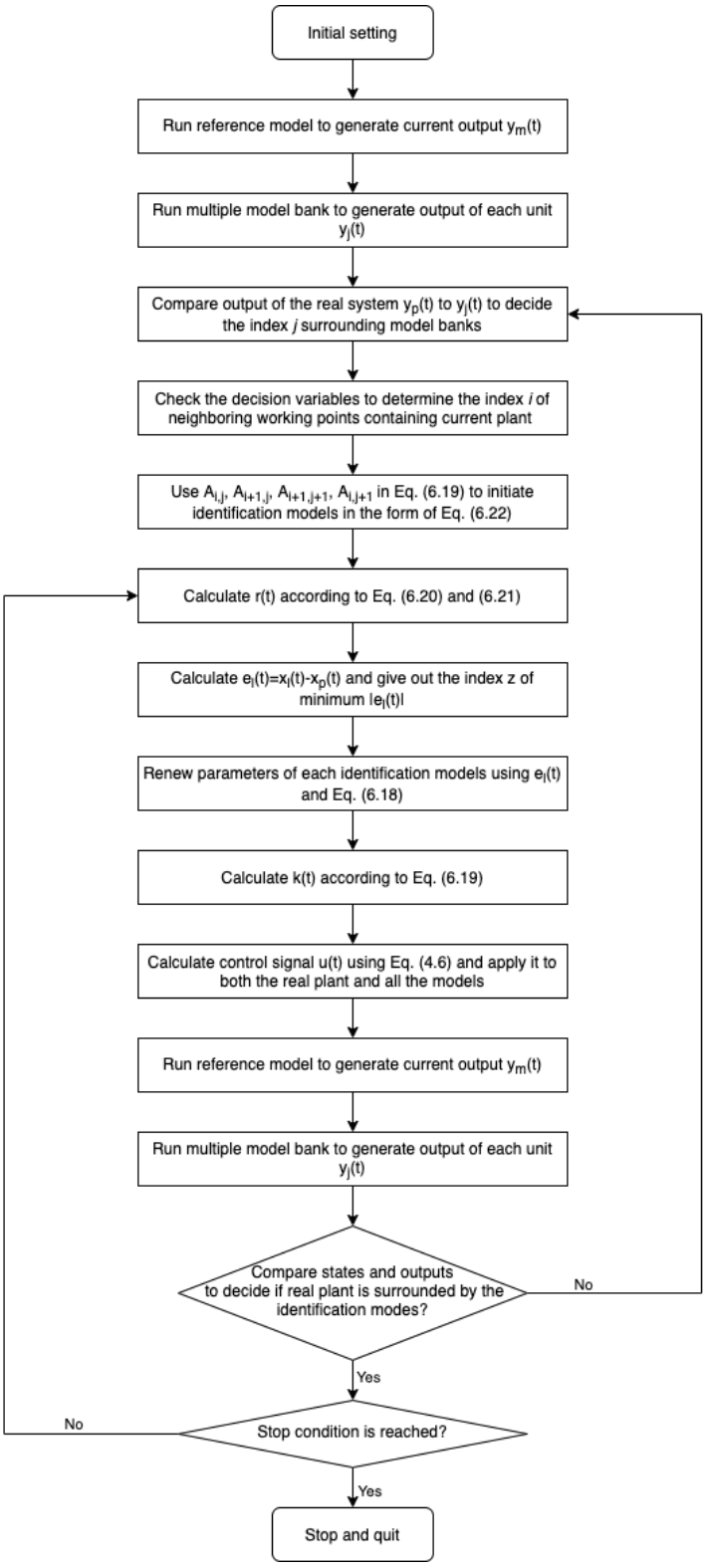

Figure 6.3: Strategy of fault tolerant control using multiple adaptive models

6.3 Simulation results

For the strategy proposed above, simulations of a second order system are shown to introduce the implementation steps and validate the proposed FTC strategy.

6.3.1 System parameters and initial setting

In these simulations, we assume that the two-layer multiple model bank has be created and parameters of the local models are known. The reference model is chosen to have $\theta_m = [-1.5, -2.5]^T$ all the time:

$$\begin{cases} \dot{x}_m(t) = \begin{bmatrix} 0 & 1 \\ -1.5 & -2.5 \end{bmatrix} x_m(t) + \begin{bmatrix} 0 \\ 1 \end{bmatrix} r(t) \\ y_m(t) = \begin{bmatrix} 1 & 0 \end{bmatrix} x_m(t) \end{cases} \tag{6.23}$$

Assume the real system in one operating point has parameter $\theta_p = [-2.1, -1.5]^T$ according to the structure of 6.1 under nominal situation. It is expressed in second order model as:

$$\begin{cases} \dot{x}_p(t) = \begin{bmatrix} 0 & 1 \\ -2.1 & -1.5 \end{bmatrix} x_p(t) + \begin{bmatrix} 0 \\ 1 \end{bmatrix} u(t) \\ y_p(t) = \begin{bmatrix} 1 & 0 \end{bmatrix} x_p(t) \end{cases} \tag{6.24}$$

During the adaptation process, the algorithm doesn't know the exact value of the real system or its equivalent model. According to the strategy of Figure 6.3, we assume that there are four sub-models in the two-layer multiple model set surrounding the real system after the detection process. Their parameters are $\theta_{11} = [-3, 3]^T$, $\theta_{12} = [3, 3]^T$, $\theta_{21} = [-3, -3]^T$ and $\theta_{22} = [3, -3]^T$ respectively. Therefore, four identification models could be initiated after the substitution of reference model A_m and the four vertex model to the structure (6.17):

$$\begin{cases} \dot{x}_l(t) = \begin{bmatrix} 0 & 1 \\ -1.5 & -2.5 \end{bmatrix} x_l(t) + \left[\begin{bmatrix} 0 & 1 \\ \theta_{l1}(t) & \theta_{l2}(t) \end{bmatrix} - \begin{bmatrix} 0 & 1 \\ -1.5 & -2.5 \end{bmatrix} \right] x_p(t) + \begin{bmatrix} 0 \\ 1 \end{bmatrix} u(t) \\ y_l(t) = \begin{bmatrix} 1 & 0 \end{bmatrix} x_l(t) \end{cases} \tag{6.25}$$

where $l \in [1, 4]$ indicates l^{th} surrounding model and identification model. Parameters $\theta_{l2}(t_0)$ are given by surrounding models.

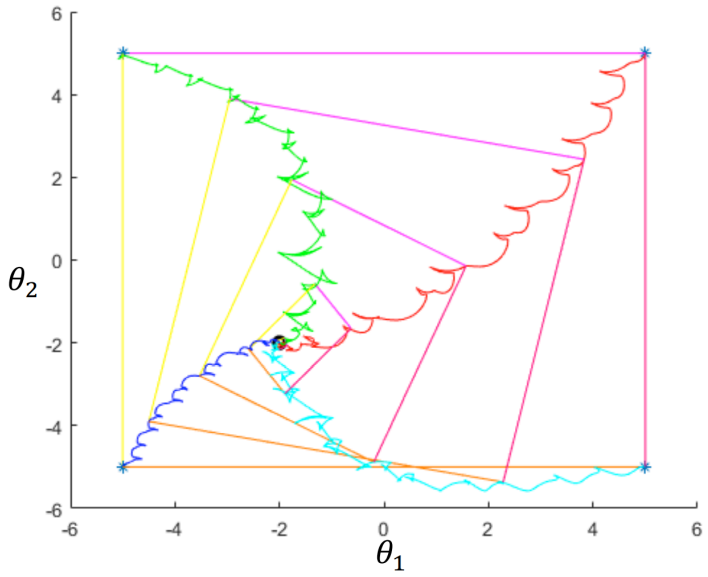

Figure 6.4: Strategy of fault tolerant control using multiple adaptive models

6.3.2 Simulations of multiple adaptive model

The concept of multiple adaptive model is illustrated by Figure 6.4. In this process, several adaptive models initiated from surrounding models to chase the unknown system. This adaptation process is conducted according to the idea given in section 6.1. It achieves the goal to estimate the accurate parameters of the target system.

To test the effectiveness of chasing the unknown system and achieving the control goal, the idea of multiple adaptive model combined with reference model controller is simulated without the introduction of fault in this section. We will compare the single and multiple adaptive model Section 6.1.3 in the two cases of single and multiple adaptive models cases when using the strategy of 6.1.3.

A square-wave with a period time of 37.5s is set as the initial reference input and MPC is constructed for the reference model. First, a single model with $\theta_{11} = [-3, 3]^T$ is chosen to initiate the identification model and launch the adaptive law. Simulation results of single adaptive model are shown in the following Figure6.5.

From Figure6.5, it is clear that the MPC controller works well. Output of the reference model could follow the changing initial reference input even if it is not given in square-wave. Overshoots in the output of reference model y_m could be adjusted by tuning parameters of the MPC controller. This controller also gives out the intermediate reference signal u_{mpc} which is renamed as $r(t)$ and applied both to the reference model and the adaptive law as is shown in Figure 6.2.

After that, we update the single adaptive model into multiple case. Like this we can

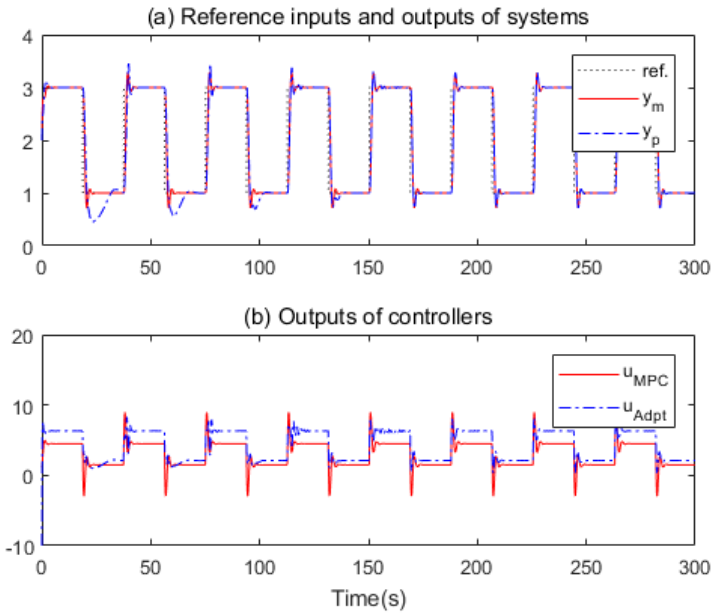

Figure 6.5: Simulation result of single adaptive models under normal condition

evaluate if there's any improvements. The simulation results are illustrated in Figure 6.6.

Comparing to Figure 6.5, the introduction of multiple adaptive model makes it converges to the unknown system much faster in 6.6. The clear comparison of converge errors is shown in Figure 6.7.

From Figure 6.7 and Figure 6.5 we can notice that for the single adaptive model case, output of the real system y_p is approaching that of the reference model gradually. It is relatively large at first, especially in the overshoot area. And it converged after about 150 seconds. This indicates that the adaptive model works also, even though the identification speed is not ideal.

Apparently, by fully using information of the surrounding models to initiate the adaptive models, identification speed is accelerated in a large scale. It takes only 50 seconds to approach the unknown real system (see Figure 6.7 and Figure 6.6).

6.3.3 FTC simulation under multiple adaptive model matching strategy

This section simulates the fault-tolerant control scheme proposed in Figure 6.3 under the multiple adaptive model matching strategy. The target system and the multiple model bank are set the same as in the previous sections. The original reference input is also set as a square wave with period $T = 37.5s$. The difference is that a system

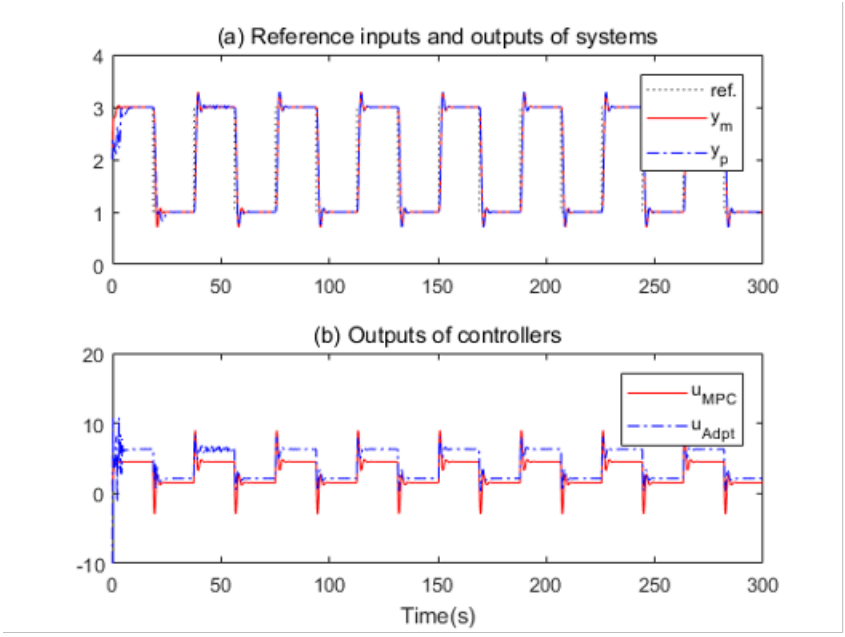

Figure 6.6: Simulation result of multiple adaptive models under normal condition

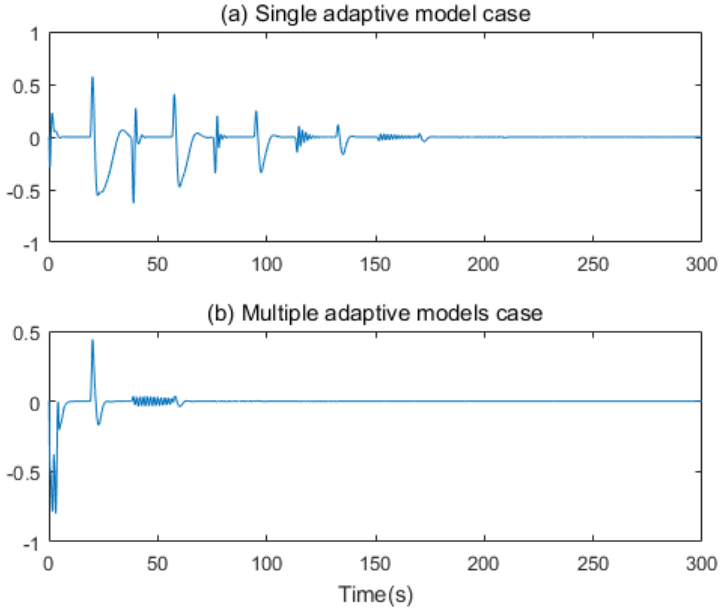

Figure 6.7: Comparison of output error between single and multiple adaptive models

fault is introduced at $t = 124s$. This fault causes a relatively large change in the parameters of the target system, and the parameters of its equivalent linear model switch from $\theta_p = [-2.1, -1.5]^T$ to $\theta_{p,f} = [6.9, 5.1]^T$. From this setting, the fault value is still relatively large. For the original system, the equivalent linear model is equivalent to change from (6.24) to (6.26).

$$\begin{cases} \dot{x}_{p,f}(t) = \begin{bmatrix} 0 & 1 \\ 6.9 & 5.1 \end{bmatrix} x_{p,f}(t) + \begin{bmatrix} 0 \\ 1 \end{bmatrix} u(t) \\ y_{p,f}(t) = \begin{bmatrix} 1 & 0 \end{bmatrix} x_{p,f}(t) \end{cases} \tag{6.26}$$

where f denotes the faulty state.

According to the strategy in Figure 6.3, the fault diagnosis module monitors the target system in real time through output feedback. When it determines that the target system is no longer enveloped by the current surrounding local models, it indicates that an operating point change or a fault occurs. Therefore, a new search can be performed in the framework of the two-layer multiple model structure to determine the new surrounding models that contain the target system. And a new round of multiple model adaptation process is initiated by the new surrounding models to accomplish the fault-tolerant goal. According to fault setting and the two-layer multiple model set, the new surrounding models have the following parameters $\theta_{11} = [3, 3]^T, \theta_{12} = [3, 9]^T, \theta_{21} = [9, 9]^T, \theta_{22} = [9, 3]^T$. The simulation results are shown in the following figures (6.8) and (6.9).

As can be seen from Figure 6.8, the system operates the same way as the simulation in Figure 6.6 when there's no fault. The adaptive law, which is initiated by multiple sub-models in parallel, ensures fast approximation to the target unknown system. The presence of the reference model controller makes it follow the original reference input. At $t = 124s$, the introduction of a fault causes a large fluctuation in the system output. The fault diagnosis module then gives a new system parameter interval. The predefined fault tolerant strategy re-initializes the multiple adaptive model, starting a new round of approximation and control compensation for the system with unknown faulty parameters. In this way it stabilizes the faulty system and makes its output follow the original reference input even in faulty situations. As can be seen in Figure 6.8(b), the FTC strategy compensates more for the control of the faulty system after the fault's occurrence, and its control output changed dramatically under the same reference input. Because of this change, the effect of the fault on the system output is compensated. Therefore, the system can still be adjusted to follow the original reference to achieve the purpose of fault-tolerant control. Figure 6.9 illustrates this process

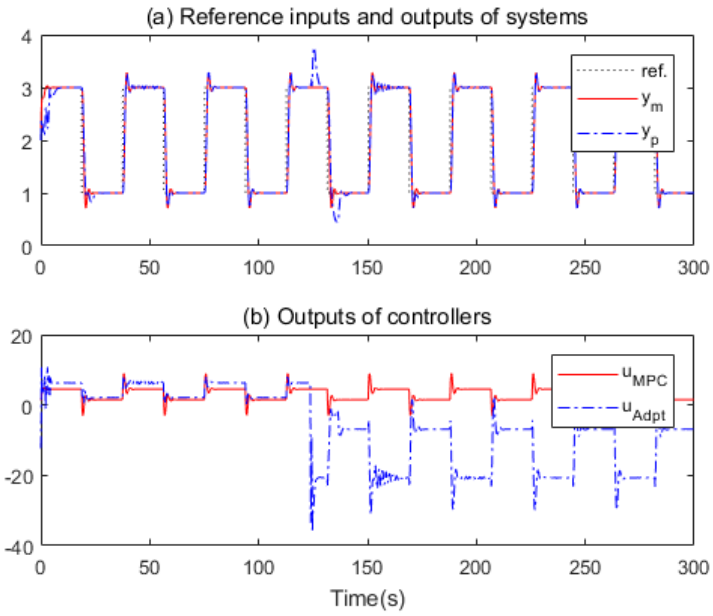

Figure 6.8: Fault tolerant control simulation of multiple adaptive models (plant fault is introduced at $t = 124s$)

from the perspective of the output error, allowing us to see the fault tolerance effect more clearly.

Figure 6.9(a) is the errors between the outputs of the reference model and the given initial reference inputs. It shows there's still improvement space for optimizing the MPC parameters. The big overshoots is caused by the time delay for detecting the change of reference inputs. Since this signal is set manually, we could adjust the rule and give it to the controller one step ahead to avoid it. Figure 6.9(b) shows the output errors between the system and the reference model. It tells us that when the fault is introduced, the behavior of the adaptation process supports the discussion given before. Therefore, the simulation showed the validity of the proposed strategy.

Figure 6.10 gives the traces of the adaptation process of the FTC simulation.

In Figure 6.10, the target system is in the left lower corner of the parameter space. It is inside an interval of four surrounding models. The adaptive process starts from these four sub-models and gradually converges to the actual system. We can notice that the target system has the nearest Euclidean distance to the sub-system with parameters $\theta_{21} = [-3, -3]^T$. When the multiple adaptive model scheme is used, there is a higher probability that the identification model initiated by this closest sub-system can be selected for iteration and computation of control signal, which results in a faster convergence than the case of a single model in probability aspect of view. When a

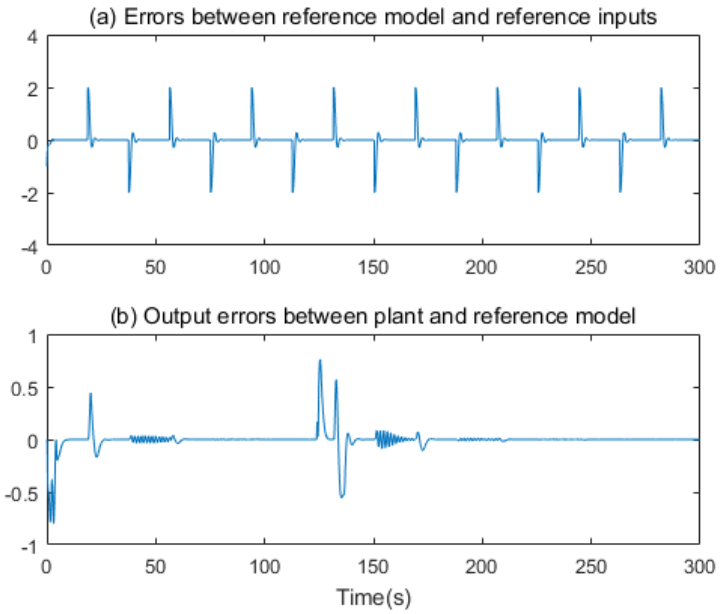

Figure 6.9: Error curves of the FTC Simulation

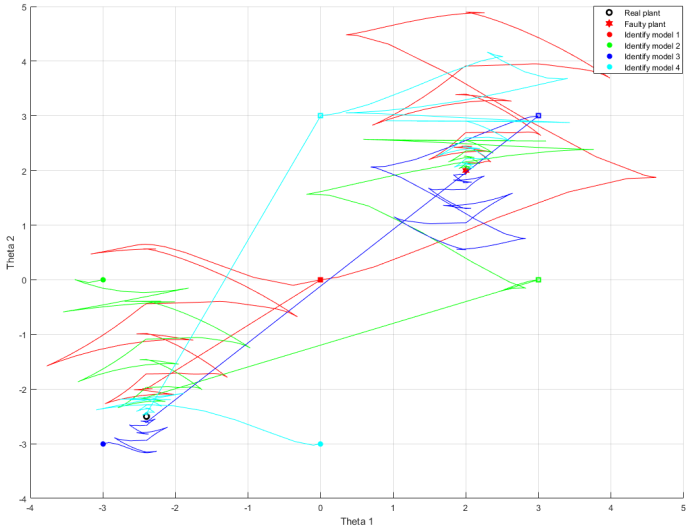

Figure 6.10: Multiple adaptive models approaching to the parameter unknown system in initialization and faulty condition

fault occurs, the parameters of the target system are changed, and the fault-tolerant strategy re-initializes multiple identification models and starts the adaptation process. This is based on the new parameter interval given by the fault diagnosis module. The adaptation process thus achieves an accurate approximation of the faulty system.

6.4 Summary

Based on the proposed multi-dimensional multiple model architecture, this chapter presented a FTC design strategy for plant fault after the inspiration of the literature. It firstly described the idea of multiple adaptive models which have the ability to assure convex hull property. Combinations of the two concepts are presented and a MPC controller is added to generating proper intermediate reference signal while achieving the overall control goal. Simulations showed that multiple adaptive models obviously have a better performance than the single one, that it took far less time for convergence. This idea is perfect for the two-layer multiple model structure. The FTC simulation showed that when a plant fault occurs, the validity of the proposed strategy, that the system can achieve control goal and follow the reference input after a short period of adjusting, is confirmed.

Chapter 7

Conclusions and Future Works

This chapter makes a summary of this thesis and points out some potential directions in this area. Directions and plans of the future works are also mentioned and discussed in this chapter.

7.1 Conclusions

This thesis investigates the problem of designing fault-tolerant control strategies for nonlinear dynamic systems. The industrialization continues to speed up, which leads to the construction of giant sized and complex modern systems. Their demands for safeties keeps increasing at the same time. Fault diagnosis and fault-tolerant control are the key research directions to improve the reliability and safety of systems. In this thesis, after introducing the basic background knowledge and systematic review of fault diagnosis and fault-tolerant control techniques, we combine and extend the classical multiple model approach and propose various fault-tolerant control strategies based on different model matching schemes.

We started from the perspective of model matching to real systems, discussed the possibility of designing controllers based on model matching strategies. To realize this, a two-layer multiple model structure is proposed by increasing the dimension of traditional multiple model approach. This architecture considers system faults as well as nonlinear system representation. The design and scheduling of a controller bank for both nominal and faulty conditions using this structure are investigated. The idea of using the multidimensional multiple model structure for model matching and thus fault-tolerant control is presented in the presence of a fault. In addition, this thesis proposed FTC strategies based on the model matching schemes via optimization and unified assessment.

The thesis starts with a detailed modeling work for an integrated heat exchanger/reactor which has been studied by our collaborators. The validity of the developed model is determined by comparing the simulation results with the experimental data. After that, an active fault-tolerant strategy using direct model matching is designed for the target HEX/Reactor by introducing the idea of the two-layer multiple model structure. Firstly, the model bank of the HEX/Reactor is established using a strategy combining model-based and data-driven approaches. Then model predictive control is used to the target models to build the corresponding controller bank. The fault diagnosis part is then designed based on the unscented Kalman filter. Finally, simulations are performed for two fault assumptions, the fault affecting heat transfer coefficient and the fault concerning the input temperature of utility fluid. Simulation results are discussed to verify the performance of the proposed fault tolerance strategy when used for the given HEX/Reactor.

After that, inspired by the concept of adaptive model, this thesis incorporates the idea of adaptive control in the structure proposed in Chapter 3. When the adaptive

model is introduced to the two-layer multiple model architecture, an idea of fault-tolerant control is given after completing the design of the fault diagnosis module. For the concept of adaptive model, the relevant derivation and proof are given for the single model case, and then the method is extended to the multiple adaptive model case. Besides that, this thesis presented the idea and the specific structure of designing additional controller for the reference model of the adaptation process. After giving a fault-tolerant control strategy that integrates the above methods, simulations are carried out to compare the performance of single and multiple adaptive model cases. In the end, simulations that show the accomplishment of the fault-tolerant control objective using multiple adaptive model in a two-layer multiple model framework are presented and analyzed. In contrast with the direct model matching FTC strategy, the one using the concept of adaptive model takes longer time to converge. However, it is more precise.

7.2 Future works

Based on different model matching methods, the thesis proposed several fault-tolerant control strategies. In addition to the model matching algorithms based on classical methods (switching and mixing, multiple adaptive models), a model matching strategy based on heuristic methods is innovatively proposed. In order to take full advantages of classical and heuristic methods, this thesis designed a higher-level unified evaluation framework, based on which model matching and optimization are carried out. This strategy gives excellent modulation solutions that can achieve fault-tolerance regardless of the normal condition or in the case of a fault. With the rapid development of computer hardware and software technology, the computational burden of the heuristic optimization algorithm is gradually not an obstacle that restricts its implementations. Based on the efforts in this thesis, the directions of the future works are as follows.

(1) The programmatic problem of model set construction. In this thesis, the multiple model approach and its extensions are chosen to describe nonlinear complex systems with a combination of simple linear models and make model matching to optimize control strategies when there's a fault. Such an approach and design idea are attempted methodologically. But more specific, operational, reproducible and widely applicable design steps should be investigated when it comes to practical engineering applications. For the construction of the model bank, it is difficult to obtain the exact nonlinear model of the target system in many cases. How to build a multiple model bank

based on simple models to achieve following control and fault-tolerant applications is a problem worth exploring.

(2) Fault simulation problem. In this thesis, as a methodological discussion, the construction of a faulty model bank is achieved by simulating the model of a faulty system to obtain sufficient I/O data for system identification. This construction method is not yet universal. In particular, for systems that are difficult to build accurate models, the nominal states can be constructed by applying the operational data of the actual system, while the faulty scenarios are difficult to achieve from the operating equipment. Therefore, it is difficult to establish the faulty model bank. Therefore, a universally applicable construction method of the faulty model bank is urgently needed.

Finally, the research in this thesis is still limited to the methodology and the validation sections are based only on simulations. There is still a long way to go and a lot of work to be done for future applications specifically in industrial sites. And there are still numerous variables and specific factors to be considered before the engineering applications can be landed.

Bibliography

[1] M. Abid. "Fault Detection in Nonlinear Systems: An Observer-Based Approach". en. In: (Sept. 2010).

[2] A. A. Adeniran and S. E. Ferik. "Modeling and Identification of Nonlinear Systems: A Review of the Multimodel ApproachPart 1". In: *IEEE Transactions on Systems, Man, and Cybernetics: Systems* 47.7 (July 2017), pp. 1149–1159. DOI: 10.1109/TSMC.2016.2560147.

[3] A. Akhenak, E. Duviella, L. Bako, and S. Lecoeuche. "Online Fault Diagnosis Using Recursive Subspace Identification: Application to a Dam-Gallery Open Channel System". en. In: *Control Engineering Practice* 21.6 (June 2013), pp. 797–806. DOI: 10.1016/j.conengprac.2013.02.013.

[4] F. Alrowaie. "Fault Isolation and Alarm Design in Non-Linear Stochastic Systems". PhD thesis. Jan. 2015. DOI: 10.13140/RG.2.2.10342.52801.

[5] A. A. Amin and K. M. Hasan. "A Review of Fault Tolerant Control Systems: Advancements and Applications". en. In: *Measurement* 143 (Sept. 2019), pp. 58–68. DOI: 10.1016/j.measurement.2019.04.083.

[6] T. Andrea and A. Lazzaretto. "Energy System Diagnosis by a Fuzzy Expert System with Genetically Evolved Rules". In: *International Journal of Thermodynamics* 11 (Sept. 2008). DOI: 10.5541/ijot.219.

[7] Z. Anxionnaz, M. Cabassud, C. Gourdon, and P. Tochon. "Heat Exchanger/Reactors (HEX Reactors): Concepts, Technologies: State-of-the-Art". en. In: *Chemical Engineering and Processing: Process Intensification* 47.12 (Nov. 2008), pp. 2029–2050. DOI: 10.1016/j.cep.2008.06.012.

[8] Z. Anxionnaz, F. Théron, P. Tochon, R. Couturier, C. Gourdon, M. Cabassud, et al. *RAPIC Project: Toward Competitive Heat-Exchanger/Reactors*. en. 2011.

[9] Z. Anxionnaz-Minvielle, M. Cabassud, C. Gourdon, and P. Tochon. “Influence of the Meandering Channel Geometry on the Thermo-Hydraulic Performances of an Intensified Heat Exchanger/Reactor”. en. In: *Chemical Engineering and Processing: Process Intensification* 73 (Nov. 2013), pp. 67–80. DOI: 10.1016/j.cep.2013.06.012.

[10] E. Arslan, M. C. Çamurdan, A. Palazoglu, and Y. Arkun. “Multimodel Scheduling Control of Nonlinear Systems Using Gap Metric”. In: *Industrial & Engineering Chemistry Research* 43.26 (Dec. 2004), pp. 8275–8283. DOI: 10.1021/ie049610o.

[11] B. Aufderheide and B. W. Bequette. “Extension of Dynamic Matrix Control to Multiple Models”. en. In: *Computers & Chemical Engineering*. 2nd Pan American Workshop in Process Systems Engineering 27.8 (Sept. 2003), pp. 1079–1096. DOI: 10.1016/S0098-1354(03)00038-3.

[12] S. Bahroun, S. Li, C. Jallut, C. Valentin, and F. D. Panthou. “Control and Optimization of a Three-Phase Catalytic Slurry Intensified Continuous Chemical Reactor”. en. In: *Journal of Process Control* 20.5 (June 2010), pp. 664–675. DOI: 10.1016/j.jprocont.2010.03.002.

[13] R. Ball and B. F. Gray. “Thermal Instability and Runaway Criteria: The Dangers of Disregarding Dynamics”. en. In: *Process Safety and Environmental Protection* 91.3 (May 2013), pp. 221–226. DOI: 10.1016/j.psep.2012.05.008.

[14] R. V. Beard. “Failure Accomodation in Linear Systems through Self-Reorganization.” eng. Thesis. Massachusetts Institute of Technology, 1971.

[15] S. Ben Chabane, C. S. Maniu, E. F. Camacho, T. Alamo, and D. Dumur. “Fault Tolerant Control Approach Based on Multiple Models and Set-Membership State Estimation”. In: *2016 European Control Conference (ECC)*. June 2016, pp. 1105–1110. DOI: 10.1109/ECC.2016.7810437.

[16] W. Benaissa, S. Elgue, N. Gabas, M. Cabassud, D. Carson, and M. Demissy. “Dynamic Behaviour of a Continuous Heat Exchanger/Reactor after Flow Failure”. en. In: *International Journal of Chemical Reactor Engineering* 6 (2008).

[17] A. Boukhris, G. Mourot, and J. Ragot. “Non-Linear Dynamic System Identification: A Multi-Model Approach”. In: *International Journal of Control* 72.7-8 (Jan. 1999), pp. 591–604. DOI: 10.1080/002071799220795.

[18] S. Bracco, M. Troilo, and I. Faccioli. "A Numerical Discretization Method for the Dynamic Simulation of a Double-Pipe Heat Exchanger". In: *International Journal of Energy* 1 (Jan. 2007), pp. 47–58.

[19] M. Chadli. "On the Stability Analysis of Uncertain Fuzzy Models". In: 8.4 (Dec. 2006).

[20] *Chemical Reactor Design and Operation, 2nd Edition | Wiley*. en-us. https://www.wiley.com/en-us/Chemical+Reactor+Design+and+Operation%2C+2nd+Edition-p-9780471917304.

[21] H. Chen and S. Lu. "Fault Diagnosis Digital Method for Power Transistors in Power Converters of Switched Reluctance Motors". In: *IEEE Transactions on Industrial Electronics* 60.2 (Feb. 2013), pp. 749–763. DOI: 10.1109/TIE.2012.2207661.

[22] L. Chen, A. Tulsyan, B. Huang, and F. Liu. "Multiple Model Approach to Nonlinear System Identification with an Uncertain Scheduling Variable Using EM Algorithm". en. In: *Journal of Process Control* 23.10 (Nov. 2013), pp. 1480–1496. DOI: 10.1016/j.jprocont.2013.09.013.

[23] Z. CHEN, Y. HU, S. TIAN, H. LU, and L. XU. "Non-stationary signal combined analysis based fault diagnosis method". ; in: *Journal on Communications* 41.05 (2020), pp. 187–195.

[24] E. Chow and A. Willsky. "Analytical Redundancy and the Design of Robust Failure Detection Systems". In: *IEEE Transactions on Automatic Control* 29.7 (July 1984), pp. 603–614. DOI: 10.1109/TAC.1984.1103593.

[25] E. Y. Chow and A. S. Willsky. "Issues in the Development of a General Design Algorithm for Reliable Failure Detection". In: *1980 19th IEEE Conference on Decision and Control Including the Symposium on Adaptive Processes*. Dec. 1980, pp. 1006–1012. DOI: 10.1109/CDC.1980.271954.

[26] D. Dochain. "State and Parameter Estimation in Chemical and Biochemical Processes: A Tutorial". en. In: *Journal of Process Control* 13.8 (Dec. 2003), pp. 801–818. DOI: 10.1016/S0959-1524(03)00026-X.

[27] D. Dougherty and D. Cooper. "A Practical Multiple Model Adaptive Strategy for Single-Loop MPC". en. In: *Control Engineering Practice*. Automotive Systems 11.2 (Feb. 2003), pp. 141–159. DOI: 10.1016/S0967-0661(02)00106-5.

[28] D. Dougherty and D. Cooper. “A Practical Multiple Model Adaptive Strategy for Single-Loop MPC”. en. In: *Control Engineering Practice*. Automotive Systems 11.2 (Feb. 2003), pp. 141–159. DOI: 10.1016/S0967-0661(02)00106-5.

[29] J. Du, C. Song, and P. Li. “Multilinear Model Control of Hammerstein-like Systems Based on an Included Angle Dividing Method and the MLD-MPC Strategy”. In: *Industrial & Engineering Chemistry Research* 48.8 (Apr. 2009), pp. 3934–3943. DOI: 10.1021/ie8009395.

[30] R. F. Escobar, C. M. Astorga-Zaragoza, A. C. Téllez-Anguiano, D. Juárez-Romero, J. A. Hernández, and G. V. Guerrero-Ramírez. “Sensor Fault Detection and Isolation via High-Gain Observers: Application to a Double-Pipe Heat Exchanger”. en. In: *ISA Transactions* 50.3 (July 2011), pp. 480–486. DOI: 10.1016/j.isatra.2011.03.002.

[31] J. C. Etchells. “Process Intensification: Safety Pros and Cons”. en. In: *Process Safety and Environmental Protection*. Hazards XVIII 83.2 (Mar. 2005), pp. 85–89. DOI: 10.1205/psep.04241.

[32] T. Evgeniou, C. A. Micchelli, and M. Pontil. “Learning Multiple Tasks with Kernel Methods”. In: *Journal of Machine Learning Research* 6.21 (2005), pp. 615–637.

[33] S. E. Ferik and A. A. Adeniran. “Modeling and Identification of Nonlinear Systems: A Review of the Multimodel ApproachPart 2”. In: *IEEE Transactions on Systems, Man, and Cybernetics: Systems* 47.7 (July 2017), pp. 1160–1168. DOI: 10.1109/TSMC.2016.2560129.

[34] P. M. Frank and X. Ding. “Survey of Robust Residual Generation and Evaluation Methods in Observer-Based Fault Detection Systems”. en. In: *Journal of Process Control* 7.6 (Dec. 1997), pp. 403–424. DOI: 10.1016/S0959-1524(97)00016-4.

[35] P. M. Frank. “Fault Diagnosis in Dynamic Systems Using Analytical and Knowledge-Based Redundancy: A Survey and Some New Results”. en. In: *Automatica* 26.3 (May 1990), pp. 459–474. DOI: 10.1016/0005-1098(90)90018-D.

[36] C. T. Gálvez. “Fault detection and fault tolerant control in wind turbines”. es. http://purl.org/dc/dcmitype/Text. Universitat Politècnica de Catalunya (UPC), 2018.

[37] D. Gao, C. Wu, B. Zhang, and X. Ma. “Signed Directed Graph and Qualitative Trend Analysis Based Fault Diagnosis in Chemical Industry”. en. In: *Chinese Journal of Chemical Engineering* 18.2 (Apr. 2010), pp. 265–276. DOI: 10.1016/S1004-9541(08)60352-3.

[38] Z. Gao, C. Cecati, and S. X. Ding. “A Survey of Fault Diagnosis and Fault-Tolerant TechniquesPart I: Fault Diagnosis With Model-Based and Signal-Based Approaches”. In: *IEEE Transactions on Industrial Electronics* 62.6 (June 2015), pp. 3757–3767. DOI: 10.1109/TIE.2015.2417501.

[39] Z. Gao, C. Cecati, and S. X. Ding. “A Survey of Fault Diagnosis and Fault-Tolerant TechniquesPart II: Fault Diagnosis With Knowledge-Based and Hybrid/Active Approaches”. In: *IEEE Transactions on Industrial Electronics* 62.6 (June 2015), pp. 3768–3774. DOI: 10.1109/TIE.2015.2419013.

[40] K. Gasso. “Identification des systèmes dynamiques non-linéaires : approche multi-modèle”. fr. PhD thesis. Institut National Polytechnique de Lorraine, Dec. 2000.

[41] G. C. Goodwin and K. S. Sin. *Adaptive Filtering Prediction and Control*. en. Courier Corporation, May 2014.

[42] A. Green, B. Johnson, and A. John. “Process Intensification Magnifies Profits.” In: *Chemical Engineering*. Vol. 106. 1999, pp. 66–73.

[43] A. V. Gribok, I. K. Attieh, J. W. Hines, and R. E. Uhrig. “Stochastic Regularization of Feedwater Flow Rate Evaluation for the Venturi Meter Fouling Problem in Nuclear Power Plants”. In: *Inverse Problems in Engineering* 9.6 (June 2001), pp. 671–696. DOI: 10.1080/174159701088027786.

[44] T. M. Guerra and L. Vermeiren. “LMI-Based Relaxed Nonquadratic Stabilization Conditions for Nonlinear Systems in the TakagiSugeno’s Form”. en. In: *Automatica* 40.5 (May 2004), pp. 823–829. DOI: 10.1016/j.automatica.2003.12.014.

[45] X. Han, Z. Li, B. Dahhou, M. Cabassud, and M. He. “Nonlinear Observer Based Fault Diagnosis for an Innovative Intensified Heat-Exchanger/Reactor”. en. In: *Proceedings of the 11th International Conference on Modelling, Identification and Control (ICMIC2019)*. Ed. by R. Wang, Z. Chen, W. Zhang, and Q. Zhu. Lecture Notes in Electrical Engineering. Singapore: Springer, 2020, pp. 423–432. DOI: 10.1007/978-981-15-0474-7_40.

[46] Z. Han and K. S. Narendra. "New Concepts in Adaptive Control Using Multiple Models". In: *IEEE Transactions on Automatic Control* 57.1 (Jan. 2012), pp. 78–89. DOI: 10.1109/TAC.2011.2152470.

[47] Z. Han and K. Narendra. "Second Level Adaptation Using Multiple Models". In: *Proceedings of the American Control Conference*. Aug. 2011, pp. 2350–2355. DOI: 10.1109/ACC.2011.5991086.

[48] M. HE, Z. LI, and B. DAHHOU. "Fault Tolerant Control Strategy Using Two-Layer Multiple Adaptive Models for Plant Fault". In: *2020 International Conference on Control, Automation and Diagnosis (ICCAD)*. Oct. 2020, pp. 1–6. DOI: 10.1109/ICCAD49821.2020.9260565.

[49] M. He, Z. Li, B. Dahhou, and M. Cabassud. "The Fault Tolerant Control Design of an Intensified Heat-Exchanger/Reactor Using a Two-Layer, Multiple-Model Structure". en. In: *Sensors* 20.17 (Jan. 2020), p. 4888. DOI: 10.3390/s20174888.

[50] M. He, Z. Li, X. Han, M. Cabassud, and B. Dahhou. "Development of a Numerical Model for a Compact Intensified Heat-Exchanger/Reactor". English. In: *Processes* 7.7 (July 2019), p. 454. DOI: 10.3390/pr7070454.

[51] D. C. HENDERSHOT. "Process Minimization: Making Plants Safer". In: *Process minimization: Making plants safer* 96.1 (2000), pp. 35–40.

[52] C. HUANG, Y. GAO, and L. PENG. "Research on multiple modeling and identification method of industrial process". ; in: *Computer Engineering and Applications* 52.20 (2016), pp. 251–256+262.

[53] R. Isermann and P. Ballé. "Trends in the Application of Model-Based Fault Detection and Diagnosis of Technical Processes". en. In: *Control Engineering Practice* 5.5 (May 1997), pp. 709–719. DOI: 10.1016/S0967-0661(97)00053-1.

[54] R. Isermann. "Process Fault Detection Based on Modeling and Estimation MethodsA Survey". en. In: *Automatica* 20.4 (July 1984), pp. 387–404. DOI: 10.1016/0005-1098(84)90098-0.

[55] R. Isermann. "Model-Based Fault-Detection and Diagnosis Status and Applications". en. In: *Annual Reviews in Control* 29.1 (Jan. 2005), pp. 71–85. DOI: 10.1016/j.arcontrol.2004.12.002.

[56] R. Isermann. *Fault-Diagnosis Applications: Model-Based Condition Monitoring: Actuators, Drives, Machinery, Plants, Sensors, and Fault-Tolerant Systems*. en. Berlin Heidelberg: Springer-Verlag, 2011. DOI: 10.1007/978-3-642-12767-0.

[57] I. Izadi, S. L. Shah, D. S. Shook, and T. Chen. “An Introduction to Alarm Analysis and Design”. en. In: *IFAC Proceedings Volumes*. 7th IFAC Symposium on Fault Detection, Supervision and Safety of Technical Processes 42.8 (Jan. 2009), pp. 645–650. DOI: 10.3182/20090630-4-ES-2003.00107.

[58] A. Jarrou. “Diagnostic de défauts et commande tolérante aux défauts des systèmes à énergie renouvelable”. fr. PhD thesis. Université de Lorraine, July 2020.

[59] J. Jiang and X. Yu. “Fault-Tolerant Control Systems: A Comparative Study between Active and Passive Approaches”. en. In: *Annual Reviews in Control* 36.1 (Apr. 2012), pp. 60–72. DOI: 10.1016/j.arcontrol.2012.03.005.

[60] T. A. Johansen, K. J. Hunt, P. J. Gawthrop, and H. Fritz. “Off-Equilibrium Linearisation and Design of Gain-Scheduled Control with Application to Vehicle Speed Control”. en. In: *Control Engineering Practice* 6.2 (Feb. 1998), pp. 167–180. DOI: 10.1016/S0967-0661(98)00015-X.

[61] S. J. Julier and J. K. Uhlmann. “A New Extension of the Kalman Filter to Nonlinear Systems”. In: *Signal Processing, Sensor Fusion, and Target Recognition VI*. Vol. 3068. International Society for Optics and Photonics, July 1997, pp. 182–193. DOI: 10.1117/12.280797.

[62] S.-W. Kau, H.-J. Lee, C.-M. Yang, C.-H. Lee, L. Hong, and C.-H. Fang. “Robust H∞ Fuzzy Static Output Feedback Control of T-S Fuzzy Systems with Parametric Uncertainties”. In: *Fuzzy Sets and Systems* 158 (Jan. 2007), pp. 135–146. DOI: 10.1016/j.fss.2006.09.010.

[63] C. Kravaris, J. Hahn, and Y. Chu. “Advances and Selected Recent Developments in State and Parameter Estimation”. en. In: *Computers & Chemical Engineering*. CPC VIII 51 (Apr. 2013), pp. 111–123. DOI: 10.1016/j.compchemeng.2012.06.001.

[64] H. Kumamoto, K. Ikenchi, K. Inoue, and E. J. Henley. “Application of Expert System Techniques to Fault Diagnosis”. en. In: *The Chemical Engineering Journal*. An International Journal of Research and Development 29.1 (Aug. 1984), pp. 1–9. DOI: 10.1016/0300-9467(84)80001-5.

[65] Z.-t. Li, B. Dahhou, M. Zhang, and M. Cabassud. “Actuator Gain Fault Diagnosis for Heat-Exchanger/Reactor”. In: *2015 Chinese Automation Congress (CAC)*. Wuhan, China: IEEE, Nov. 2015, pp. 940–945. DOI: 10.1109/CAC.2015.7382633.

[66] Z. Li. “Contribution à l’élaboration d’algorithmes d’isolation et d’identification de défauts dans les systèmes non linéaires”. fr. PhD thesis. INSA de Toulouse, July 2006.

[67] Z. LI and B. DAHHOU. “Fault-Tolerant Control Based on Insufficient Fault Information”. In: *Journal of Nanjing University of Science and Technology* 35.Sup (2011).

[68] Z. Li and B. Dahhou. “A New Fault Isolation and Identification Method for Nonlinear Dynamic Systems: Application to a Fermentation Process”. en. In: *Applied Mathematical Modelling* 32.12 (Dec. 2008), pp. 2806–2830. DOI: 10.1016/j.apm.2007.09.036.

[69] Z. Li, B. Dahhou, Q. Li, and M. Zhang. “Design of Passive Fault Tolerant Control of a Process System”. In: *The 27th Chinese Control and Decision Conference (2015 CCDC)*. Qingdao, China: IEEE, May 2015, pp. 2776–2781. DOI: 10.1109/CCDC.2015.7162401.

[70] J. Liu, Q. Meng, and F. Fang. “Minimum Variance Lower Bound Ratio Based Nonlinearity Measure for Closed Loop Systems”. en. In: *Journal of Process Control* 23.8 (Sept. 2013), pp. 1097–1107. DOI: 10.1016/j.jprocont.2013.06.012.

[71] D. Magill. “Optimal Adaptive Estimation of Sampled Stochastic Processes”. In: *IEEE Transactions on Automatic Control* 10.4 (Oct. 1965), pp. 434–439. DOI: 10.1109/TAC.1965.1098191.

[72] A. Mirzaee and K. Salahshoor. “Fault Diagnosis and Accommodation of Nonlinear Systems Based on Multiple-Model Adaptive Unscented Kalman Filter and Switched MPC and H-Infinity Loop-Shaping Controller”. en. In: *Journal of Process Control* 22.3 (Mar. 2012), pp. 626–634. DOI: 10.1016/j.jprocont.2012.01.002.

[73] B. Mogens, K. Michel, L. Jan, and S. Marcel. *Diagnosis and Fault-Tolerant Control*. 2006.

[74] J. Mohd Ali, N. Ha Hoang, M. A. Hussain, and D. Dochain. “Review and Classification of Recent Observers Applied in Chemical Process Systems”. en. In: *Computers & Chemical Engineering* 76 (May 2015), pp. 27–41. DOI: 10.1016/j.compchemeng.2015.01.019.

[75] T. D. Murphey. “On Multiple Model Control for Multiple Contact Systems”. en. In: *Automatica* 44.2 (Feb. 2008), pp. 451–458. DOI: 10.1016/j.automatica.2007.05.018.

[76] R. Murray-Smith and T. Johansen. *Multiple Model Approaches To Nonlinear Modelling And Control*. en. CRC Press, Nov. 2020.

[77] N. N. Nandola and S. Bhartiya. “A Multiple Model Approach for Predictive Control of Nonlinear Hybrid Systems”. en. In: *Journal of Process Control* 18.2 (Feb. 2008), pp. 131–148. DOI: 10.1016/j.jprocont.2007.07.003.

[78] K. S. Narendra and K. Esfandiari. “Second Level Adaptation in Periodically Varying Environments”. en. In: (2019), p. 29.

[79] K. S. Narendra and A. M. Annaswamy. *Stable Adaptive Systems*. en. Courier Corporation, July 2012.

[80] A. Niederlinski. “A Heuristic Approach to the Design of Linear Multivariable Interacting Control Systems”. en. In: *Automatica* 7.6 (Nov. 1971), pp. 691–701. DOI: 10.1016/0005-1098(71)90007-0.

[81] M. Nikolaou and P. Misra. “Linear Control of Nonlinear Processes: Recent Developments and Future Directions”. en. In: *Computers & Chemical Engineering*. 2nd Pan American Workshop in Process Systems Engineering 27.8 (Sept. 2003), pp. 1043–1059. DOI: 10.1016/S0098-1354(03)00036-X.

[82] N. M. Nor, C. R. C. Hassan, and M. A. Hussain. “A Review of Data-Driven Fault Detection and Diagnosis Methods: Applications in Chemical Process Systems”. en. In: *Reviews in Chemical Engineering* 36.4 (May 2020), pp. 513–553. DOI: 10.1515/revce-2017-0069.

[83] J. Oravec, M. Trafczynski, M. Bakosova, M. Markowski, A. Mészáros, and K. Urbaniec. “Robust Model Predictive Control of Heat Exchanger Network in the Presence of Fouling”. In: *Chemical Engineering Transactions* 61 (Aug. 2017), pp. 334–342. DOI: 10.3303/CET1761054.

[84] R. Orjuela, B. Marx, J. Ragot, and D. Maquin. “Nonlinear System Identification Using Heterogeneous Multiple Models”. en. In: *International Journal of Applied Mathematics and Computer Science* 23.1 (Mar. 2013), pp. 103–115. DOI: 10.2478/amcs-2013-0009.

[85] M. Oudghiri. “Commande Multi-Modèles Tolérante Aux Défauts : Application Au Contrôle de La Dynamique d’un Véhicule Automobile.” In: (Oct. 2008).

[86] M. Oudghiri. "H∞ Tracking Observer-Based Control for TS Uncertain Fuzzy Models". en. In: ().

[87] P. Overloop. "Model Predictive Control on Open Water Systems". In: (Jan. 2006).

[88] C. H. Phillips, G. Lauschke, and H. Peerhossaini. "Intensification of Batch Chemical Processes by Using Integrated Chemical Reactor-Heat Exchangers". en. In: *Applied Thermal Engineering* 17.8 (Aug. 1997), pp. 809–824. DOI: 10.1016/S1359-4311(96)00061-0.

[89] Z. Qu, B. Dahhou, and G. Roux. "Fault Tolerant Control System Based on Subspace Predictive Control and Multiple Model Predictive Control". In: *2016 3rd Conference on Control and Fault-Tolerant Systems (SysTol)*. Sept. 2016, pp. 724–729. DOI: 10.1109/SYSTOL.2016.7739834.

[90] D. Rotondo, F. Nejjari, and V. Puig. "Passive and Active FTC Comparison for Polytopic LPV Systems". In: *2013 European Control Conference (ECC)*. July 2013, pp. 2951–2956. DOI: 10.23919/ECC.2013.6669235.

[91] W. J. Rugh. "Analytical Framework for Gain Scheduling". In: *IEEE Control Systems Magazine* 11.1 (Jan. 1991), pp. 79–84. DOI: 10.1109/37.103361.

[92] W. J. Rugh and J. S. Shamma. "Research on Gain Scheduling". en. In: *Automatica* 36.10 (Oct. 2000), pp. 1401–1425. DOI: 10.1016/S0005-1098(00)00058-3.

[93] W. E. Sayed, M. Abd El Geliel, and A. Lotfy. "Fault Diagnosis of PMSG Stator Inter-Turn Fault Using Extended Kalman Filter and Unscented Kalman Filter". en. In: *Energies* 13.11 (Jan. 2020), p. 2972. DOI: 10.3390/en13112972.

[94] T. SHEN. *H-Infinity Control Theory and Its Applications*. Beijing: Tsinghua University Press, 1996.

[95] H. Shi, P. Li, C. Su, Y. Wang, J. Yu, and J. Cao. "Robust Constrained Model Predictive Fault-Tolerant Control for Industrial Processes with Partial Actuator Failures and Interval Time-Varying Delays". en. In: *Journal of Process Control* 75 (Mar. 2019), pp. 187–203. DOI: 10.1016/j.jprocont.2018.09.003.

[96] S. Simani, C. Fantuzzi, and R. J. Patton. *Model-Based Fault Diagnosis in Dynamic Systems Using Identification Techniques*. en. Advances in Industrial Control. London: Springer-Verlag, 2003. DOI: 10.1007/978-1-4471-3829-7.

[97] A. Slimani, P. Ribot, E. Chanthery, and N. Rachedi. “Fusion of Model-Based and Data-Based Fault Diagnosis Approaches”. en. In: *IFAC-PapersOnLine*. 10th IFAC Symposium on Fault Detection, Supervision and Safety for Technical Processes SAFEPROCESS 2018 51.24 (Jan. 2018), pp. 1205–1211. DOI: 10.1016/j.ifacol.2018.09.698.

[98] H. Song, P. Han, J. Zhang, and C. Zhang. “Fault Diagnosis Method for Closed-Loop Satellite Attitude Control Systems Based on a Fuzzy Parity Equation”. In: *International Journal of Distributed Sensor Networks* 14 (Oct. 2018). DOI: 10.1177/1550147718805938.

[99] A. J. Stack and F. J. Doyle. “The Optimal Control Structure: An Approach to Measuring Control-Law Nonlinearity”. en. In: *Computers & Chemical Engineering* 21.9 (June 1997), pp. 1009–1019. DOI: 10.1016/S0098-1354(96)00339-0.

[100] M. Staroswiecki. “FAULT TOLERANT CONTROL : THE PSEUDO-INVERSE METHOD REVISITED”. en. In: *IFAC Proceedings Volumes*. 16th IFAC World Congress 38.1 (Jan. 2005), pp. 418–423. DOI: 10.3182/20050703-6-CZ-1902.01872.

[101] E. H. Stitt. “Alternative Multiphase Reactors for Fine Chemicals: A World beyond Stirred Tanks?” en. In: *Chemical Engineering Journal*. Catalytic Reaction and Reactor Engineering EuropaCat V Limerick, Sept 2-7 2001 90.1 (Nov. 2002), pp. 47–60. DOI: 10.1016/S1385-8947(02)00067-0.

[102] T. Takagi and M. Sugeno. “Fuzzy Identification of Systems and Its Applications to Modeling and Control”. In: *IEEE Transactions on Systems, Man, and Cybernetics* SMC-15.1 (Jan. 1985), pp. 116–132. DOI: 10.1109/TSMC.1985.6313399.

[103] W. Tan, H. J. Marquez, T. Chen, and J. Liu. “Multimodel Analysis and Controller Design for Nonlinear Processes”. en. In: *Computers & Chemical Engineering* 28.12 (Nov. 2004), pp. 2667–2675. DOI: 10.1016/j.compchemeng.2004.08.005.

[104] K. Tanaka and H. O. Wang. *Fuzzy Control Systems Design and Analysis: A Linear Matrix Inequality Approach*. en-us. New York: John Wiley & Sons, Inc., 2001.

[105] F. Théron, Z. Anxionnaz-Minvielle, M. Cabassud, C. Gourdon, and P. Tochon. "Characterization of the Performances of an Innovative Heat-Exchanger/Reactor". en. In: *Chemical Engineering and Processing: Process Intensification* 82 (Aug. 2014), pp. 30–41. DOI: 10.1016/j.cep.2014.04.005.

[106] P. Tochon, R. Couturier, Z. Anxionnaz, S. Lomel, H. Runser, F. Picard, et al. "Toward a Competitive Process Intensification: A New Generation of Heat Exchanger-Reactors". In: *Oil & Gas Science and Technology - Revue d'IFP Energies nouvelles* 65.5 (2010), pp. 785–792. DOI: 10.2516/ogst/2010020.

[107] P. S. Varbanov, J. J. Kleme, and F. Friedler. "Cell-Based Dynamic Heat Exchanger ModelsDirect Determination of the Cell Number and Size". en. In: *Computers & Chemical Engineering*. Selected Papers from ESCAPE-20 (European Symposium of Computer Aided Process Engineering - 20), 6-9 June 2010, Ischia, Italy 35.5 (May 2011), pp. 943–948. DOI: 10.1016/j.compchemeng.2011.01.033.

[108] A. Vasikaninová, M. Bakoová, A. Mészáros, and J. J. Kleme. "Neural Network Predictive Control of a Heat Exchanger". en. In: *Applied Thermal Engineering*. Selected Papers from the 13th Conference on Process Integration, Modelling and Optimisation for Energy Saving and Pollution Reduction 31.13 (Sept. 2011), pp. 2094–2100. DOI: 10.1016/j.applthermaleng.2011.01.026.

[109] V. Venkatasubramanian, R. Rengaswamy, and S. N. Kavuri. "A Review of Process Fault Detection and Diagnosis: Part II: Qualitative Models and Search Strategies". en. In: *Computers & Chemical Engineering* 27.3 (Mar. 2003), pp. 313–326. DOI: 10.1016/S0098-1354(02)00161-8.

[110] V. Venkatasubramanian, R. Rengaswamy, S. N. Kavuri, and K. Yin. "A Review of Process Fault Detection and Diagnosis: Part III: Process History Based Methods". en. In: *Computers & Chemical Engineering* 27.3 (Mar. 2003), pp. 327–346. DOI: 10.1016/S0098-1354(02)00162-X.

[111] V. Venkatasubramanian, R. Rengaswamy, K. Yin, and S. N. Kavuri. "A Review of Process Fault Detection and Diagnosis: Part I: Quantitative Model-Based Methods". en. In: *Computers & Chemical Engineering* 27.3 (Mar. 2003), pp. 293–311. DOI: 10.1016/S0098-1354(02)00160-6.

[112] Y. Vidal, L. Acho, and F. Pozo. "Robust Fault Detection in Hysteretic Base-Isolation Systems". en. In: *Mechanical Systems and Signal Processing* 29 (May 2012), pp. 447–456. DOI: 10.1016/j.ymssp.2011.11.025.

[113] H. Wang, W. Bai, and P. X. Liu. “Finite-Time Adaptive Fault-Tolerant Control for Nonlinear Systems with Multiple Faults”. In: *IEEE/CAA Journal of Automatica Sinica* 6.6 (Nov. 2019), pp. 1417–1427. DOI: 10.1109/JAS.2019.1911765.

[114] L. Wang. *Model Predictive Control System Design and Implementation Using MATLABő*. en. Springer Science & Business Media, Feb. 2009.

[115] B. WU. “A multiple model approach integrated operating space partition and optimal control for nonlinear system”. ;. Zhejiang University, 2017.

[116] X. Wu, Z. Xie, X. Bai, and T. Kwan. “Design of a 1-Bit MEMS Gyroscope Using the Model Predictive Control Approach”. en. In: *Sensors* 19.3 (Jan. 2019), p. 730. DOI: 10.3390/s19030730.

[117] L. Xiaodong and Z. Qingling. “New Approaches to H∞ Controller Designs Based on Fuzzy Observers for T-S Fuzzy Systems via LMI”. en. In: *Automatica* 39.9 (Sept. 2003), pp. 1571–1582. DOI: 10.1016/S0005-1098(03)00172-9.

[118] X. Yan, Y. Liu, M. Jia, and Y. Zhu. “A Multi-Stage Hybrid Fault Diagnosis Approach for Rolling Element Bearing Under Various Working Conditions”. In: *IEEE Access* 7 (2019), pp. 138426–138441. DOI: 10.1109/ACCESS.2019.2937828.

[119] H. Yang, B. Jiang, and M. Staroswiecki. “Supervisory Fault Tolerant Control for a Class of Uncertain Nonlinear Systems”. en. In: *Automatica* 45.10 (Oct. 2009), pp. 2319–2324. DOI: 10.1016/j.automatica.2009.06.019.

[120] Youmin Zhang and Jin Jiang. “Design of Proportional-Integral Reconfigurable Control Systems via Eigenstructure Assignment”. In: *Proceedings of the 2000 American Control Conference. ACC (IEEE Cat. No.00CH36334)*. Vol. 6. June 2000, 3732–3736 vol.6. DOI: 10.1109/ACC.2000.876918.

[121] B. YU. “Fault-Tolerant Control with Applications to Aircraft Using Linear Quadratic Design Framework”. PhD thesis. 2016.

[122] X. Yu and Y. Zhang. “Design of Passive Fault-Tolerant Flight Controller against Actuator Failures”. en. In: *Chinese Journal of Aeronautics* 28.1 (Feb. 2015), pp. 180–190. DOI: 10.1016/j.cja.2014.12.006.

[123] A. Zakharov, V. .-M. Tikkala, and S. .-L. Jämsä-Jounela. “Fault Detection and Diagnosis Approach Based on Nonlinear Parity Equations and Its Application to Leakages and Blockages in the Drying Section of a Board Machine”. en. In: *Journal of Process Control* 23.9 (Oct. 2013), pp. 1380–1393. DOI: 10.1016/j.jprocont.2013.03.006.

[124] A. Zavala-Río and R. Santiesteban-Cos. “Reliable Compartmental Models for Double-Pipe Heat Exchangers: An Analytical Study”. en. In: *Applied Mathematical Modelling* 31.9 (Sept. 2007), pp. 1739–1752. DOI: 10.1016/j.apm.2006.06.005.

[125] M. ZHANG. “Fault Diagnosis & Root Cause Analysis of Invertible Dynamic System”. PhD thesis. UPS-GZU, 2017.

[126] M. Zhang, B. Dahhou, M. Cabassud, and Z. Li. “Faults Isolation in Intensified Continuous HEX Reactor with Parameter Uncertainties”. In: *The 26th International Workshop on Principles of Diagnosis (DX-2015)*. Paris, France, Aug. 2015.

[127] M. Zhang, Z.-t. Li, M. Cabassud, and B. Dahhou. “An Integrated FDD Approach for an Intensified HEX/Reactor”. en. In: *Journal of Control Science and Engineering* 2018 (Jan. 2018), e5127505. DOI: 10.1155/2018/5127505.

[128] Y. Zhang and J. Jiang. “Integrated Active Fault-Tolerant Control Using IMM Approach”. In: *IEEE Transactions on Aerospace and Electronic Systems* 37.4 (Oct. 2001), pp. 1221–1235. DOI: 10.1109/7.976961.

[129] Y. Zhang and J. Jiang. “Bibliographical Review on Reconfigurable Fault-Tolerant Control Systems”. en. In: *Annual Reviews in Control* 32.2 (Dec. 2008), pp. 229–252. DOI: 10.1016/j.arcontrol.2008.03.008.

[130] Z. Zhang, Z. Zhao, X. Li, X. Zhang, S. Wang, R. Yan, et al. “Faster Multiscale Dictionary Learning Method With Adaptive Parameter Estimation for Fault Diagnosis of Traction Motor Bearings”. In: *IEEE Transactions on Instrumentation and Measurement* 70 (2021), pp. 1–13. DOI: 10.1109/TIM.2020.3032193.

[131] D. Zhou and X. Ding. “Theory and Applications of Fault Tolerant Control”. ; in: *ACTA AUTOMATICA SINICA* 06 (2000), pp. 788–797.

[132] D. Zhou and Y. Hu. “Fault Diagnosis Techniques for Dynamic Systems”. ; in: *ACTA AUTOMATICA SINICA* 35.06 (2009), pp. 748–758.